

A free-flow isotachophoresis (FFITP) device with a
selectable output by using flow control which was used
as an interface for sample purification and
concentration

Dissertation
zur Erlangung des Grades
des Doktors der Ingenieurwissenschaften
der Naturwissenschaftlich - Technischen Fakultät
der Universität des Saarlandes

von

Jukyung Park

Saarbrücken
2016

Tag des Kolloquiums:

06.DEZ.2016

Dekan:

Prof. Dr. rer. nat. Guido Kickelbick

**Mitglieder des
Prüfungsausschusses:**

Vorsitzender:

Prof. Dr.-Ing. habil. Joachim Rudolph

Gutachter:

Prof. Dr. sc. techn. Andreas Manz

Prof. Dr. rer. nat. Andreas Schütze

Akademischer Mitarbeiter:

Dr. rer. nat. Andreas Leschhorn

Contents

1	Introduction	3
1.1	Motivation	3
1.2	Electrophoresis	4
1.2.1	Double layer	5
1.2.2	Electroosmotic flow	7
1.2.3	Electrophoresis	9
1.3	Isotachophoresis	11
1.4	Miniaturization	12
1.4.1	On hips capillary electrophoresis	13
1.4.2	Free-flow electrophoresis	14
1.5	Detection methods	15
1.5.1	Optical detection	15
1.5.2	Electrospray Ionization Mass Spectrometry (ESI-MS)	15
2	Fabrication	19
2.1	Glass chip fabrication	19
2.1.1	Gold and chrome sputtering	19
2.1.2	Spin coating of photoresist	20
2.1.3	Exposure of the photoresist	20
2.1.4	Development of the pattern	21
2.1.5	Wet etching	21
2.1.6	Removal of the photoresist and Gold/Chrome layers	22
2.1.7	Making inlets	22
2.1.8	Bonding and dicing	24
2.2	Connector mounting	25
2.3	Cleaning protocol	26
3	Isotachophoresis free-flow on a glass chip using side flow for selectable output	31
3.1	Introduction	31

3.2	Experimental	32
3.2.1	Chemicals	32
3.2.2	Device layout	32
3.2.3	Optical setup	32
3.2.4	Experimental procedure	33
3.3	Result and discussion	34
3.3.1	FFITP concentration factors	34
3.3.2	Hydrodynamic flow control	35
3.4	Conclusion	38
4	Coupling to the Mass spectrometer	41
4.1	Introduction	41
4.2	Simulation of ITP	43
4.3	Experimental	44
4.3.1	Chemicals	44
4.3.2	Chip layout and tubing	44
4.3.3	Experiment setup	45
4.3.4	Interface from chip to MS	46
4.3.5	Experimental Procedure	46
4.4	Result and discussion	46
4.4.1	Isotachopheresis	46
4.4.2	FFITP-ESI-MS interface test	47
4.4.3	FFITP-ESI-MS	48
4.5	Conclusion	51
5	FFITP enhanced ISFET Based Biosensor	55
5.1	Introduction	55
5.2	Experimental	56
5.2.1	Chemicals	56
5.2.2	Surface modification for attaching GFP antibody to the sensor . . .	57
5.2.3	Experiment setup	57
5.3	Experimental Procedures	57
5.4	Result and Discussion	58
5.4.1	FFITP	59
5.4.2	DGFET	59
5.4.3	FFITP-DGFET connection	59
5.4.4	Coupling of FFITP and DGFET	62
5.5	Conclusion	62
6	Conclusion	65

7	Appendix	67
7.1	fabrication protocol	67
7.1.1	Glass chip	67
7.1.2	SU8 chip	79
7.2	Connector mounting protocol	92
7.3	Cleaning protocol	94
7.3.1	Glass chip	94
7.3.2	SU8 chip	98

List of Figures

1.1	(A) The schematic drawing of the Helmholtz double layer. (B) The inner layer in which the potential changes linearly with the distance it comprises the absorbed anions.	5
1.2	(A) The schematic drawing of the Gouy-Chapman model (B) The potential change is exponential which follows the Boltzmann statistical distribution .	6
1.3	(A) The schematic drawing of the stern model model (B) The potential change is exponential which follows the Boltzmann statistical distribution .	7
1.4	Electroosmotic Flow Schematic	8
1.5	Schematic of electrophoresis	11
1.6	An Isotachophoretic Separation. (A) Before Applying electric field (B) Separation Commenced (C)Steady state	12
1.7	Conceptual drawing of free flow electrophoresis where a perpendicular electric field is applied to the pressure driven flow	14
1.8	Conceptual drawing of free flow electrophoresis where a perpendicular electric field is applied to the pressure driven flow	16
1.9	Conceptual drawing of free flow electrophoresis where a perpendicular electric field is applied to the pressure driven flow	17
1.10	Conceptual drawing of free flow electrophoresis where a perpendicular electric field is applied to the pressure driven flow	17
2.1	Gold and chrome sputtering	19
2.2	Spin coating of photoresist	20
2.3	Exposure of the photoresist and cadence desing	20
2.4	Development of the pattern	21
2.5	Wet etching. Where (A) is chrome etching, (A) is gold etching, and (A) is glass etching	21
2.6	Removal of the photoresist(A), Gold(B). and Chrome(C) layers	22
2.7	Drilling with a drill machine	22
2.8	Drilling with a CNC machine	23
2.9	Making inlets by etching	24

2.10	Etching procedure	24
2.11	Making inlets by etching with photoresist	25
2.12	Connenctor bonding 1	25
2.13	Connenctor bonding 2	26
2.14	Connenctor bonding 3	26
2.15	Connenctor bonding 4	27
2.16	Cleaning 1	27
2.17	Cleaning 2	27
2.18	Cleaning 3	28
2.19	Cleaning 4	28
2.20	Cleaning 5	29
2.21	Cleaning 6	29
3.1	Chip schematic showing all chambers. The side chambers are separated from the main chamber by $25\mu m$ wide channels and pillars were used in order to avoid collapse during thermal bonding which is shown by an SEM picture left top. Connections for the syringes and the side reservoirs which are used to connect the electrodes are shown at the left bottom figure.	33
3.2	(A) Laminar flow before applying the separation voltage (B) Focused stream line of fluorescein with 200V separation voltage.	34
3.3	PMT output signal as function of applied voltage with a constant flow rate of $5 \mu L/min$. It could be observed that the concentration of the fluorescein is increased by applying a higher	35
3.4	PMT output signal change by a constant voltage (100 V) and increasing the flow rate. It could be observed that the fluorescein concentration is decreasing by increasing the flow rate.	35
3.5	: Schematic operation of the ITP device. By applying an electric field perpendicular to the flow direction, the sample will be focused. This focused stream can be control by applying an additional flow which is called as control flow. Three possibilities is considered for the control flow; applying positive pressure from the outlet, applying positive pressure from the inlet and applying negative pressure from the outlet.	36
3.6	Simplified drawing of the device showing the velocity vectors. For shifting the stream, the flow rate at inlet 1 was increased.	37
3.7	The x-component of the velocity at the outlet of the device as function of the flow at inlet 1. The point at which the x-component becomes zero shifts towards the right with increasing flow, by increasing the flow rate with a $0.1 \mu L/min$ step.	38

3.8	Comparison of the experimental data and the simulation of the hydrodynamic control of the focused stream line. Indicated on the vertical axes is the x-position the outlet at which the x-component of the velocity is zero. This point, at which the liquid no longer displaces in x-direction, is shifting to the left side with increasing flow at input 1.	39
4.1	Principle of operation of the FFITP chip. By applying an electric field perpendicular to the flow direction, the target analytes are focused between the leading (LE) and terminating buffer (TE). Increasing the flow at inlet 5 will shift the stream to a desired outlet (13)	42
4.2	Result of the ITP simulation, showing Alexa fluor 488 and citric acid being concentrated in the ITP window while fluorescein dissipates into the TE. The ITP system is depicted right to left with the relative position of the window positioned at 0, LE at negative values and TE at the positive values.	43
4.3	(A) Photograph of the device implementation in glass. The side chambers are separated from the main chamber by 25 \hat{I} $\frac{1}{4}$ m wide grooves. Pillars were introduced to avoid collapse during thermal bonding and to prevent breaking by the high back pressure inside the chamber (B) Connections for the tubing and the side reservoirs which are used to connect the electrodes. (C) Connection of the FFITP chip to the MS with a diagram showing the connection points for the electric field, syringe pumps and ESI-MS. The chip is mounted on an inverted optical microscope (photograph).	45
4.4	Microscope image of the FFITP device which showing the focusing of Alexa fluor into a sharp band and dissipating fluorescein. (C) PMT signal output which showing the intensity of Alexa fluor and fluorescein.	48
4.5	PMT signal output which showing the intensity of Alexa fluor and fluorescein.	49
4.6	Online connection test with fluorescein for 40 min	49
4.7	Online connection with fluorescein and Citric acid	50
4.8	Normalized value of the output of the online connection of fluorescein and citric acid	51
4.9	The MS data output during FFITP-ESI-MS. A mixture of Alexa fluor 488, Citric acid, Glycolic acid, and fluorescein was used as sample, using Alexa fluor for optical guidance. By controlling the flow rate at the inlets the flow through the outlet connected with the MS was moved from LE to TE for 7 min and then shifted back to LE. Throughout this process, first citric acid (191 m/z) was detected, followed by glycolic acid and back to citric acid	52
4.10	Normalized value of the output of the online connection of fluorescein, citric acid, and glycolic acid	52

4.11	Selected ion isotachopherograms for glycolic acid ($m/z=73$), citric acid ($m/z=191$) and fluorescein ($m/z=331$).	54
5.1	Schematic operation of the FFITP-DGFET.	56
5.2	3 Left top: FFITP with connector. Left bottoms: EG-DG FET where the antibody and the antigens was injected. Right bottom: Probe station where the DGFET was mounted	58
5.3	The ITP process of GFP. (A) Electric field on (B) Electric field off (C) The zoomed version when the electric field is applied	60
5.4	The concentration change from DGFET with GFP in PBS buffer	61
5.5	The V-I curve by increasing the voltage at the FFITP device.	62
5.6	The V-I curve with injection of fluorescein to the DGFET via FFITP.	63
5.7	Left: TRIS buffer which was injected to the EG via pipette. Right: the threshold voltage change when the GFP concentration was increased from 1 fg/ml to 1 ng/ml	63

Acknowledgements

Firstly, I would like to express my sincere gratitude to my advisor Prof. Andreas Manz for the continuous support of my Ph.D. study and related research, for his patience, motivation, and immense knowledge. His guidance helped me in all the time of research and writing of this thesis. I could not have imagined having a better advisor and mentor for my Ph.D. study. I would also like to thank Prof. Pavel Neuzil, for providing wise advice for the chip fabrication. Prof. Leon Abelmann for insightful comments and encouragement. Prof. Rosanne Guijt for guidance and teaching in the chemical field. Finally, I must express my very profound gratitude to my parents and to my wife Sehwa Lee for un-failing support and continuous encouragement throughout my years of study and though the process of researching and writing this thesis. This accomplishment would not have been possible without them.

Thank you

Eidesstattliche Versicherung

Hiermit versichere ich an Eides statt, dass ich die vorliegende Arbeit selbständig und ohne Benutzung anderer als der angegebenen Hilfsmittel angefertigt habe. Die aus anderen Quellen oder indirekt übernommenen Daten Konzepte sind unter Angabe der Quelle gekennzeichnet. Die Arbeit wurde bisher weder im In- noch Ausland in gleicher oder ähnlicher Form in einem Verfahren zur Erlangung eines Akademischen Grades vorgelegt.

(Ort, Datum)

(Jukung Park)

Abstract

Isotachopheresis (ITP) is a powerful technology capable of simultaneously concentrating analytical targets and removal of interferences. Free flow electrophoresis (FFE) is an electrophoretic separation technique where an electric field is applied perpendicular to the flow direction in order to have a continuous separation system. FFITP is the mode of FFE where a discontinuous buffer system consisting of a LE and TE flows through the separation chamber. FFITP is especially attractive because it provides a continuous separation combined with selective concentration of the analytes. Two applications were studied in this thesis. First, the online coupling of a FFITP to an electrospray ionization mass spectrometer. This combination decouples the separation and detection time frame because the electrophoretic separation and concentration takes place perpendicular to the flow direction. Second, the FFITP was coupled to a dual gate field effect transistor (DGFET). DGFET is a self-made sensor which consists of an extended gate where antibodies are bound on the surface. When the target antigen is entering to the extended gate (EG) the DGFET will change the threshold voltage. The online coupling with FFITP a DGFET will lower the detection limit by pre-concentration of the target sample. Based on the result future applications of this approach are expected in monitoring biochemical changes and proteomics.

Zusammenfassung

Die Isotachophorese (ITP) ist eine leistungsfähige Analysenmethode, mit der man gleichzeitig das zu analysierende Molekül aufkonzentrieren und NebenkompONENTEN abtrennen kann. Die Elektrophorese im freien Fluss, die sogenannte "Free Flow Electrophoresis (FFE)" ist eine elektrophoretische Trennmethode, mit der man kontinuierlich Ionen durch ein elektrisches Feld senkrecht zur Strömungsrichtung auftrennen kann. "Free-Flow-Isotachophoresis (FFITP)" ist eine Kombination aus FFE und ITP. FFITP ist besonders attraktiv, weil es Trennung und Erhöhung der Konzentration der zu analysierenden Moleküle kontinuierlich ermöglicht. Zwei Anwendungen wurden in dieser Arbeit untersucht:

1. Die Online-Kopplung von einem FFITP mit der Elektrospray-Ionisations-Massenspektrometrie:

Diese Kombination ermöglicht die Auswahl einer bestimmten Fraktion der Trennung aus komplexen Gemischen und überführt sie kontinuierlich in ein Massenspektrometer. Dabei kann die Fraktionsdauer frei gewählt werden.

2. Die Kombination von FFITP mit einem Biosensor, einem sogenannten "Dual Gate Field Effect Transistor" (DGFET): Das ist ein Sensor, bei dem Antikörper auf der Oberfläche eines Extended Gate (EG) immobilisiert sind. Wenn die Ziel-Antigene über das EG fließen und sich mit den Antikörpern verbinden, verändert sich die Schwellenspannung des DGFET. Durch die vorherige Trennung und Aufkonzentration mittels FFITP wird eine niedrigere Nachweisgrenze erzielt.

Chapter 1

Introduction

1.1 Motivation

Isotachopheresis (ITP) is a powerful technology capable of simultaneously concentrating analytical targets and removal of interferences. An ITP system consists of different electrolytes, with the co-ion selected based on the electrophoretic mobility in relationship to the target. The co-ion in the leading electrolyte (LE) has mobility higher than the target analytes, whilst the co-ion in the terminating electrolyte (TE) has mobility lower than the target. When the ITP system establishes, ions arrange according to their mobility according to the Kohlrausch regulating function, positioning the analytical target(s) between the LE and TE. Free flow electrophoresis (FFE) is an electrophoretic separation technique where an electric field is applied perpendicular to an electric field in order to have a continuous separation system. Analogous to the terminology used in capillary electrophoresis, FFITP is the mode of FFE where a discontinuous buffer system consisting of a LE and TE flows through the separation chamber. FFITP is especially attractive because it provides a continuous separation combined with selective concentration of the analytes. Hydrodynamic flow control was used in order to guide the concentrated sample to the desired outlet. Two applications were studied in this thesis. First, the online coupling of a free-flow isotachopheresis (FFITP) chips to an electrospray ionization mass spectrometer (ESI-MS) for continuous online monitoring without extensive sample preparation. The online coupling of FFITP to ESI-MS decouples the separation and detection timeframe because the electrophoretic separation takes place perpendicular to the flow direction, which can be beneficial for monitoring (bio) chemical changes and/or extensive MSn studies. We have demonstrated the coupling of FFITP with ESI-MS for simultaneous concentration of target analytes and sample clean-up. Furthermore, we demonstrated hydrodynamic control of the fluidic fraction injected into the MS, allowing for fluidically controlled scanning of the ITP window. Future applications of this approach are expected in monitoring biochemical changes and proteomics. Second, the FFITP was coupled to a

dual gate field effect transistor (DGFET). DGFET is a self made sensor which consists of a extended gate where antibodies are bind on the surface. When the target antigen is entering to the extended gate the DGFET will change the threshold voltage. The online coupling with FFITP a DGFET will lower the detection limit by pre-concentration of the target sample. This is important for early detection of disease. Although the fact that the antibodies are highly selective, in real application the concentration of the unwanted protein has a much higher concentration compare to the target concentration. Which result lots of noise to the DGFET, therefore a sample clean-up is needed. The FFITP-DGFET is also compareable with the FFITP-ESI-MS. One of the big problems of the FFITP-ESI-MS coupling is that the buffer system should be chosen which is compatible with the MS. However this criterion is not easy to full fill, where the FFITP-DGFET is free of this problem. Therefore a similar approach was done where the FFITP is used as purification of the sample and concentration of the target sample which was injected to the DGFET. Based on the result with the two applications, future applications of this approach are expected in monitoring biochemical changes and proteomics.

1.2 Electrophoresis

Analytical chemistry is a study for determine the constituents of a chemical compound or a mixture of chemical compounds. Analytical chemistry has a various application such as; biological, environmental, and materials analysis. One of the problems to analyze these samples is the complexity. Therefore a separation technique is needed to separate the compound of interest from the other compounds. Several techniques are used for solve this problem including electrophoresis. Electrophoresis is a separation method based on the mobility different by applying an electric field. A detail explanation will be given in the chapter 1.2.3. Even though electrophoresis is a good separation method many practical application in analytical chemistry is suffering of a very low concentration of the compound of interest. Therefore a pre-concentration method is needed such as filtering or centrifugation. However both of these methods need an additional step for pre-concentration, an alternative for sample pre-parathion (concentration and separation) is isotachopheresis. Where isotachopheresis is mode of electrophoresis which is able to concentrate and separate the sample simultaneously (see chapter 1.3). In order to determine the compound of the sample a detection method is needed, where normally a desired volume is needed, which result to the problem to collect a separated a concentrated compound. In ordered to collect the compound a continues output is required. In this chapter I will discuss about the theory of each technology stating with the Double layer.

1.2.1 Double layer

The concept of the existence of the double layer at a charged flat surface and a spatial counter charge was first appeared by Helmholtz (1879) [19].

Helmholtz double layer

A Helmholtz double layer constitutes two layers having opposite charges, one being negatively charged and the other positively charged. A separation of charges exists like in a capacitor. Helmholtz figured it out in 1853, when an electronic conductor (metal) dissolves continuously, it become increasingly negative charge. This is due to the ions in solution adsorbed at the surface of the solid. The excess of negative charge on the metal surface attract the positive charge ion of the solution (see 1.1). The negatively charged layer is called as the inner Helmholtz layer and the positive layer is called as an outer Helmholtz layer. A potential (Ψ) drop from the surface to the outer Helmholtz layer (OHL). The potential drop is given in equation 1.1.

$$\Psi = \Psi_0 \left(1 - \frac{1}{x_{OHL}} x\right) \quad (1.1)$$

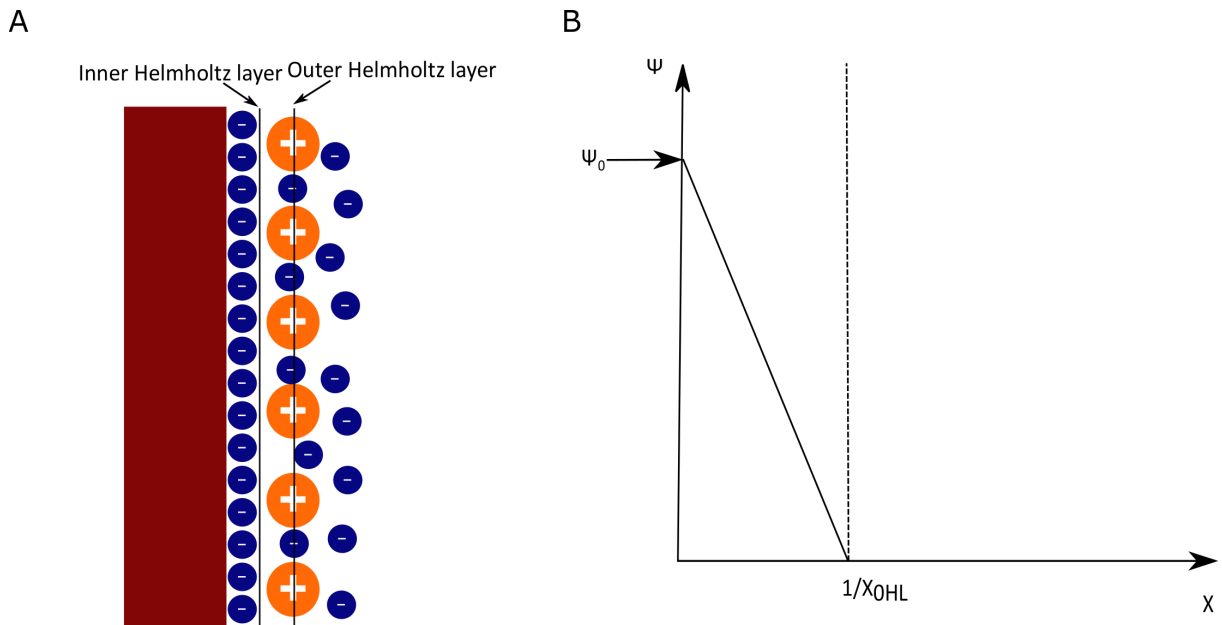


Figure 1.1: (A) The schematic drawing of the Helmholtz double layer. (B) The inner layer in which the potential changes linearly with the distance it comprises the absorbed anions.

Gouy-Chapman double layer

The Helmholtz model is a good foundation for explaining the surface charge. However it does not include important factors such as diffusion, thermal motion, adsorption onto the surface, and solvent/ surface interactions. A more realistic description of the electrostatic double layer which involves the diffuse part is suggested by Gouy-Chapman in 1910 [39] (1.2). The counter ions are not rigidly held as in the Helmholtz model, but tend to diffuse into the solvent until the counter potential is set up. The kinetic energy of the counter ions will affect the thickness of diffused double layer which know as the Debye length ($1/k$). The charge distribution of ions as a function of distance from the metal surface follows Maxwell-Boltzmann statistics to be applied. The potential drops exponentially as given in equation 1.2.

$$\Psi = \Psi_0(e^{-kx}) \quad (1.2)$$

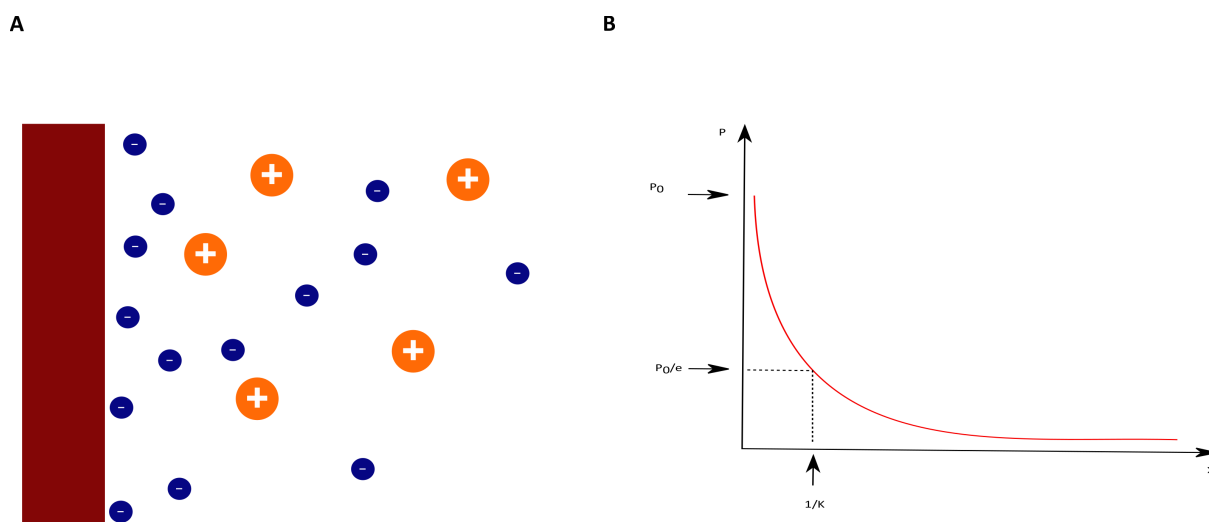


Figure 1.2: (A) The schematic drawing of the Gouy-Chapman model (B) The potential change is exponential which follows the Boltzmann statistical distribution

Stern double layer

The Gouy-Chapman theory provides a better approximation of reality than does the Helmholtz theory, but it still has limited quantitative application. It assumes that ions behave as point charges, which they cannot, and it assumes that there is no physical limits for the ions in their approach to the surface, which is not true. Stern [49], therefore, modified the Gouy-Chapman diffuse double layer. His theory states that ions do have finite size so cannot approach the surface closer than a few nm. As a result he has combined the Helmholtz model with the Gouy-Chapman model, where a compact layer is

followed by diffuse layer (see 1.3). The transition point from Helmholtz model to Gouy-Chapman model is called as a shear plane, where the potential of the plane known as zeta (ζ) potential.

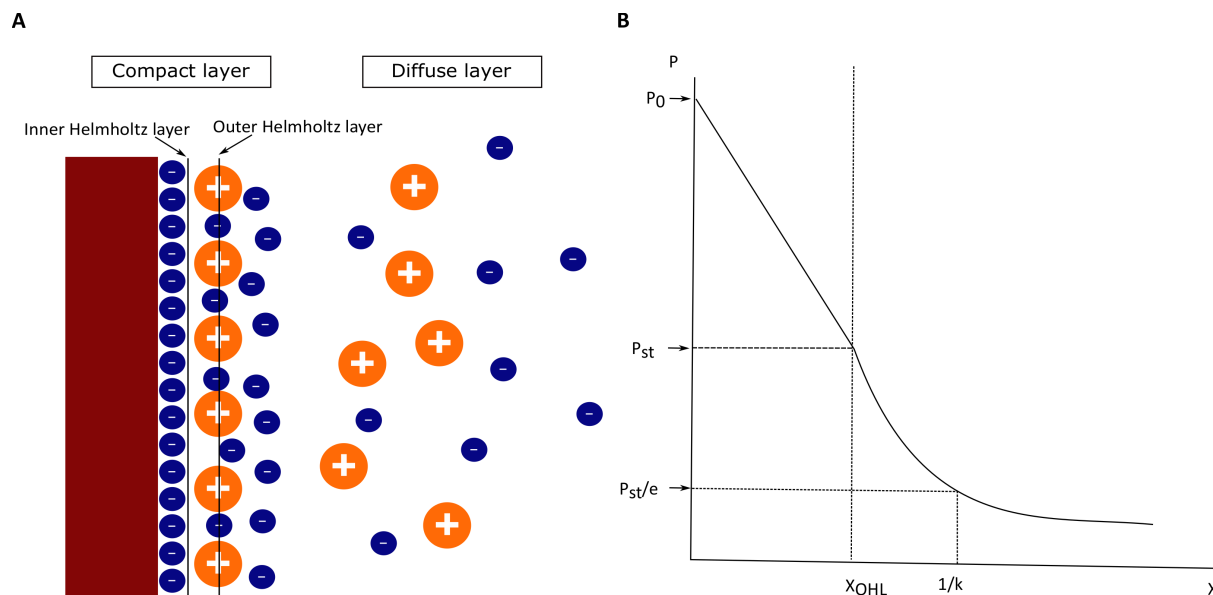


Figure 1.3: (A) The schematic drawing of the stern model (B) The potential change is exponential which follows the Boltzmann statistical distribution

1.2.2 Electroosmotic flow

When a charged particle is put in contact with a liquid in a capillary tube, double-layer forms at the wall of the capillary. The first layer is surface charge, and can be positive or negative depending on the material. As capillaries are generally borosilicate glass, the numerous silanol (SiOH) groups cause the charge of the first layer to be negative (Helmholtz layer). The second layer is made up of ionic particles in solution that are electronically attracted to the charge of the capillary surface. As the particles in this layer are not fixed, but move as a result of electrical and thermal energy, it is called the diffuse layer (Gouy-Chapman layer). When an electrical potential is placed across the capillary tube, the diffuse layer is pulled to one side. As the diffuse layer progresses to one side of the capillary tube, it drags the bulk solution along with it, creating a flow (specifically, the electro-osmotic flow) of the solution through the cathode. As shown in figure 1.4 the resulting of applying an electrical potential is a plug flow, where the velocity profile (green) is approximately planar, except of the variation near the electric double layer [53].

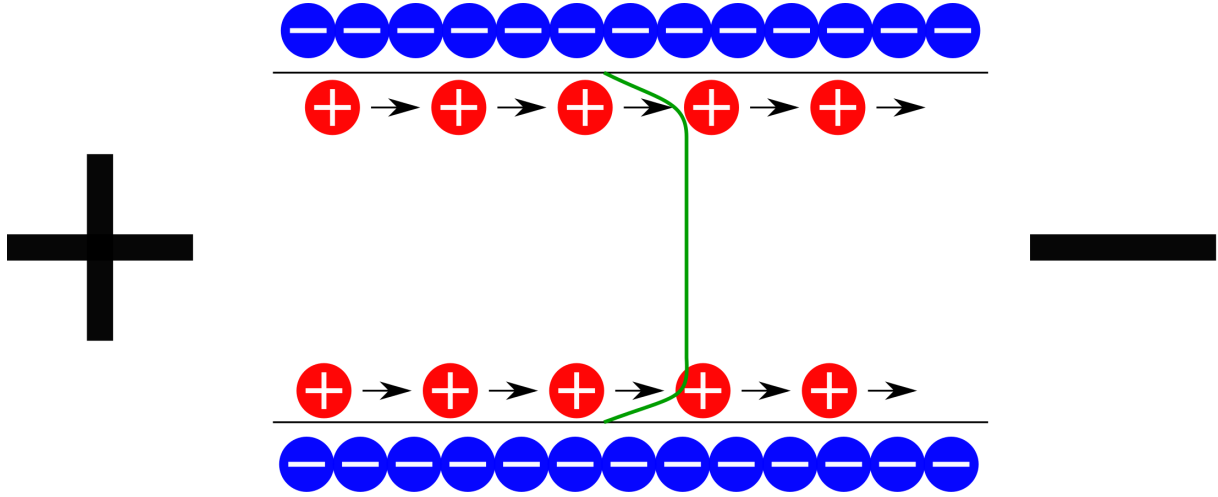


Figure 1.4: Electroosmotic Flow Schematic

Navier-Stokes Equation

The Navier-Stokes equation can be viewed as an application of Newton's second law ($F=ma$) to fluid motion, together with the assumption that the stress in the fluid is the sum of a diffusing viscous term (proportional to the gradient of velocity) and a pressure term. The density of the fluid is equivalent to the mass, and $\frac{dv}{dt} + (v \cdot \nabla)v$ is the acceleration. $\nabla \cdot \sigma$ is the shear stress and f is all other force.

$$\rho \left[\frac{dv}{dt} + (v \cdot \nabla)v \right] = \nabla \cdot \sigma + f \quad (1.3)$$

This can be rewritten as:

$$\rho \left[\frac{dv}{dt} + (v \cdot \nabla)v \right] = -\nabla p + \gamma \nabla^2 v + f \quad (1.4)$$

The divergence on velocity $((v \cdot \nabla)v)$ which describe how the divergence affects the velocity which is also called as convection. For instance when the channel is narrowing the velocity of the flow will be increased and when the channel is become wider the overall flow will become slower. However in an incompressible situation the divergence of the velocity becomes zero. Therefore equation 1.4 can be simplified as:

$$\rho \left[\frac{dv}{dt} \right] = -\nabla p + \gamma \nabla^2 v + f \quad (1.5)$$

In the case of electroosmotic flow the last term in equation 1.5, the force (f) represent as the electroosmotic body force and is equivalent to the product of the net charge density in the double layer ρ_e , multiplied by the gradient of the total potential (Ψ). It is also typical in electroosmotic flow that the channel is in micro or in even in nano meter range, where the Reynolds number ($Re = \frac{\rho l v}{\gamma}$) is low. Which result that the transient and

convective terms are neglectable. Neglecting the transient part implies that the system will reach the steady state instantaneously ($\frac{dv}{dt} = 0$). Also the pressure gradient can be eliminated since no additional pressure is applied to the system. Therefore equation 1.5 can be rewritten as:

$$0 = \gamma \nabla^2 v - \rho_e \Psi \nabla \quad (1.6)$$

The total potential is a summation of the electrical double layer and the applied electrical potential.

Helmholtz-Smoluchowski's equation

Assuming that the electrical double layer varies only in the direction normal to the surface the potential and the net charge density can be related as

$$\gamma \frac{d^2 v_x}{dy^2} - \epsilon_w \epsilon_o \frac{d^2 \Psi}{dy^2} E_x = 0 \quad (1.7)$$

where ϵ_o and ϵ_w are the dielectric permittivity of vacuum ($8.854 * 10^{-12} C/Vm$) and dielectric constant of the liquid respectively. Applying the condition when $y \rightarrow \infty$, then $\frac{dv_x}{dy} = 0$ and $\frac{d\Psi}{dy} = 0$, and that at $y = 0$, also considering the outside region of the double layer ($\Psi = 0$) yields,

$$v_{eo} = -\frac{\epsilon_w \epsilon_o \zeta}{\gamma} E_x \quad (1.8)$$

which describes the electroosmotic flow velocity. The proportionality coefficient between of the velocity (v_{eo}) and E_x is commonly used and referred to the electroosmotic mobility (μ_{eo})

$$\mu_{eo} = \frac{-\epsilon_w \epsilon_o \zeta}{\gamma} \quad (1.9)$$

1.2.3 Electrophoresis

Electrophoresis is one of the main techniques in separation science because it is not only a powerful technique but also a relative easy and inexpensive technique. The principle of electrophoresis is by applying a uniform electric field the particle will migrate [42][8].

Electrophoretic mobility

When the ions reaches a steady state velocity the accelerating force equals the friction force. The accelerating force is made by the electrical field which is proportion to the

effective electric field (q), and the field strength (E). The friction force is proportional to the velocity of the ion (v_{ep}) and the friction coefficient (ζ).

$$qE = \zeta v_{ep} \quad (1.10)$$

By dividing the friction coefficient in both side:

$$v_{ep} = \frac{q}{\zeta} E = \mu_{ep} E \quad (1.11)$$

The term in equation 1.11 is the eletrophoretic mobility of the ion, which is a constant. The friction coefficient is related to the hydrodynamic radius (r), the viscosity (γ).

$$\zeta = 6\pi\gamma r \quad (1.12)$$

Together with equation 1.11 and equation 1.12 the eletrophoretic mobility can be rewritten as

$$\mu_{ep} = \frac{q}{6\pi\gamma r} \quad (1.13)$$

The vector sum of the eletroosmotic mobility μ_{eof} and the eletrophoretic mobility (μ_{ep}) is known as the apparent mobility (μ_{app}).

Neutral ions will migrate in the same direction and velocity as eletroosmotic flow, cations and anions will separated based on their differences in their apparent mobilities. The total mobility for each ions cases can be given as

Neutral

$$\mu_{neutral} = \mu_{eof} \quad (1.14)$$

anions

$$\mu_{anion} = \mu_{eof} + \mu_{ep} \quad (1.15)$$

cations

$$\mu_{anion} = \mu_{eof} - \mu_{ep} \quad (1.16)$$

Figure 1.5 illustrate the electrophoresis for each of the ions charge. When the pH value is higher than 3, eletroosmotic flow is normally higher than the eletrophoretic flow, hence the all of the ions (anions, cations, and neutral) will move to the negative potential. However when the pH is lower than 3, the eletroosmotic flow becomes weak and therefore the anions will move to the positive potential.

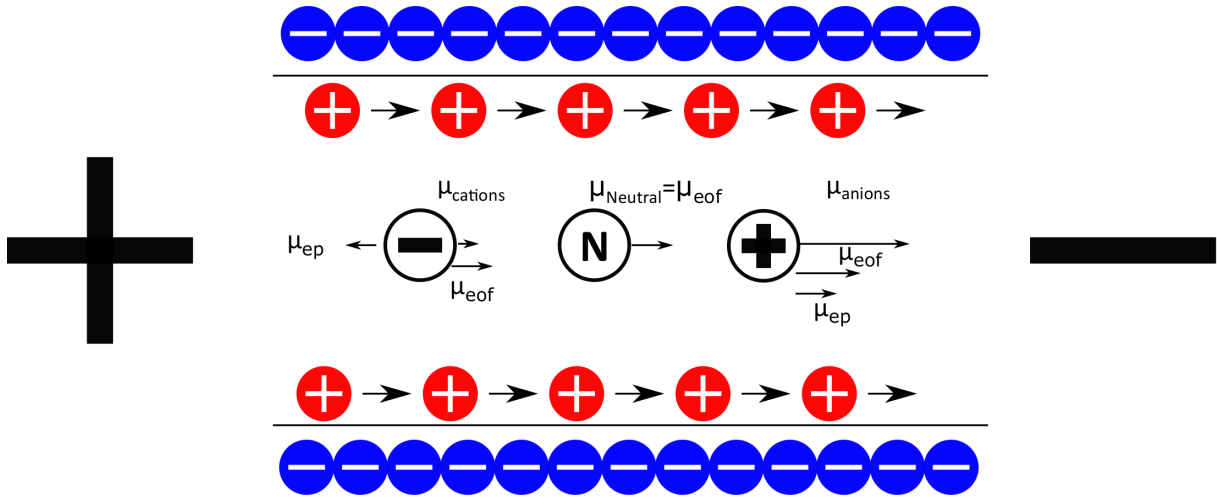


Figure 1.5: Schematic of electrophoresis

1.3 Isotachophoresis

Isotachophoresis (ITP) is one type of an electrophoresis, where the sample is placed between two different electrolytes, called leading and terminating buffer. The leading buffer contains the highest mobility ions while the terminating buffer contains the lowest mobility ions. The name isotachophoresis comes from Greek terms where, iso means equal, tacho means speed, and phoresis migration. Let consider a situation where you have a leading buffer (LB), two analytes (A,B) and a terminating buffer (TB) with a mobility given as $\mu_{LB} > \mu_A > \mu_B > \mu_{TB}$. The sample is injected in between of LB and TB as shown in 1.6A [2][15][44][9].

When the electric field is applied the ions will be first the ions will be separated according to their different migration velocity ($v_a = \mu_a \times E_{mix}$ and $v_b = \mu_b \times E_{mix}$). Since the mobility of analyte A is higher than B, A will be migrating out from the mixed zone to the leading buffer side and B will be moved out to the terminating buffer side (1.6B). When the separation is done so that the mixed zone (A+B) disappear a steady state is established which is called as the isotachophoretic condition (1.6C). When the system reaches the steady state, all of the ions move with a same velocity [21].

Based on a Kohlrausch regulation all zones reach a specific ion concentration. The Kohlrausch regulating function (KRF) is conservation law in electrophoresis which enables to calculate the concentrations of the ions. The potential drop in a capillary is related to the resistivity of the cross-sectional area. In the liquid domain the resistivity is defined through each ions charge (z), and concentration which given in the following equation :

$$\omega = \sum \frac{c_i z_i}{|\mu_i|} \quad (1.17)$$

Where Kohlrausch regulating value ω 1.17 remains constant because ions arrange ac-

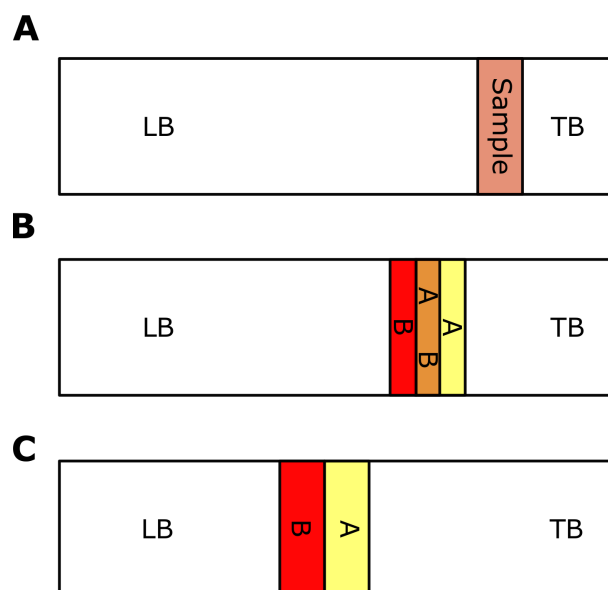


Figure 1.6: An Isotachophoretic Separation. (A) Before Applying electric field (B) Separation Commenced (C) Steady state

ording to their electrophoretic mobility (μ_i) and charge (z_i) by regulating their concentration (c_i). As this affects the current density, the electric field strength (E) in each zone is adjusted so that all zones move at an equal velocity, $v_i (v_i = \mu_i \times E)$. When dealing with samples containing compounds across a wide dynamic range in zone electrophoresis, analytes/interferences in high concentration broaden due to ion diffusion following Fick's law. In ITP, compounds outside the separation window dissipate in the LE or TE. Concentration differences within the window are evened out because high concentration compounds are diluted by lengthening their zone, low concentration compounds are concentrated by narrowing the zone.

The main advantage of ITP compare to the conventional electrophoresis is its immunity to band broadening. This phenomenon is called self-sharpening effect. It forces ions which diffused out of their band into a higher (or lower band) back into their original band. The specific ion concentration as well as the self-sharpening effect made the ITP an attractive option for miniaturized electrophoresis using microfluidics as it is capable concurrently focus and separate the sample [38] [16][36].

1.4 Miniaturization

The concept of miniaturization of analytical techniques has gain lot of interest in the past decade. This trend can be seen in various fields from the mechanical filed which focus on the novel micro fabricated structures such as in Microelectromechanical systems (MEMS). Together with the micro fabrication skills also new approached are done for the

use of this technology such as in Lab on a chip. Research into miniaturization is driven because of various advantages; 1) high throughput, 2) cost reduction, 3) less use of sample amount, 4) ability to make a handle device, and 5) automation etc. [23]. In 1982 silicon was suggested as a substrate for fabrication of micromechanical devices. This was quickly adapted to the microelectromechanical systems (MEMS) with the photolithography and the etching methods [5]. Microfluidic is essentially based on this approach [40], however because of the incompatibility with the high voltage, and also the non-transparency glass or quartz material became more preferred [22]. The introduction of Polydimethylsiloxane (PDMS) [43][54] for soft lithography obtains lots of interested, since it has the advantage of being cheap, transparent, non-toxic. However, one of the biggest problems of PDMS is that the surface is hydrophobic, therefore much effort has been focused on controlling the surface of PDMS [41]. Another common material for microfluidic chip fabrication is polymethylmethacrylate (PMMA) which usually fabricated by hot embossing [34].

1.4.1 On hips capillary electrophoresis

The structure of the Microfluidic chips are based on small platforms comprising channel system which are connected to various features such as reservoir, chamber, mixing region etc. The size of these structures is typically in the range of a few micrometers. Microfluidic chip is used in various areas one of the application of it is electrophoresis and related techniques (2-4). Beside the advantage that the amount of sample volume is reduced, the combination of microfluidic and electrophoresis has additional advantages [8][?]. The number of theoretical plates represents the efficiency and resolution of electrophoresis 1.11.

$$N = CA \quad (1.18)$$

where N is the plate number and micro is the apparent mobility and D is the diffusion coefficient. A higher plate number means a better efficiency and resolution. As it can be seen in the equation in order to increase the plate number the only parameter that we can change is the voltage. However by increasing the voltage will result to increase the temperature because of joule heating 1.19.

$$P = IV = I^2R = \frac{V^2}{R} \quad (1.19)$$

where P is the power which converted from electrical energy to thermal energy I is the current, V is the applied voltage and R is the resistance from the buffer. This temperature increase will result a non-uniform temperature gradient across the capillary, lower temperature at the wall than in the middle of capillary. Since the electrophoretic mobility is also temperature dependent this variation of temperature will also result variation of

the electrophoretic mobility across the capillary which eventually means loss of resolution. The production of heat in capillary electrophoresis inevitable since electrophoresis needs a voltage across the capillary. However, using narrow-diameter capillaries improves the situation based on two reasons. The resulting thermal gradient is proportional to the square of the diameter of the capillary as shown in equation 1.20.

$$\nabla T = 0.24 \frac{Wr^2}{4K} \quad (1.20)$$

Where W is the power, r is the capillary radius, and K is the thermal conductivity. Therefore the reduction of the capillary radius will result less thermal gradient. The second problem is ineffective heat dissipation. Narrow-diameter capillaries also help heat dissipation, which can be additionally improved by effective cooling.

1.4.2 Free-flow electrophoresis

Free-flow-electrophoresis techniques are used for continuous electrophoretic separations by applying an electric field perpendicular to the buffer and sample flows [33]. The schematic and conceptual drawing is shown in 1.7. A pressure driven flow is induced from the inlet side while an electric field is applied. The main advantage of free-flow electrophoresis compare to the capillary electrophoresis (CE) is that the separation domain is orthogonal to the flow domain. Which result a continuous separation of the analytes which can be easily collected, where CE gives a discontinuous output. Large scale FFE was first introduced in the 1960s [18]. Since 1994 several microfluidic FFE were developed with the benefit of low sample volume (nL to μ L). Also the separation time is reduced from minutes to seconds by reducing the size according to the scaling laws [37]. Furthermore the smaller separation chamber reduces the joule heating problem which allows applying a higher electric field [23].

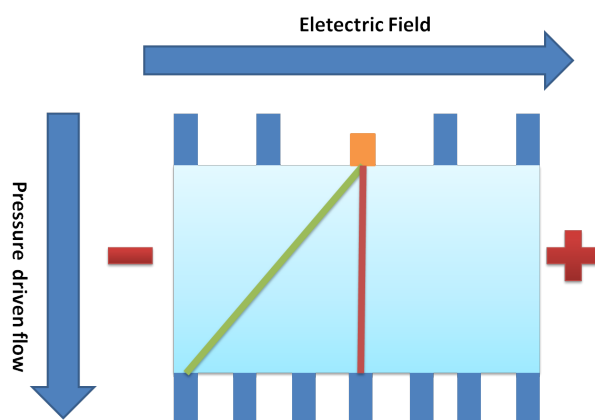


Figure 1.7: Conceptual drawing of free flow electrophoresis where a perpendicular electric field is applied to the pressure driven flow

So far different materials for FFE miniaturized chips were employed. The first chip [47] was fabricated from a silicon substrate with a channel depth of 50 μm . This silicon chip was anodically bonded to a glass cover. The decrease dissipation of Joule heat and theoretical band broadening effect were studied. However using a silicon substrate limited the effectiveness of the device due to problems with electrical isolation of the substrate and thus limited maximum applied voltage. Alternatively the polydimethylsiloxane (PDMS) was used to replace silicon as the substrate to eliminate the electrical breakdown of silicon insulating material [55]. The device had channels with depth of 10 μm . Unfortunately, the weak bonding of PDMS and glass and the elasticity of PDMS hindered the device to use a high flow rate. To solve this problem various type of glass chip was suggested [13][7][32][29][26][31][25][6][30].

1.5 Detection methods

FFE has an advantage that the separation is continuously done as described above, however observing the process is relatively difficult especially when it comes to online detection. The most common method is detecting the process optically in this chapter we will discuss about the optical method and also mass spectrometry.

1.5.1 Optical detection

Optical detection is usually done with instruments which include UV absorbance and fluorescence detectors. One of the most common instruments for optical detection is a fluorescence microscope. The principle of the fluorescence microscope is illuminating a fluorescent dye with a specific wavelength (excitation wavelength). The excitation light is absorbed by the fluorophores and emits a light in a longer wavelength (emission wavelength). 1.8 shows a schematic view of a common fluorescence microscope where a LED is used for the excitation light source, a dichroic mirror is used to guide the excitation light to the sample. The target sample will then produce the emission light which will be grant to the lens and finally of the detector. Even though optical detection is one of the most simple and common way to detect the sample it is lacked due to the need of an optical dye. Therefore a more efficient method is required.

1.5.2 Electrospray Ionization Mass Spectrometry (ESI-MS)

Electrospray Ionization Mass Spectrometry (ESI-MS) is an important technique which can provide the structure, the molecular mass, and the concentration of analyze molecules. The process of the ESI-MS is that the molecules first enter the ionization source where the molecules become ionized. These ionized molecules (ion) will travel through the mass

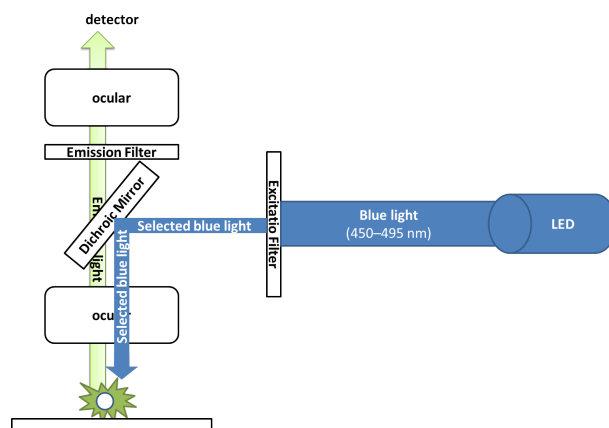


Figure 1.8: Conceptual drawing of free flow electrophoresis where a perpendicular electric field is applied to the pressure driven flow

analyzer and finally arrive at a detector. After arriving at the detector a computer system will generate a mass spectrum which shows the abundance of the relative mass to charge (m/z) ratio. Each of the components will be describe in detail in the following chapters.

Electro spray ionization

The ESI consist of three steps starting with spraying of fine droplets which are charged, followed by solvent evaporation and finally ion ejection. 1.9 shows the process in detail were the tube is made of stainless steel or quartz silica capillary. A voltage of 2.5-6.0 kV is applied to the tube which charge droplets with the same polarity. The highly charged droplets will fly to the MS inlets size which has the opposite charge of the droplets. With the aid of Nitrogen and heat the charged droplets are reducing their size by evaporating. This will reduction of size will increase the surface charge density and finally when the electric field strength inside the charge droplets reaches the critical point the droplet will be changed to a gaseous phase [10][11][48]

Mass analyzer

A quadrupole mass analyzer is commonly used which consist of four parallel metal bars which is kept in equal distance. The two metal bars which are located horizontally (1.10) has a DC voltage where the AC voltage is applied to the vertical bars. The DC voltage is used for keeping the ions flying to the z-direction where the AC voltage making an oscillation motion. The principal mechanism of the mass analyzer is that the movement of ions is an electric field is determined by their m/z ratio. With this principle the DC and AC voltages can be set so that only desired m/z ratios are able to become stable which will be lead to the detector and the other ions will collapse with metal bar which has a high temperature.

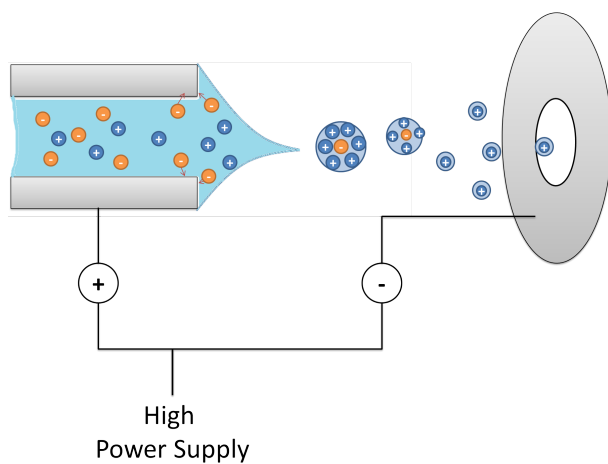


Figure 1.9: Conceptual drawing of free flow electrophoresis where a perpendicular electric field is applied to the pressure driven flow

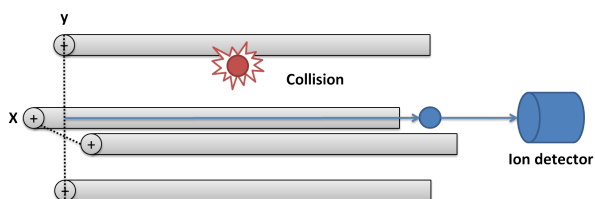


Figure 1.10: Conceptual drawing of free flow electrophoresis where a perpendicular electric field is applied to the pressure driven flow

Chapter 2

Fabrication

2.1 Glass chip fabrication

As described in the previous chapter microfluidic consist of small channels or structure which has a dimension in micrometer or even nanometer region. In order to realize this kind of structures microfabrication techniques are used which comes originally for semi-conductor fabrication methods. This technique in general consist of two big process which photolithography and etching. In the fabrication process of the glass device will be described also for more detail parameter please see also table 1.

2.1.1 Gold and chrome sputtering

The wafer was first sputtered with gold and chrome as shown in 2.1. This process is needed since after the photolithography process the wafer will be put inside HF in order to etch the glass wafer. Even though a so called photoresist which will describe in more detail in the following chapters was used to protect the part which we did not want to etch this process will be ensure that the glass wafer is protected since gold is not possible to etch through HF. The chrome layer was required in order to make the gold layer adhesive to the glass layer.

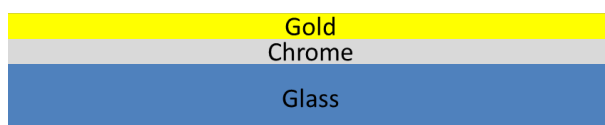


Figure 2.1: Gold and chrome sputtering

2.1.2 Spin coating of photoresist

This process was required to put a thin photoresist layer on the gold layer. The principle method was to put a small amount of the photoresist (Olin Oir 907-17) and then rotated the wafer with a speed of 4000 rpm for 30 second. To improve the adhesion and remove the solvent the glass wafer was heated at a temperature of 90 degree for 90 second, this process is called soft backing (2.2).

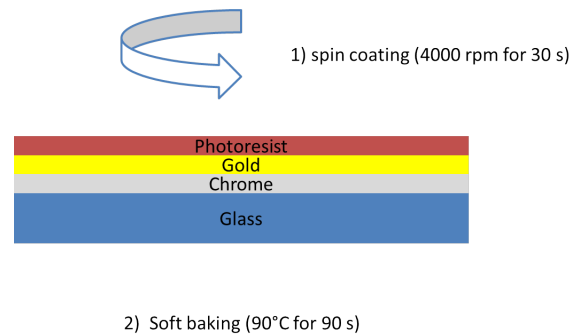


Figure 2.2: Spin coating of photoresist

2.1.3 Exposure of the photoresist

After the photoresist was spin coated on the wafer UV light was exposure to the wafer. The UV light will react with the photoresist so that the photoresist can be developed with a chemical which is called a developer. In order to protect the part where the UV light should not reach a mask is used. The mask can be made from various software such as AutoCAD, solid works, cadence, etc. 2.3 shows the conceptual drawing of the process and also a photomask which was generated by cadence.

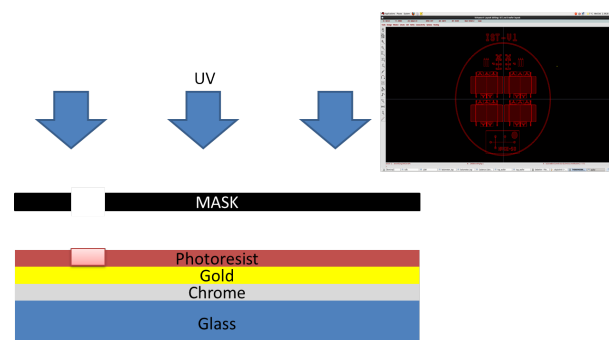


Figure 2.3: Exposure of the photoresist and cadence desing

2.1.4 Development of the pattern

The exposed plate put in a developer solution (OPD4262) so that the reacted photoresist can be removed as shown in 2.4. After the developing of the photoresist the other etchant can reach the surface and can be etched (see appendix A for more detail parameter).

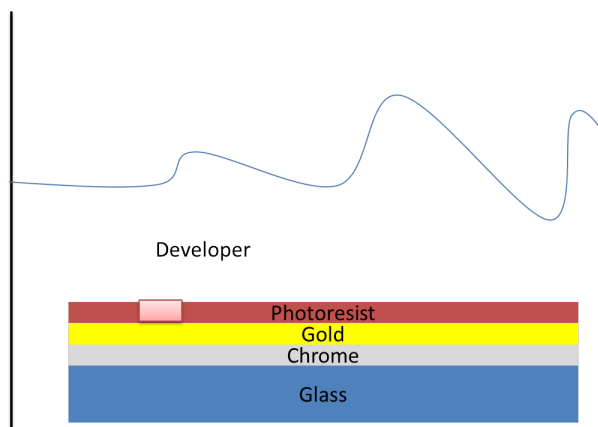


Figure 2.4: Development of the pattern

2.1.5 Wet etching

After developing the photoresist the wafer should be etched each layer starting with the gold layer (See 2.5A). The gold etchant was made of $KI : I_2 : DI = (4 : 1 : 40)$, this process will take until it was possible to see the chrome layer which has a gray color. When the gold layer was etched away the wafer is rinsed with Distilled water (DI) and the dried with a nitrogen gun. After cleaning the wafer was again put in the chrome etchant and wait until the glass surface was able to observe (See2.5B). When the wafer became transparent then the cleaning process was done as above and finally the wafer was put in HF/HCl 25percent/2.5percent. The etch rate of 25 percent HF is $1\mu m$. therefore the wafer was let in HF for 5 min to have a structure depth of $5\mu m$. One important thing that needs to be in mind is that wet etching is not only one directional but etching in all direction as shown in 2.5C. Therefore it is not possible in wet etching to have a width smaller than the height of the structure which has to consider in the designing process.

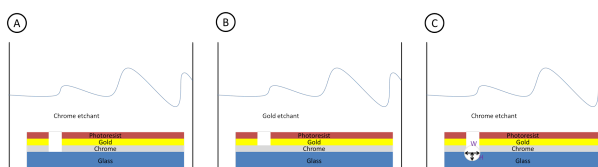


Figure 2.5: Wet etching. Where (A) is chrome etching, (A) is gold etching, and (A) is glass etching

2.1.6 Removal of the photoresist and Gold/Chrome layers

When the etching process is done and also the wafer is cleaned the wafer was put in acetone in order to remove the photoresist of the wafer. Then the wafer was put in the gold etchant and chrome etchant until only the pure glass wafer was left. 2.6 shows this process where a also in figure2.6 is showing the wafer after removing the photoresist of the wafer.

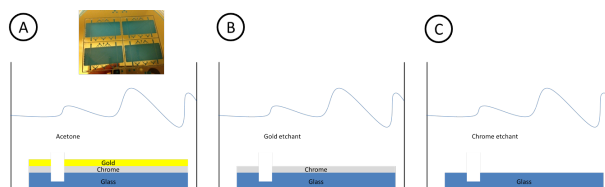


Figure 2.6: Removal of the photoresist(A), Gold(B). and Chrome(C) layers

2.1.7 Making inlets

Since the microfluidic chip needs inlet so that the fluidic can enter the chip, inlets should be made at the glass wafer. Several method are possible to make an inlets, we have used making holes at the glass wafer. This process seems very simple however making a hole in a glass wafer was not as simple as we have imaged. Therefore several approaches were done to overcome this problem.

Drilling

The first approach was simply drilling the holes by assisting a diamond drill bit. 2.7A shows the conceptual Idea of this process. The glass wafer was mounted on a table which was assembled with a stepper motor so that the table was able to move up and down. On the top of the table the diamond drill bit was mounted to a driller. 2.7B shows the setup in real, where the chip was mounted at the chip holder and the diamond drill bit was mounted on the driller.

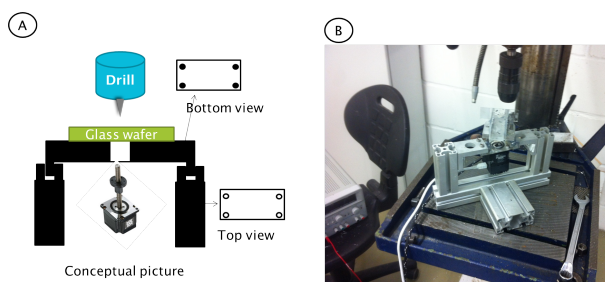


Figure 2.7: Drilling with a drill machine

This approach did give some promising result however it was very time consuming since for every single hole the user had to align the holes. Therefore with a similar concept a CNC machine as shown in 2.8 was used except of the drilling set. The CNC machine did reduce the time since the glass wafer had to be aligned only once however the number of successful result was very low which means that the wafer was broken during this process. This is because that from average after drilling 10 holes the drill bit has to be changed and the wafer was consisting at least 60 holes. This was a big problem not only it will take a lot of time but also it was expensive since the drill bit cost around 100 euros.

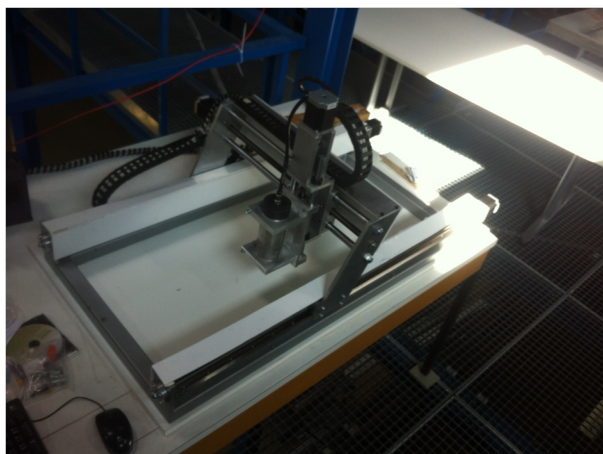


Figure 2.8: Drilling with a CNC machine

Etching

Another attempt was to etch the holes, since the inlets have a diameter of 1 mm and the wafer was 500 micro meter deep. The concept of this process was instead of making holes in the same wafer but making holes at the second wafer and then bond these wafer together as shown in 2.9.

The process of making the holes from the second layer is described as in 2.10. To protect the other side of the wafer, it was spin coated with the photoresist in both side and then it was developed and etched. Unfortunately, however this process was not able to realize because we were never able to etch the entire wafer through.

Powder blasting

Another approach was powder blasting the wafer. Here once again a photoresist film was used in this to protect the wafer from powder blasting. The whole process is shown in 2.11 where the photoresist film was first attached to the back side of the wafer and exposure (2.11A), then it was developed (2.11B). After developing the film 30 micro meters (Al_2O_3)

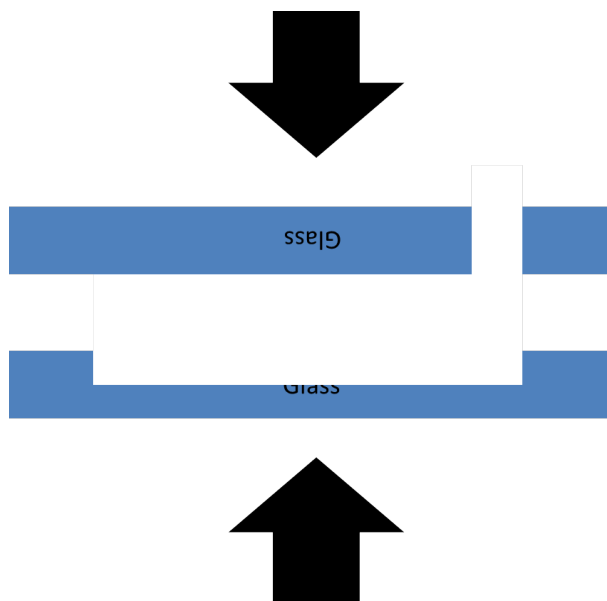


Figure 2.9: Making inlets by etching

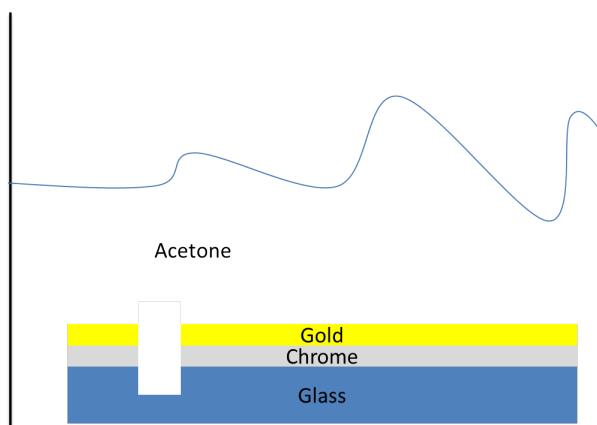


Figure 2.10: Etching procedure

particle was blasted to the wafer to make the holes (2.11C). 2.11D shows the result of this process where the inlet holes are able to be observed.

2.1.8 Bonding and dicing

The next process is sealing the microfluidic structure which is done by bonding the glass wafer to another glass wafer. This process was done by applying a temperature while pressing the two wafers together (see also table 1). The final step is dicing the chips out of the wafer which was done by a dicing machine see appendix.

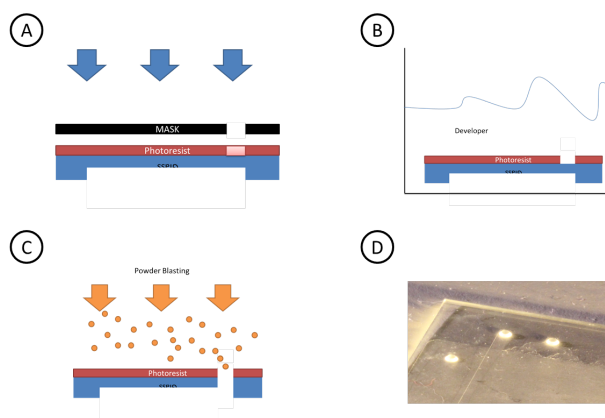


Figure 2.11: Making inlets by etching with photoresist

2.2 Connector mounting

Bootlace ferrules (OD: 1 mm, height: 8 mm, Bauhaus, Germany) was used as an interface to connect the Teflon tubing to the FFITP device. The ferrules were simply bonded to the glass surface by an epoxy, here the detail process is explained. First the FFITP device is cleaned with nitrogen gun to blow small particles and also to ensure that the device is complete dry. UHU PLUS Endfest 300 was used for the epoxy since it promised a good bonding strength between glass and metal. The UHU PLUS consists of two mixing solutions. Therefore the component was mixed with a 1:1 ratio as shown in 2.12.

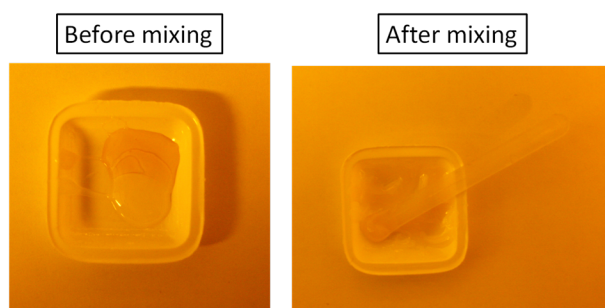


Figure 2.12: Connector bonding 1

The FFITP device is then put to a hot plate with 120 degrees, a silicon wafer was used to protect that the hotplate is contaminated through the epoxy. The ferrules were then carefully put at the inlets of the FFITP device as shown in 2.13. Here, because of particle issue the ferrules were out from one side to the other side.

Then a small amount of UHU plus 300 was put at the outer side of the ferrules and cure for 10 minutes in temperature of 120°C, to keep them stable (2.14). This process is required because the epoxy has very low viscosity when a temperature is applied. Therefore there exist high possibilities that the epoxy will flow into the other inlets where the ferrules do not exist.

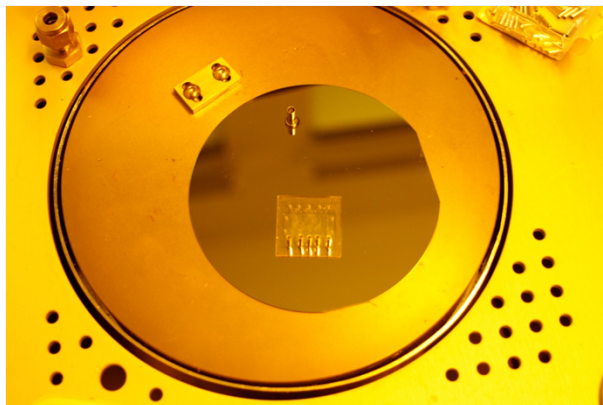


Figure 2.13: Connenctor bonding 2

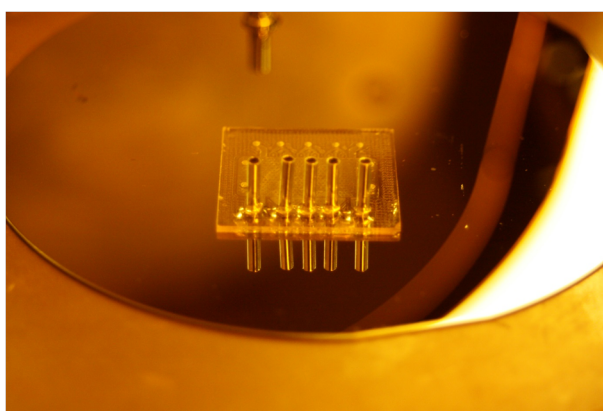


Figure 2.14: Connenctor bonding 3

This process was also repeated to the other inlets, and when all of the ferrules were stabilized on the device, UHU plus 300 was again used to seal any possible leakage from the inlets as shown in 2.15. Here once again the curing time was 10 minutes and the temperature was 120 degree. After the whole process was done, the chip was rested in room temperature for at least 2 hours.

2.3 Cleaning protocol

After the device was used the FFITP device needs to be cleaned. The cleaning method is provided in detail in this chapter. First the FFITP device was put in beaker with isopropanol and distilled water with a ratio of 2 : 10 as shown in 2.16.

In order to wash the chip also inside the chip was put in a sonicator for 2 hours with a temperature of 80 degree. The temperature was also needed not only to clean the chip but also to remove the ferrules from the FFITP device. After the sonication the ferrules will be removed from the chip as shown in 2.17.

When the ferrules were removed from the chip then nitrogen was applied to the FFITP

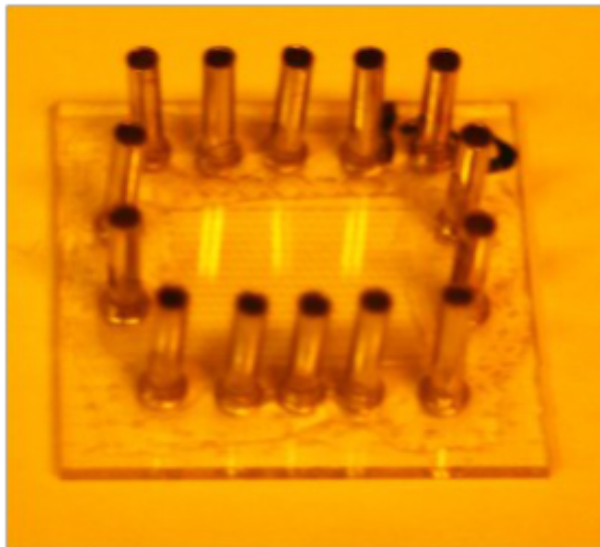


Figure 2.15: Connector bonding 4



Figure 2.16: Cleaning 1



Figure 2.17: Cleaning 2

device. This process was required to push all the residues inside the chip, however this process need a lot of caution since when a too high pressure is applied the chip will be

break. Therefore it is recommend not using the full power of the nitrogen gun and also keeping slight distance from the device as shown in 2.18.

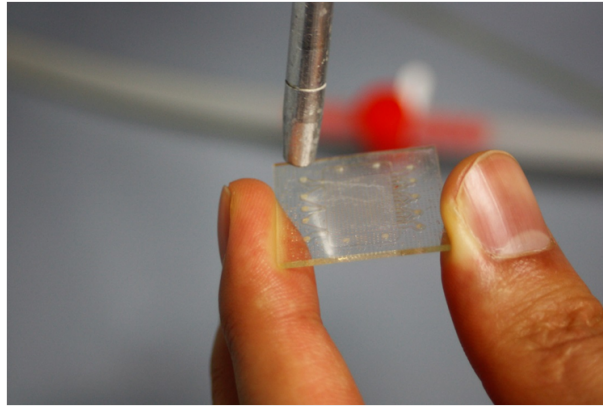


Figure 2.18: Cleaning 3

After applying nitrogen to the device the chip was put again in the isopropanol and water solution and was sonicated for 30 min in temperature of 80 degree. This process together with the nitrogen cleaning process was repeated twice more and then rinse the chip with kimtex paper as shown in ??.



Figure 2.19: Cleaning 4

In order to ensure that the device does not have any residues inside the chip was put in a vacuum chamber (see ??) with 0.2 bars for 1 hour. Finally the chip was put in an oven with a temperature of 400 degree for 6 hours to be complete sure that there are no residues inside. This process can be also used when the epoxy goes inside the inlets by accident. After the whole cleaning process the chip will be cleaned as shown in ??.



Figure 2.20: Cleaning 5

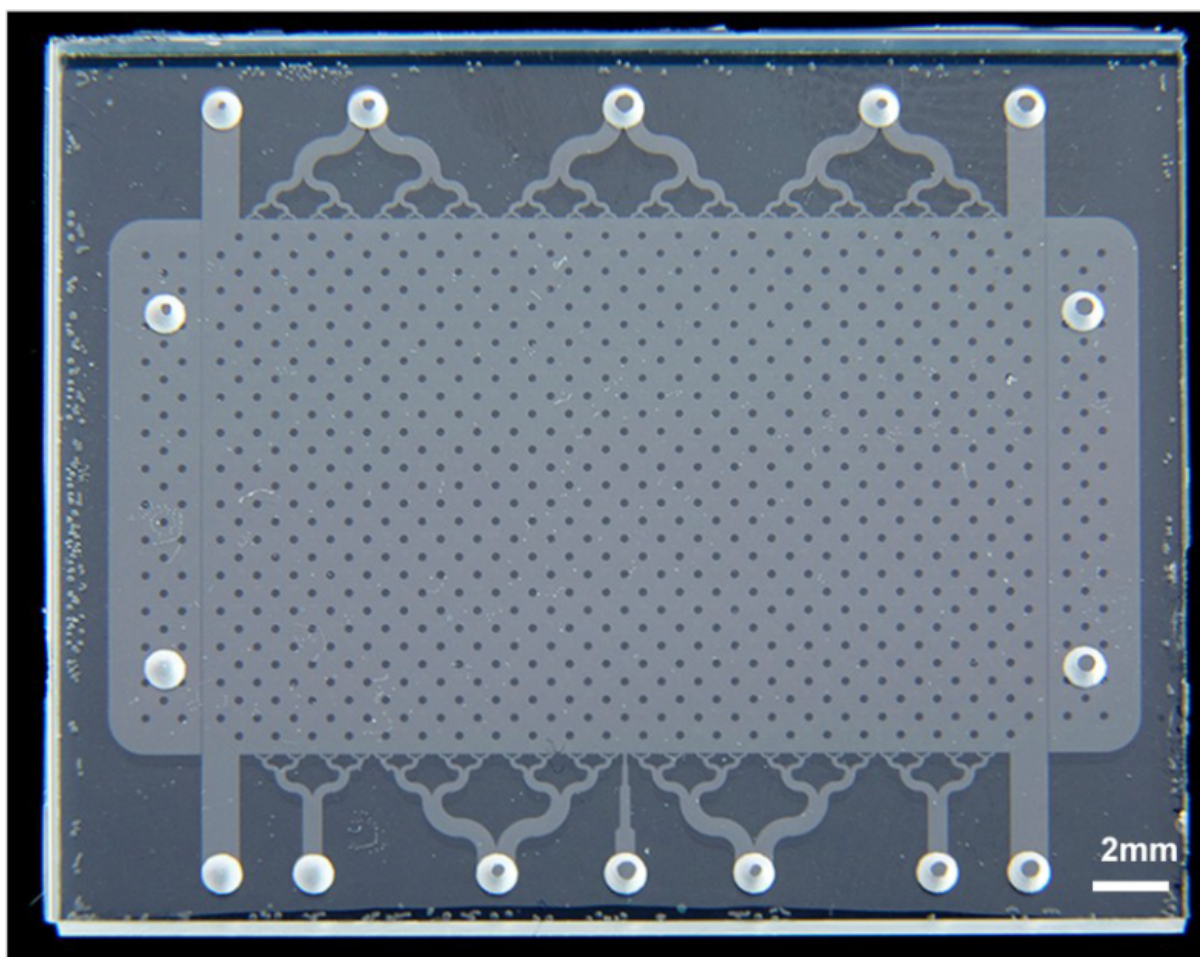


Figure 2.21: Cleaning 6

Chapter 3

Isotachophoresis free-flow on a glass chip using side flow for selectable output

3.1 Introduction

ITP is a powerful mode of electrophoresis, which allows simultaneously preconcentration and separation of samples. Free-flow electrophoresis (FFE) is a method used for continuous separation. The combination of FFE and ITP allows us to have a continuous preconcentrated and separated sample which can be used for real time online detection. The combination of ITP and FFE was first suggested in 2006 [24]. Conventional ITP has all separated bands flowing next to each other making their optical detection as well as collection of a specific band a challenging task [45][20][27]. Collecting a specific band after the separation of the sample is commonly done by sample shifting. Sample shifting means that the focused ITP stream is moving by the changing the flow ratio [3]. One of the method to shift the ITP window is using the electric field as shifting force [28][4]. The device consist three inlets where the middle inlet is used for sample injection, the out side two inlets is made also for applying an electric field to the device. By changing the voltage at the inlet side of the device, the sample was guided to the desired location. However this method has some limititations, such as precise control is not posible and also the range of the shifting is small. In order to overcome this problems our FFITP glass device use hydrodynamic flow control to shift the sample to the desired location. Three possible method were tested and compared, which was using an additional flow at the outlet of the device, using negative pressure (suction) at the outlet, and changing the flow rate at the inlet. Also to optimize and to know the relationship between concentration change based on the electric field and the flow rate optical detection was uesd with an optical microscope and also with a photomultiplier tube (PMT) to observe the distribution and

concentration of the device.

3.2 Experimental

3.2.1 Chemicals

All buffers were prepared using deionized water with final pH of 9. The leading buffer was made from 10 mM NaCl solution mixed with tris(hydroxymethyl) aminomethane (TRIS) buffer for pH adjustment. The terminating buffer was made from 5 mM solution of 2-[4-(2-hydroxyethyl)-1-piperazinyl]-ethanosulphonic acid (HEPES) mixed with TRIS. The sample for testing was prepared by adding 0.1 mM solution of fluorescein into the terminating buffer. All chemicals were purchased from Sigma Aldrich GmbH.

3.2.2 Device layout

The layout of the device is shown in 3.1 (left). Arrays of pillars prevented the chamber collapsing during the thermal bonding process. The device consisted of five inlets (I), a separation (*main*) chamber with the size of $23\text{mm} \times 15\text{mm}$, two side chambers for connecting the electrodes and seven outlets (O). Three middle inlets were equipped with binary tree structures to evenly distribute input solutions into the chamber. The outer two inlets (I_1 and I_5) were designed to guide the flow direction into the chamber. All outlets were designed similarly as the inlets except the middle one (O_4) which has narrow entrance for sample collection. The side chambers are separated from the main chamber by $25\mu\text{m}$ wide channels to prevent gas bubbles entering the main chamber. The side channels and the pillars (3.1). Reservoirs were also used for connecting the electrodes, as well as to reduce the pH change inside the chamber. 3.1 right bottom shows the side reservoir and the connectors which are used for connecting the syringes.

3.2.3 Optical setup

The chip was mounted on an Axiovert 100 (Zeiss, GmbH) inverted microscope. We have used LED type M470L3 (Thorlabs, GmbH) with 470 nm principal wavelength and maximum optical power of 650 mW for sample illumination. For all fluorescence imaging and measurement experiments we have used a filter set model 49002 (Chroma Technology Corp.). Imaging was performed with $5\times$ objective lens and with color CCD camera model C5 (Jenoptik, GmbH). The LED intensity was adjusted by 1600 mA electrical current. The concentration measurement was performed as single point detection with $50\times$ objective lens and with a photomultiplier tube (PMT) model H10722-01 (Hamamatsu, Co.). Its gain was set by 0.5 V bias. The LED intensity was adjusted by 16 mA electrical current.

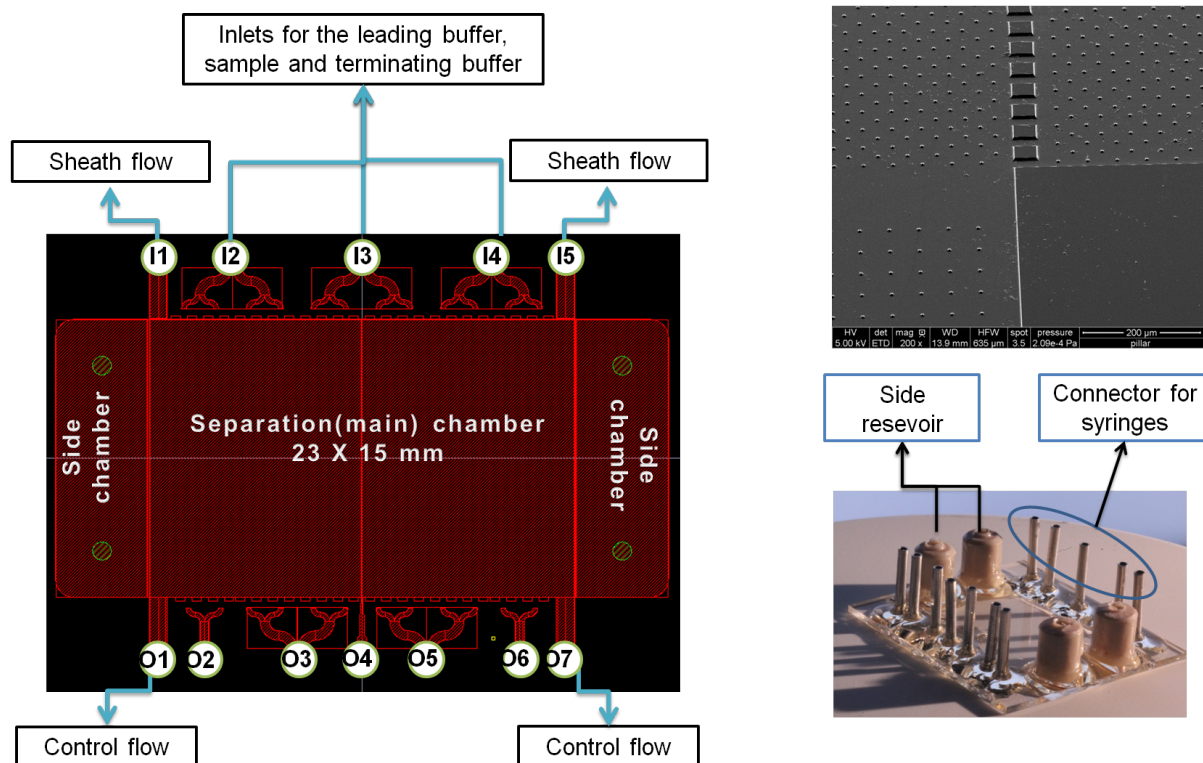


Figure 3.1: Chip schematic showing all chambers. The side chambers are separated from the main chamber by $25\mu m$ wide channels and pillars were used in order to avoid collapse during thermal bonding which is shown by an SEM picture left top. Connections for the syringes and the side reservoirs which are used to connect the electrodes are shown at the left bottom figure.

3.2.4 Experimental procedure

The experiment consisted of four steps: filling, steady-state laminar flow, applying separation voltage, hydrodynamic control. The chip was first filled with the terminating and leading buffers. The leading buffer was introduced by inlets I_1 and I_2 and the terminating buffer by inlets I_4 and I_5 , all with flow rate of $10\ \mu L/min$. First the chamber was filled with buffers which also contained air bubbles. It was impossible to push the bubbles out by external positive pressure. A negative pressure at the outlets was then applied to remove those bubbles. Once the main chamber and side reservoirs were filled the electrodes were introduced into the side chamber and sealed. Then the sample was introduced and all flow rates adjusted to $5\ \mu L/min$. Once the laminar flow was achieved $+100\ V$ was applied to the leading buffer and $-100\ V$ to the terminating buffer. 3.2A shows the steady state situation before applying the voltage, and 3.2B shows the fluorescein focused after applying the separation voltage.

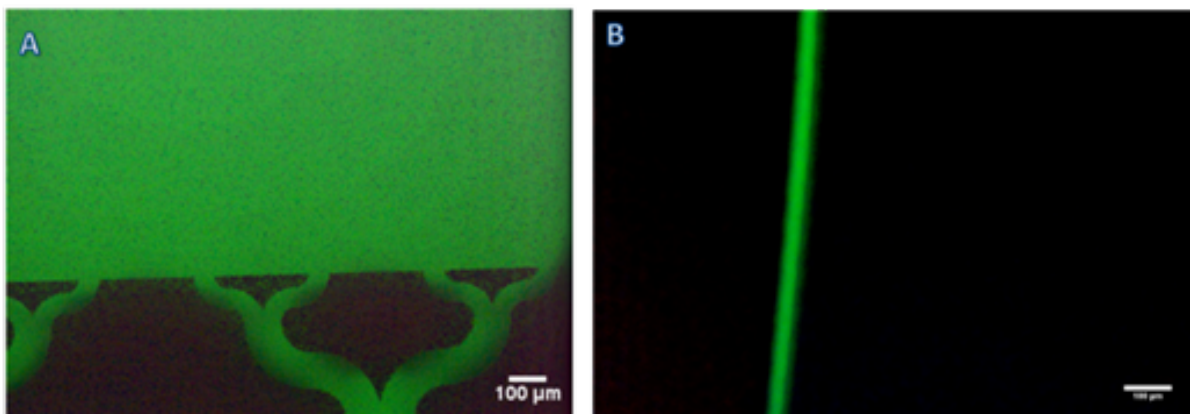


Figure 3.2: (A) Laminar flow before applying the separation voltage (B) Focused stream line of fluorescein with 200V separation voltage.

3.3 Result and discussion

3.3.1 FFITP concentration factors

The concentration of ITP will be happen at the isoelectric point (PI) which means the charged particles which are not at the point should move toward the point. The velocity of the charged particle is proportional to the applied electric field; $v = \mu_e \times E$ where v is the drift velocity μ_e is the electrophoretic mobility and E is the electric field. In FFITP it could happen that the applied electric filed is not high enough so that not all of the charged particle reaches the PI point. Since there is not enough time given before the particles is leaving the chip. Therefore PMT observation was done to check the change of the concentration, while changing the voltage with a flow rate of $5 \mu L/min$. 3.3 shows the concentration change while increasing the voltage. It could be observed a linear increase of concentration till the 600 V and no more increase after this point. When the voltage was higher than 2000 V bubble generation was able to observe. It could be caused by either extensive buffer electrolysis or Joule heat dissipation.

Next we have tested the system with flow rate as a parameter. As discussed in the former chapter the concentration of ITP has a relation with the time until the charged particle are drift to the PI point. Therefore if we give more time inside the separation chamber it is possible that the concentration will increase. In order to verify this principle an experiment was done where a constant electric field was applied and the flow rate was increased. As expected the intensity of fluorescein decrease when the flow rate was increased (see 3.4). As the expectation it could be observed that the fluorescein intensity was decreasing when the flow rate was increasing also a exponential graph was able to observe which also fit with the result of the voltage increase.

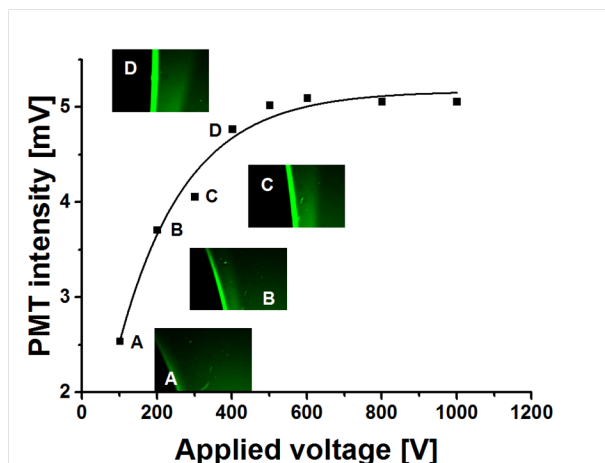


Figure 3.3: PMT output signal as function of applied voltage with a constant flow rate of $5 \mu\text{L}/\text{min}$. It could be observed that the concentration of the fluorescein is increased by applying a higher

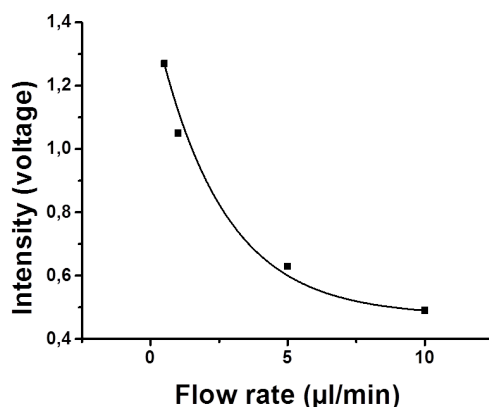


Figure 3.4: PMT output signal change by a constant voltage (100 V) and increasing the flow rate. It could be observed that the fluorescein concentration is decreasing by increasing the flow rate.

3.3.2 Hydrodynamic flow control

One of the key features of the FFITP chip design was the possibility to collect specific fractions at one of the outlets. Three possible method was studied (see 3.5). First applying a positive pressure at the outlets O_1 and O_7 . Second applying a negative pressure at the outlet O_1 and O_7 by suction. Last increasing the flow rate at the at inlets I_1 and I_7 . Each of the method was compared, based on two parameters the settling time and the preciseness to move the focused stream line. The settling time means the needed time until the focused stream line is not moving further.

Applying positive pressure at outlet

This method was done by introducing a flow to the outlet O_1 and O_7 . The FFITP settling

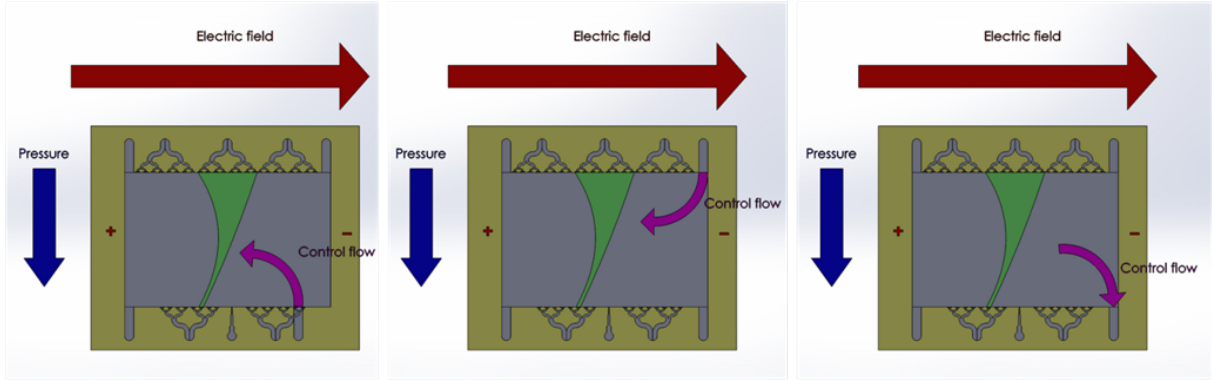


Figure 3.5: : Schematic operation of the ITP device. By applying an electric field perpendicular to the flow direction, the sample will be focused. This focused stream can be control by applying an additional flow which is called as control flow. Three possibilities is considered for the control flow; applying positive pressure from the outlet, applying positive pressure from the inlet and applying negative pressure from the outlet.

time was below 30 second and we were able to achieve precise control of the focused line. Nevertheless the pressure inside the chamber was often too high leading to the chamber destruction. It was probably caused by high pressure drop at the fluid outlet channel, which can be calculated by Hagen-Poiseuille equation (3.1).

$$\Delta P = \frac{12 \times \mu \times l \times Q}{h^3 \times w} \quad (3.1)$$

where ΔP is pressure drop, l is length of the channel, μ is dynamic viscosity of the fluid, Q is volumetric flow rate, h and w are the height and the width of the channel, respectively. For the calculation purpose we assumed a simple straight channel with length of 4 mm and width of 1 mm. The channel depth was left at $5 \mu m$. Total applied volumetric flow inside the chamber was $25 \mu l/min$ (5 inlets in parallel each with a flow rate of $5 \mu l/min$) with all outlets opened. With those assumptions the calculated pressure drop at the outlet channels and thus also pressure inside the chamber was 0.24 bar. Once the outlets O_1 and O_7 are used for flow control with positive pressure, the pressure inside the chamber rose to 0.395 bar, far too high for glass chip integrity.

Applying negative pressure at outlet

Second option to control the focused line is applying a negative pressure to the outlets O_1 and O_7 . Suction was used to realise this method. By changing the suction speed of the syringe pump the focused stream was controlled to the desired location. Since no further pressure were applied no destruction was able to observe during the process. However a very long settling time (3 min) was required, and also it had also a precision control below $100 \mu m$ was no possible.

Applying positive pressure at inlet

The mechanism of this method is to increase the flow rate either from I_1 or I_7 to control the focused line. In order to achieve the exact relationship of the flow ratio change and the shifted streamline, simulations were conducted using FreeFEM++28 simulation software using a slight simplification of the design (3.6).

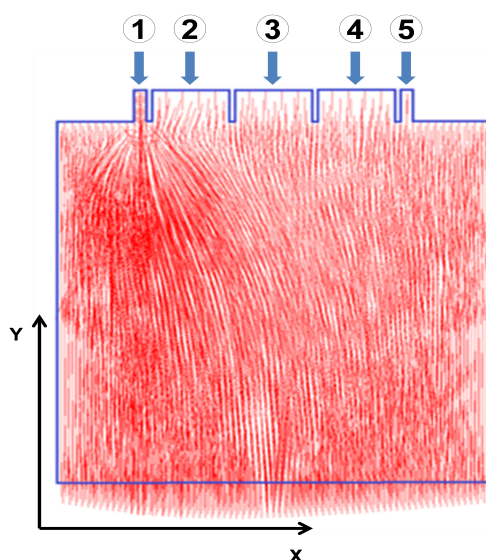


Figure 3.6: Simplified drawing of the device showing the velocity vectors. For shifting the stream, the flow rate at inlet 1 was increased.

The Stokes differential equation for an incompressible Newtonian fluid was solved, with boundary conditions set by flow velocities in both directions at all surfaces. Grid resolution was tested by decreasing the grid size by a factor of two, accepting the resolution if the difference in flow shift was less than 5 percent. An example of an obtained flow pattern is shown in 3.6. In 3.7, the x-component of the velocity is given for a change in flow rate at inlet 1 from 5 to 6 $\mu\text{l}/\text{min}$ by 0.1 $\mu\text{l}/\text{min}$ increments, reducing the flow rate through inlet 5 from 5 to 4 $\mu\text{l}/\text{min}$ to maintain a constant total flow rate of 10 $\mu\text{l}/\text{min}$. The outlet position for the sample stream line is defined at the point where the x-component of the velocity is zero, and shows a trend towards the right with an increase in flow rate from inlet 1. The measured displacement is plotted as a function of the flow

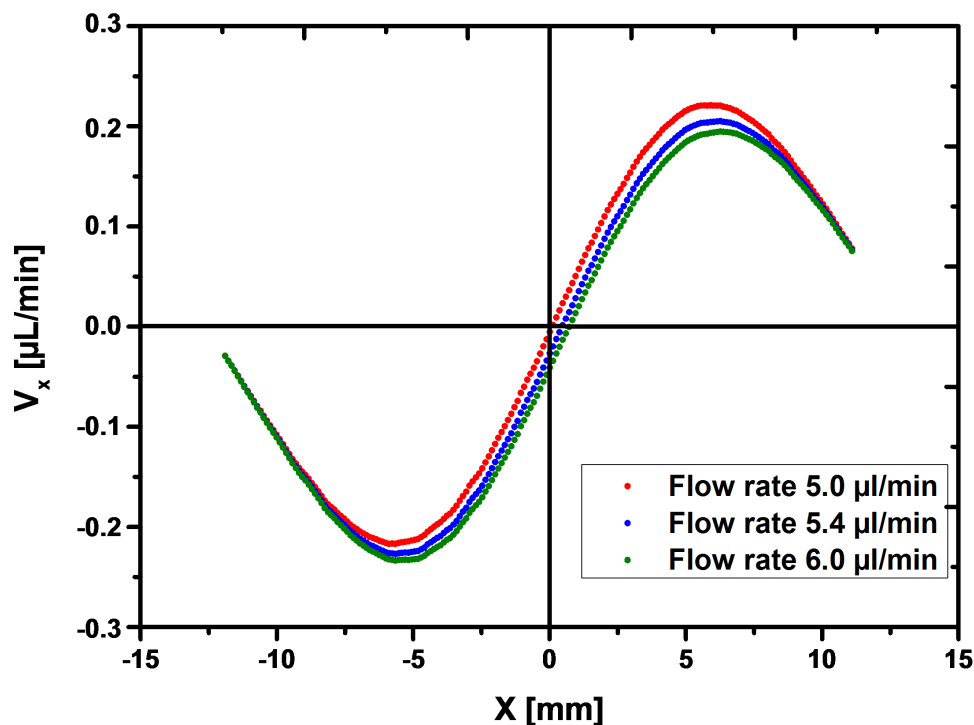


Figure 3.7: The x-component of the velocity at the outlet of the device as function of the flow at inlet 1. The point at which the x-component becomes zero shifts towards the right with increasing flow, by increasing the flow rate with a $0.1 \mu\text{L}/\text{min}$ step.

rate change at inlet 1 for a total flow rate of $10 \mu\text{L}/\text{min}$ in reffig:flowcontrolex using black dots, demonstrating good agreement with the simulated results (indicated with red line). A linear relationship was found between the flow rate and displacement, with a $0.1 \mu\text{L}/\text{min}$ increment resulting in a $30 \mu\text{m}$ shift. After a flow rate change at the inlet, approximately 45 seconds were required for the outlet flow to stabilize at its new position. Inserts 1 and 2 in reffig:flowcontrolex are microscope images taken at $5 \mu\text{L}/\text{min}$ and $6 \mu\text{L}/\text{min}$, again taken at a total flow rate of $10 \mu\text{L}/\text{min}$, to illustrate the shift of the focused stream line.

3.4 Conclusion

A free-flow Isotachopheresis has been fabricated on a glass wafer with $5 \mu\text{m}$ depth channel. The device consists of five inlets, a separation chamber with the size of $23 \times 15 \text{ mm}$, two side chambers for connecting the electrodes and five outlets. The three middle inlets are split with a binary tree structure for equal distribution of samples and buffers. Two outer two inlets used to guide flow direction into the main chamber. The side chambers are

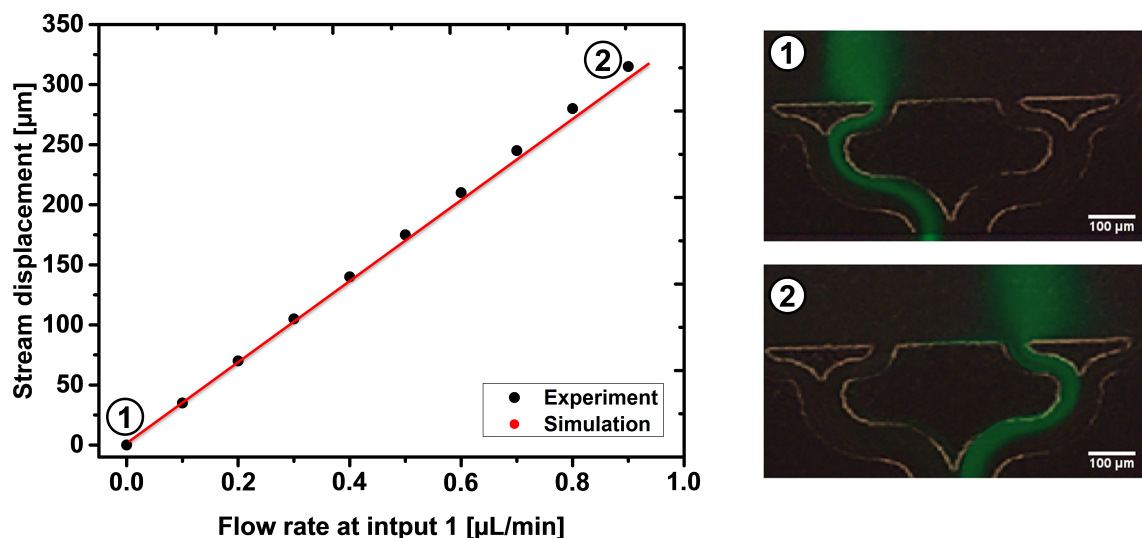


Figure 3.8: Comparison of the experimental data and the simulation of the hydrodynamic control of the focused stream line. Indicated on the vertical axes is the x-position the outlet at which the x-component of the velocity is zero. This point, at which the liquid no longer displaces in x-direction, is shifting to the left side with increasing flow at input 1.

separated from the main chamber by $15 \mu\text{m}$ wide channels to prevent gas bubbles entering the main chamber. The outlets are designed in similar fashion as the inlets. Steady flow of buffers and a sample was achieved by syringe pumps with flow rate of $5 \mu\text{L}/\text{min}$. The relationship between concentration and voltage was studied in a constant injection flow rate. As the theory already predicted a Logarithmic relation was able to observe. When the applied electric field was higher than 2000 V bubble generation was able to observe. Therefore, instead of increasing the voltage an alternative was studied by reducing the flow rate. A similar relation was observed with the concentration and the flow rate. Also fluid scanning method of the ITP window was realised by controlling the inlet flows, changing the flow rate ratio supplied to either side of the device. A computational model predicting the shift of the outlet flow as a function of flow rate ratio was experimentally confirmed, enabling a shift of $300 \mu\text{m}$ with $30 \mu\text{m}$ steps. With result we were confident that the FFITP is working and also that we were able to control the focused stream, so that we can collect the desired sample for other applications.

Chapter 4

Coupling to the Mass spectrometer

4.1 Introduction

Biochemical pathways are complex and typically involve a wide range of compounds covering a wide dynamic range. The elucidation of these pathways and their control mechanisms requires sophisticated analytical methods, typically removing interferences and enhancing the concentration of targets to allow for their detection. High resolution analytical techniques such as high performance liquid chromatography (HPLC) and capillary electrophoresis (CE) are often coupled with mass spectrometry to obtain information about the amount and identity of these compounds [12]. The biggest limitation of the CE-MS method is that it is common that the amount of the sample of interest is very low. Furthermore the concentration of the contaminants are much higher, therefore lots of sample preparation is needed. To solve this problem ITP,MS (Advanced electrolyte tuning and selectivity enhancement for highly sensitive analysis of cations by capillary ITP-ESI MS.) was suggested. Since ITP is powerful technique to pre concentrate and also separate the sample as discussed in the other chapters. This facilitates the handling of samples across a wide dynamic range making it a very attractive technique for studying biochemical processes with high complexity in chemical diversity and dynamic range. ITP has been extensively used in capillaries and on microchips, as discussed in various review articles [2] [46]. FFITP is advantageous since it has a continuous sample output. However detection in FFITP is a challenging task. The most common way is optical detection, which done by fluorescent labelling of the samples. Optical detection, however, is complicated in ITP because the separated analyte zones are stacked next to each other, requiring the use of spacers [24]. More serious problem is that in real sample the labelling is difficult and also very time consuming. Therefore we suggest a online coupling of an FFITP device with ESI-MS, enabling continuous analyte concentration and clean-up before injection into the MS where.

Hydrodynamic flow control was used to direct zones of interest into the MS, and en-

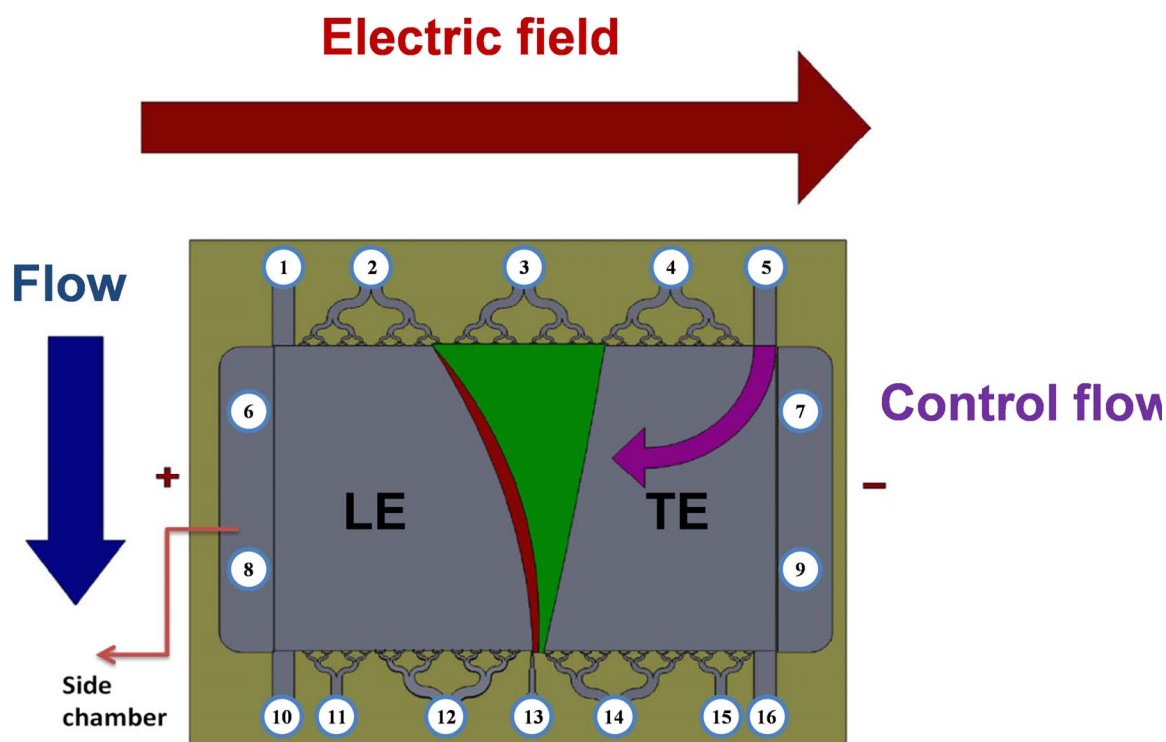


Figure 4.1: Principle of operation of the FFITP chip. By applying an electric field perpendicular to the flow direction, the target analytes are focused between the leading (LE) and terminating buffer (TE). Increasing the flow at inlet 5 will shift the stream to a desired outlet (13)

abled scanning of the ITP system as discussed in chapter 3. As mentioned before, analyte identification in analytical ITP with universal detection is complicated by the changes in migration time with sample composition. Connection with an MS eliminates this issue by allowing for the identification of the analyte based on its mass. In plateau mode, the hydrodynamically controlled scanning also provides a measure for the zone width, and hence analyte concentration. The proposed method is ideally suited for proteomic and metabolic studies, where the FFITP can simultaneously concentrate trace analytes in a specific mobility range in peak mode ITP, whilst removing interferences with mobilities outside the ITP window. The concentrated targets are then continuously directed into the MS, providing its resolving power to identify and analyse the concentrated analytes in a timeframe independent of the analytical separation.

4.2 Simulation of ITP

In capillary and free flow ITP, conductivity and optical detection are most frequently used, but this method can also be used in conjunction with a mass spectrometer. The limited range of ESI-MS compatible buffers, however, restricts the range of LEs and TEs that can be used. Gebauer et al. [17] recently proposed manipulating the ITP window by adjusting the pH and therefore effective mobility of the LE and TE. Here, a similar approach was followed, and resulted in the selection of formic acid as the leader and propionic acid as the terminator. With the LE adjusted to pH 4.3 using NH_4OH ; the resulting effective mobilities are shown in Table 130. The ITP process was modeled using SIMUL31 in constant current mode ($-1.125 \mu\text{A}$). The LE was 10 mM formic acid adjusted to pH 4.3 with 8 mM ammonium, and the TE was 7 mM propionic acid with a pH of 3.5. Alexa fluor 488 (3 mM), citric acid (1 mM), fluorescein (2 mM) and glycolic acid (1 mM) were used as model analytes, with their effective mobilities given in Table 1.

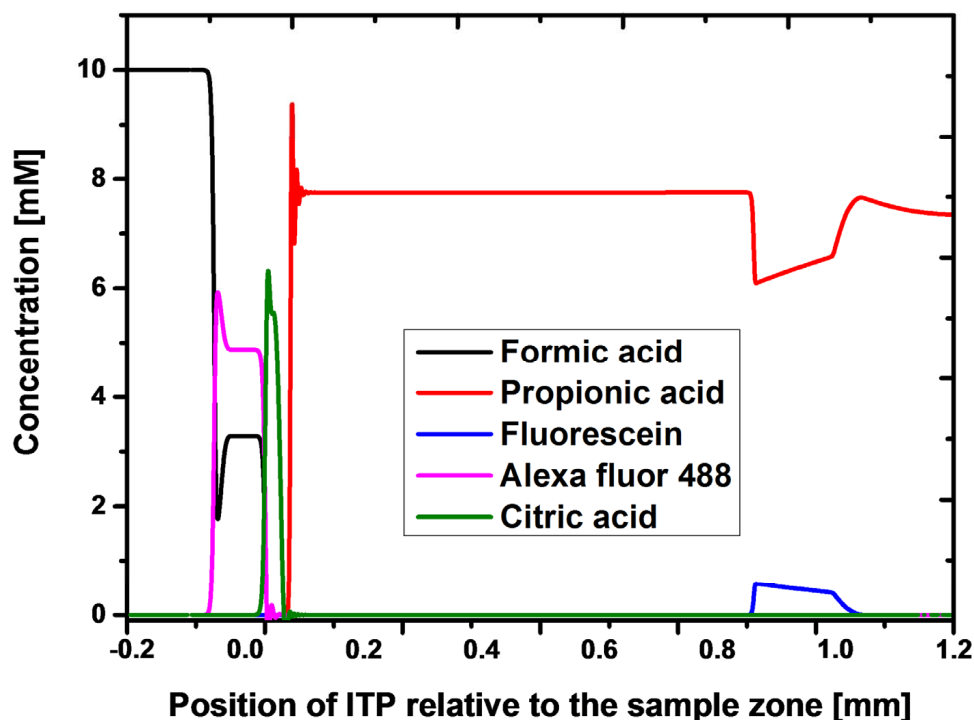


Figure 4.2: Result of the ITP simulation, showing Alexa fluor 488 and citric acid being concentrated in the ITP window while fluorescein dissipates into the TE. The ITP system is depicted right to left with the relative position of the window positioned at 0, LE at negative values and TE at the positive values.

The SIMUL results are presented in 4.2. To maintain continuity in the figures through-

out the manuscript, the LE is on the left, TE on the right hand side. The ITP window defined between the LE (formic acid) and TE (propionic acid). The target analytes stack in the window in order of decreasing mobility, with the fast Alexa fluor 488 adjacent to the LE followed by Alexa fluor 488. Fluorescein, the model contaminant, has mobility lower than the TE and therefore dissipated from the ITP window into the TE zone.

Compund	pka	$\mu(10^{-9}m/V.s)$	$\mu_{eff}(10^{-9}m/V.s)$
Alexa Fluor 488	-	-	36
Fluorescein	6.8;4.4	35.9,19	0.5
Citric acid	6.41;4.76;3.13	74.4;54.7;28.7	28.9
Formic acid	3.89	42.4	27.1
Propionic acid	4.87	37.1	1.6

4.3 Experimental

4.3.1 Chemicals

As LE, we used 10 mM Formic acid adjusted to pH 4.29 with ammonium hydroxide, 7mM propionic acid (pH 3.55) was used as TE. For the MS scanning study, samples contained 1 mM fluorescein, 1 mM citric acid, 1 mM Alexa Fluor 488, and 1 mM glycolic acid. All chemicals were purchased from Sigma Aldrich (Germany) with the exception of Alexa fluor 488, which was purchased from Life Technology (Germany).

4.3.2 Chip layout and tubing

The layout of the device is shown in 4.1. The device consisted of five inlets (1-5), a 23×15 mm separation chamber, two side chambers for connecting the electrodes (6-9) and seven outlets (10-16). The three middle inlets were equipped with binary tree structures to evenly distribute the input solutions into the chamber. The outer two inlets (1 and 5) were designed for hydrodynamic control. All outlets were designed similarly to the inlets except for the middle outlet (13), which has a narrower ($100 \mu m$ wide) outlet channel for sample collection. The electrode chambers are connected to the main chamber using an array of $25 \mu m$ wide channels, $50 \mu m$ apart. Arrays of pillars were introduced to strengthen the support of the chamber wall (4.3A). The voltages were applied to the buffer-filled reservoirs to minimize the pH changes inside the chamber. Gas bubbles, generated by electrolysis, were prevented from entering the main chamber by reservoirs and an array of channels in the side chamber. 4.3B shows the side reservoir and the connectors, which are used for connecting the tubing. To provide fluidic access by Teflon tubing (ID: 0.5 mm, OD: 1.6 mm, ProLiquid GmbH, Germany) to the chip, bootlace ferrules (OD: 1 mm, height: 8 mm, Bauhaus, Germany) were bonded to inlets 1-4 and outlets 10-12 and 14-16 using epoxy (UHU, Germany). Outlet 13 was connected using a one-Piece Fitting and

Bonded-Port Connector (Labsmith, USA). The metal bootlace ferules were also mounted to the four electrode outlets (6-9) to act as buffer reservoirs.

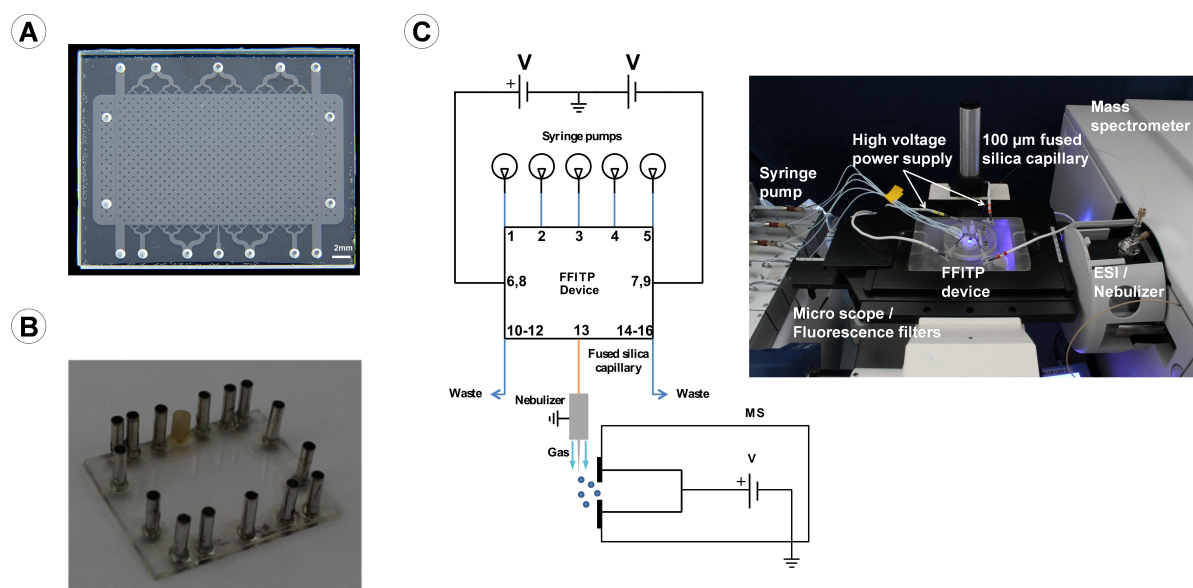


Figure 4.3: (A) Photograph of the device implementation in glass. The side chambers are separated from the main chamber by $25 \hat{I}\frac{1}{4}$ m wide grooves. Pillars were introduced to avoid collapse during thermal bonding and to prevent breaking by the high back pressure inside the chamber (B) Connections for the tubing and the side reservoirs which are used to connect the electrodes. (C) Connection of the FFITP chip to the MS with a diagram showing the connection points for the electric field, syringe pumps and ESI-MS. The chip is mounted on an inverted optical microscope (photograph).

4.3.3 Experiment setup

The setup of the experiment is shown in 4.3C. The FFITP device was mounted on an Axiovert 100 (Zeiss GmbH, Germany) inverted microscope. LEDs (type M470L3, Thorlabs GmbH, Germany) with a 470 nm principal wavelength and maximum optical power of 650 mW were used for sample illumination. All fluorescence imaging and measurement experiments were done using a 470/525*ex/em* filter set (model 49002, Chroma Technology Corp. USA). Imaging was performed using a 5x objective lens (Zeiss GmbH, Germany) and a color CCD camera model C5 (Jenoptik GmbH, Germany) with the LED intensity adjusted to 1.6 A. The fluorescence intensity measurements were performed using a single point detector made using a 50x objective lens and photomultiplier tube (PMT) (model H10722-01, Hamamatsu Photonics, Co., Germany) with the gain set by a 0.5 V bias. Samples and buffer were injected through a nEMESYS Low Pressure Syringe Pump system comprised of five syringe modules (Cetoni GmbH, Germany). To connect the tubing from

the syringes to the device, bootlace ferrules were bonded to the glass chip using epoxy (UHU, Germany), shown in 4.3B. The potential difference was applied using a HVS448 High Voltage Sequencer (Labsmith, USA).

4.3.4 Interface from chip to MS

A fused silica capillary with an outer diameter of 360 μm , inner diameter of 100 μm and length of 30 cm was used to connect the FFITP chip to the ESI interface of the 1100 LC/MSD mass spectrometer (Agilent, Germany). A commercially available connector (One-Piece Fitting and Bonded-Port Connector, Labsmith, USA) was used to connect the fused silica capillary to the chip. A 1/32" OD PEEK tubing Sleeve (IDEX, USA) was used to guide the capillary into the ESI interface of the 1100 LC/MSD mass spectrometer (Agilent, Germany). The mass spectrometer was operated in negative mode with a potential of 4000 V, fragmentation factor 100, and nitrogen was used as nebulizing gas. No sheath flow was used. The flow rate from the chip outlet through the capillary was 1.5 $\mu\text{L}/\text{min}$ as determined by collection and weighing at 10 minute intervals when the free flow device operated at 2 $\mu\text{L}/\text{min}$. At this flow rate, there is a 2 minute delay between the analytes leaving the device and entering the MS.

4.3.5 Experimental Procedure

The FFITP device was first filled with LE (inlets 1 and 2) and TE (inlets 4 and 5). Once the main chamber and electrode reservoirs were filled, the reservoirs at the side chambers were sealed using the Platinum electrodes. Then the sample was introduced at inlet 3, and after equilibration of the flows, the electric field was applied across the chamber.

4.4 Result and discussion

4.4.1 Isotachopheresis

The main advantage of ITP over zone electrophoresis is that clean-up and concentration of trace analytes can be achieved simultaneously through the selection of the LE and TE. To demonstrate the FFITP-MS, model compounds were selected because they could be visualized using fluorescence microscopy and/or determined by MS. Fluorescein was used as a model contaminant with a lower mobility than the TE and the targets. Citric acid was selected as target analyte because its electrophoretic mobility is similar to that of Alexa Fluor 488, but unlike Alexa Fluor 488 it yields a response in the MS. This allows the visualization of the ITP window using Alexa Fluor 488, and the analysis of the effluent by MS. In order to determine the optimal separation voltage, the fluorescence intensity

of the Alexa Fluor 488 zone was studied as a function of the potential difference applied across the FFITP device with a constant flow rate of $2 \mu\text{L}/\text{min}$. The intensity increased with the applied potential difference, leveling off around 1200 V ($E = 520 \text{ V}/\text{cm}$, $I = 100 \mu\text{A}$), indicating that steady state was achieved. Using a flow rate of $2 \mu\text{L}/\text{min}$ and a potential difference of 1200 V, a sample comprising of fluorescein, Alexa fluor 488 and citric acid was loaded. The microscope image in 4.4 confirms the validity of the selected electrolyte system. The fluorescein is effectively removed from the sample, demonstrated by a faint zone representing the dissipating fluorescein at the TE side. The Alexa Fluor 488 is stacked in the ITP window, visualised by the bright zone. Citric acid acts as a non-fluorescent spacer between Alexa Fluor 488 and the TE containing the dissipating fluorescein and cannot be observed by fluorescence microscopy. The fluorescence intensity was quantified using a PMT using the microscope stage to move the chip. 4.5 shows the fluorescence intensity measured using a PMT as a function of the scan time. A narrow peak with high intensity is recorded for Alexa Fluor 488, indicating the ITP window passes the detection spot. Further down in the terminator, a broad zone of lower intensity corresponds to the fluorescein dissipating ion the TE. Regular drops in the fluorescence intensity are caused by the pillars used to support the microfluidic chamber, passing across the detection spot.

4.4.2 FFITP-ESI-MS interface test

Before applying an electric field to the FFITP device and test the compatibility of the FFITP-MS, it had to be test first whether the simple connection through fused silica tubing was appropriate as an interface. Also electrolyte system (LE, TE) had to be tested if the electrolytes give any interference at the signal. Therefore a simple test was done where fluorescein was used as optical guidance as well as the detection guidance for the MS. This simple test was done by inducing the fluorescein at inlet 3 the LE was injected at inlet 1 and 2, and the TE at inlet 4 and 5 all of the inlet flowrate was $1 \mu\text{L}/\text{min}$ which was the minimum flow rate where the MS was able to give a stable output. After achieving a laminar flow the FFITP device was connected to MS and a scanning from LE to TE was done. 4.6 shows the result of this process where it can be observed that the abundant number is very low. This is time region is when the LE was entering the MS, also it can be seen that the signal is increasing after 10 minutes which is the time when fluorescein is entering the MS. In the time domain between 17-25 min the signal is decreasing which is the time domain when the TE was entering. After 25 min the signal is increasing again which is the time where fluorescein was entering again. This result was able to make us to conclude that the interface of the FFITP-MS was working and also the electrolyte system for the ITP does not give interferences.

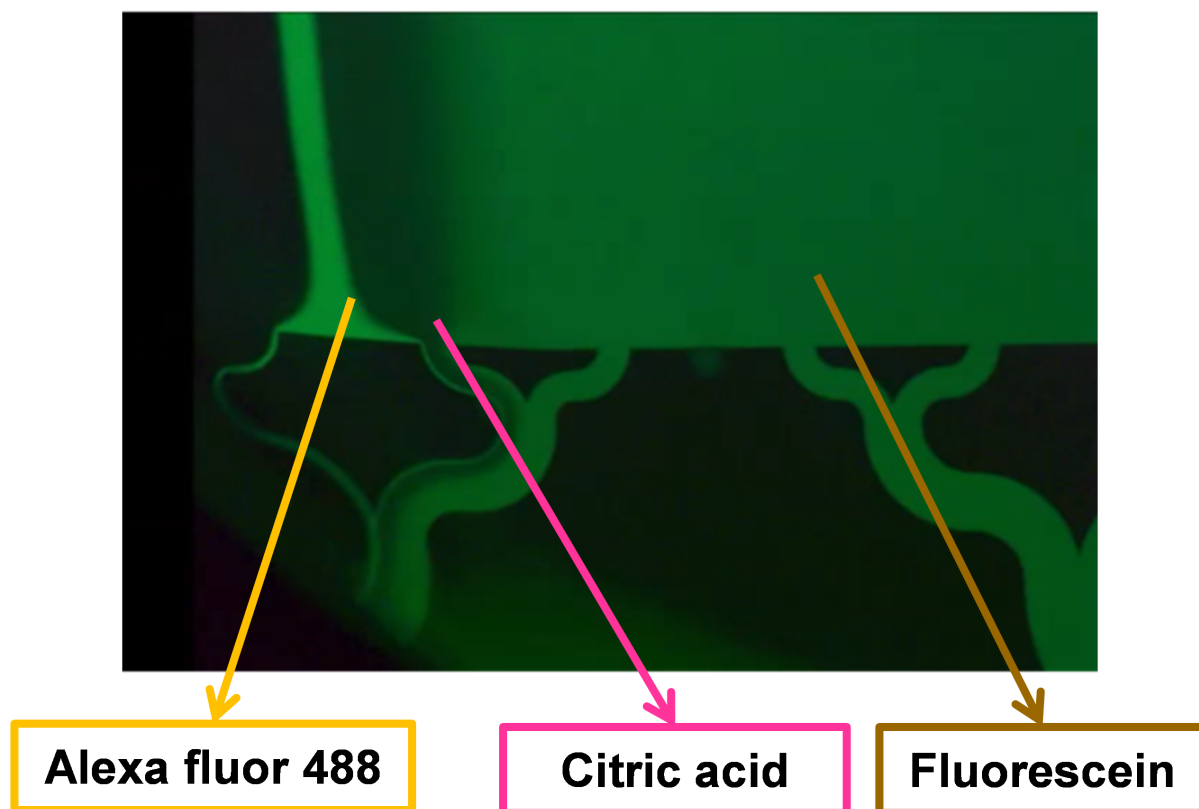


Figure 4.4: Microscope image of the FFITP device which showing the focusing of Alexa fluor into a sharp band and dissipating fluorescein. (C) PMT signal output which showing the intensity of Alexa fluor and fluorescein.

4.4.3 FFITP-ESI-MS

Having confirmed the validity of the FFITP system, the device was connected to the MS interface. Two concepts were studied by the on line connection of the FFITP to the ESI-MS. First, the use of the ITP window for the elimination of a contaminant in combination with the concentration of the target analyte and its continuous infusion into the MS. Citric acid was selected as target analyte together with fluorescein as contaminant. Alexa Fluor 488 was only used as an optical maker to guide the ITP zone into the MS, since it does not yield an MS response. Citric acid and fluorescein were chosen as analyte and contaminant respectively. 4.7 show the result of raw MS data which agreed with the fluorescence microscopy experiments and showed fluorescein dissipating in the TE and citric acid forming and ITP zone. 4.8 shows the normalized data of 4.7 where it is possible to observe the concentration of citric acid increased while the concentration of fluorescein decreased, with the ratio of citric acid to fluorescein increasing from 1:2.6 to 1:8.4. More significant enhancements are expected in peak mode when the initial concentration of citric acid is lower or when the concentration of fluorescein is higher.

The second question would it be possible to have several interest of analytes which

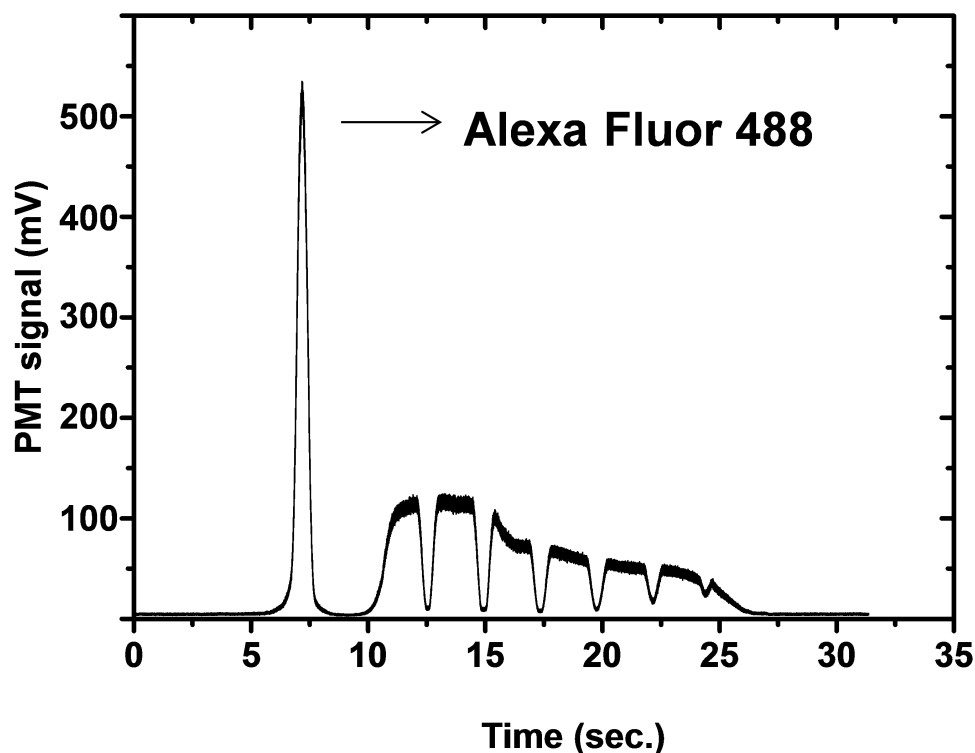


Figure 4.5: PMT signal output which showing the intensity of Alexa fluor and fluorescein.

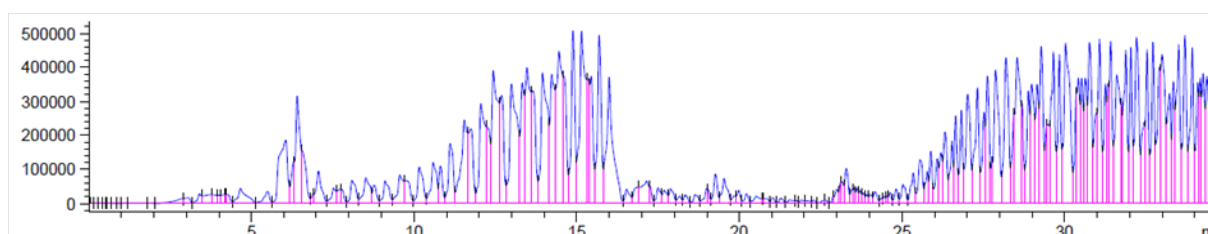


Figure 4.6: Online connection test with fluorescein for 40 min

will be concentrated by the FFITP and then by hydrodynamic control shift the stream line so that we can scan the focused stream line in such that only one of the analytes will enter the MS. In order to proof this concept an additional acid (glycolic acid) was mixed to the sample which will be concentrated next to the citric acid. 4.9 shows the MS data output as a function of the scanning time of this process, moving from the LE to the TE and back. First citric acid is detected between 2 and 4 minutes, characterised by the signal at mass to charge ratio (m/z) of 191, glycolic acid with m/z of 73 can be observed around 6 minutes. After reaching the TE at around 7 minutes of scan time, the flows were shifted back to the original location, showing first glycolic and then citric acid. It is important to realise that fluorescein ($m/z=331$), added as interference, is not detected

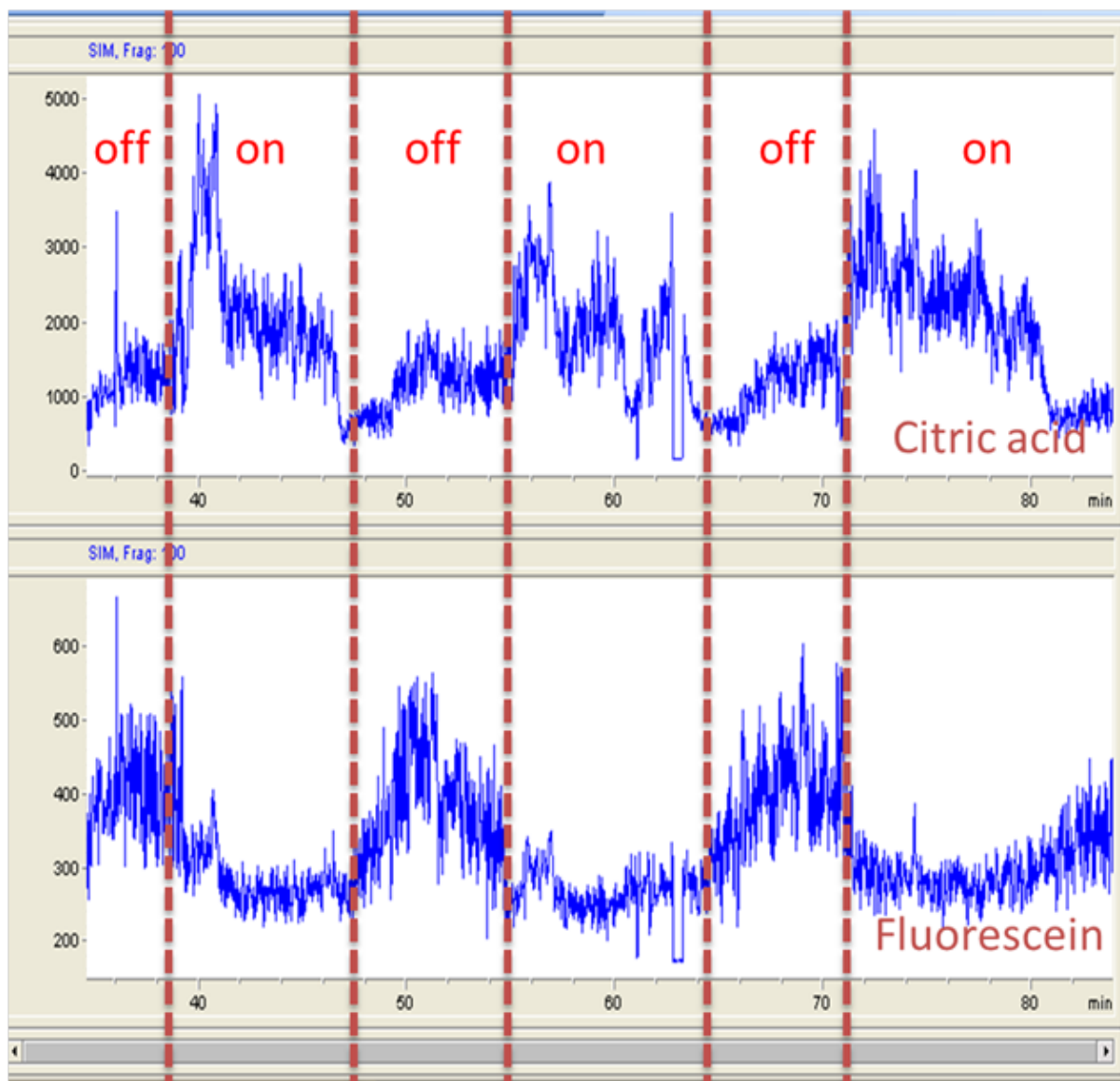


Figure 4.7: Online connection with fluorescein and Citric acid

in the ITP window.

4.10 shows the MS data output of this scanning process with a percentage value which was made by dividing the highest value of each time and multiplied with hundred. Where it is more clearly to observe that citric acid is entering first which has a mass to charge ratio (m/z) 191. By shifting the stream line further to terminating buffer, glycolic acid ($73 m/z$) is able to observe, and in the whole time domain fluorescein was not able to observe.

The extracted ion isotachopherograms for the three compounds over the period scanning back from TE to LE are given in 4.11. The flat baseline signal for $m/z=331$ confirms fluorescein has been effectively removed from the ITP window. 4.11 also demonstrates

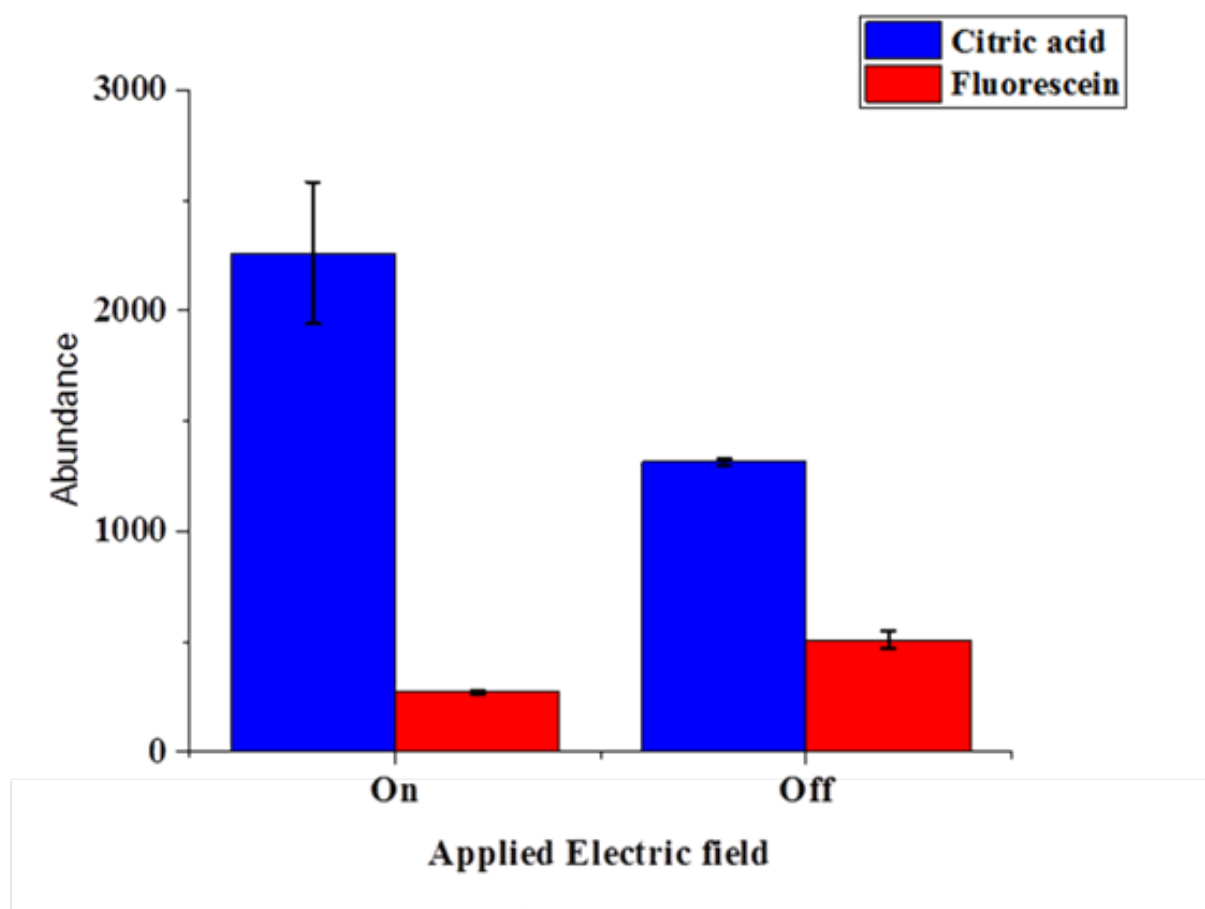


Figure 4.8: Normalized value of the output of the online connection of fluorescein and citric acid

glycolic and citric acid have been separated into their respective ITP zones, with the slower glycolic acid forming the zone closest to the TE preceding the faster citric acid. Without the use of a spacer, the overlap in signal for the adjacent glycolic and citric acid bands is normal. It is important to note the absence of citric acid in the glycolic acid zone and vice versa, confirming steady state has been reached

4.5 Conclusion

The coupling of FFITP with ESI-MS decouples the separation and detection time frame, whilst benefiting from the power of ITP to simultaneously concentrate and purify analytical targets. We have demonstrated the online coupling of FFITP-ESI-MS by the removal of fluorescein from a set of target analytes. Fluidic scanning of the ITP window was realised by controlling the inlet flows, changing the flow rate ratio supplied to either side of the device. The connection between the chip and MS was realised using a 100

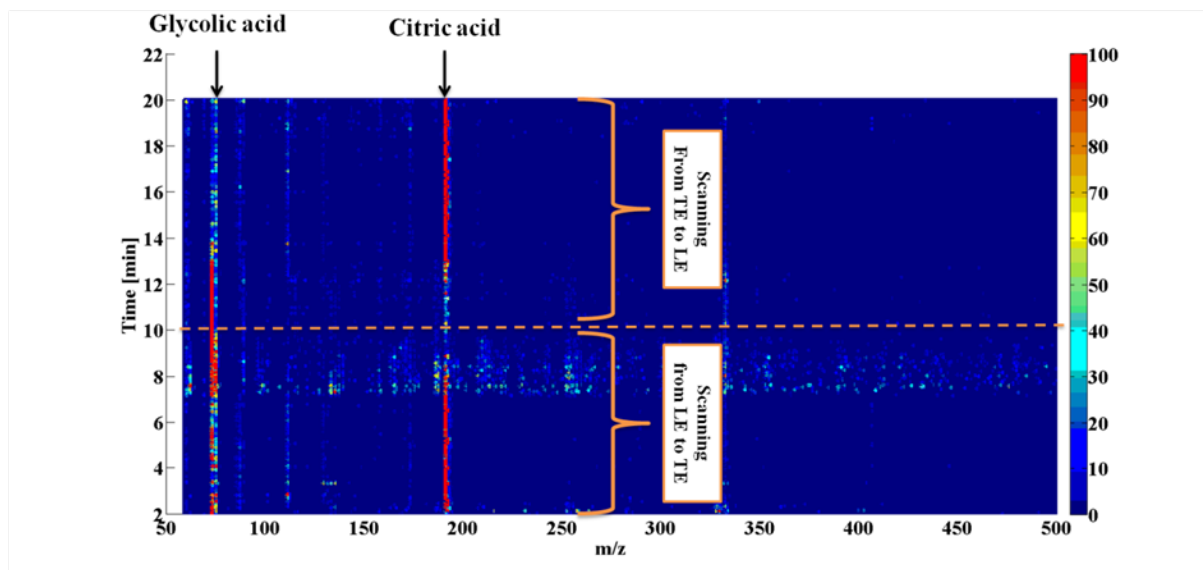


Figure 4.9: The MS data output during FFITP-ESI-MS. A mixture of Alexa fluor 488, Citric acid, Glycolic acid, and fluorescein was used as sample, using Alexa fluor for optical guidance. By controlling the flow rate at the inlets the flow through the outlet connected with the MS was moved from LE to TE for 7 min and then shifted back to LE. Throughout this process, first citric acid (191 m/z) was detected, followed by glycolic acid and back to citric acid

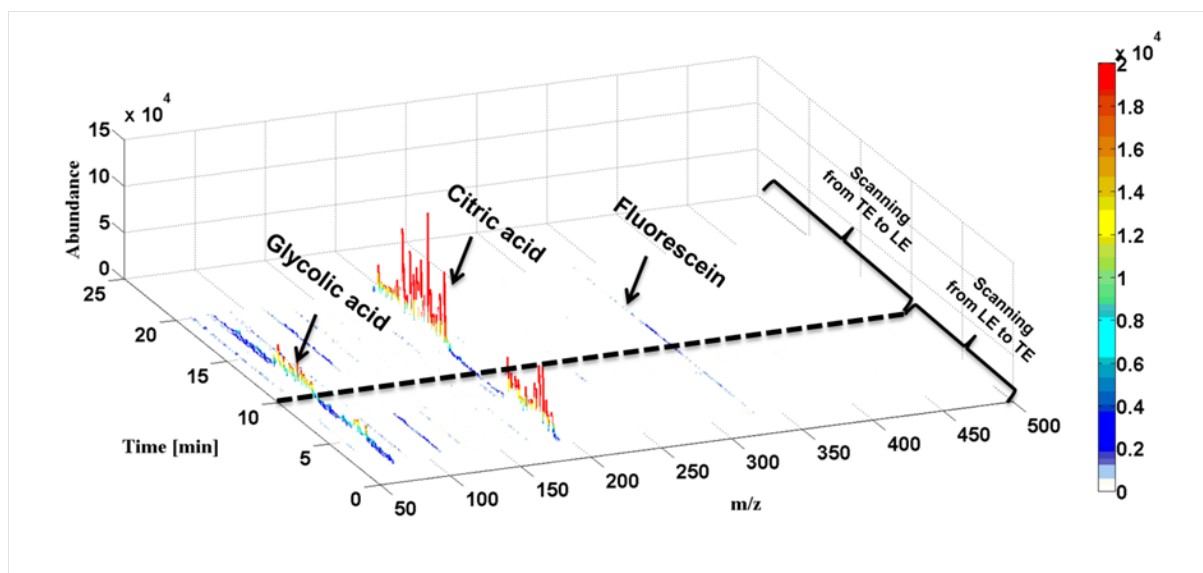


Figure 4.10: Normalized value of the output of the online connection of fluorescein, citric acid, and glycolic acid

μm ID fused silica capillary, selected to minimize flow resistance and dead volume whilst enabling visual inspection using a fluorescence microscope. For further study where the use of a microscope can be eliminated, shorter capillaries with a narrower ID can be used

to allow for lower flow rates and increased residence times in the electric field and hence the time for ITP to establish. The dissipation of fluorescein into the TE at the same time of the concentration of Alexa Fluor 488 and citric acid to the steady state concentration were recorded using a fluorescence microscope and MS, respectively. The fluorescence intensity across the device IS showing a narrow band for the Alexa Fluor 488 in the ITP window, and a broad and less intense signal for the dissipating fluorescein. The changes in abundance for the m/z corresponding to citric acid and fluorescein confirmed that the ITP was simultaneously increasing the citric acid concentration to its steady state level and removing the fluorescein. Quantification based on the changes in abundance of the MS signal in presence and absence of an applied electric field demonstrated an increase in the citric acid to fluorescein ratio by a factor of 3.2. Fluidically scanning across the ITP window past the MS demonstrated the separation of glycolic acid and citric acid by the changes in the abundance at their respective m/z ratio. Importantly, no signal was recorded at the m/z ratio for fluorescein, demonstrating it was effectively removed from the ITP window. Based on these encouraging initial results, we are confident that the online coupling of FFITP-ESI-MS will solve problems either where the concentration of the target analytes is very low compared to contaminants, and/or where extended MS studies are required for structure elucidation. Additional engineering of the ESI-MS connection is required to achieve higher spraying stability at low volumetric flow rates. Once solved, it should be possible to apply the technique to biomolecules including peptides and proteins, which may require surface modification of the glass device.

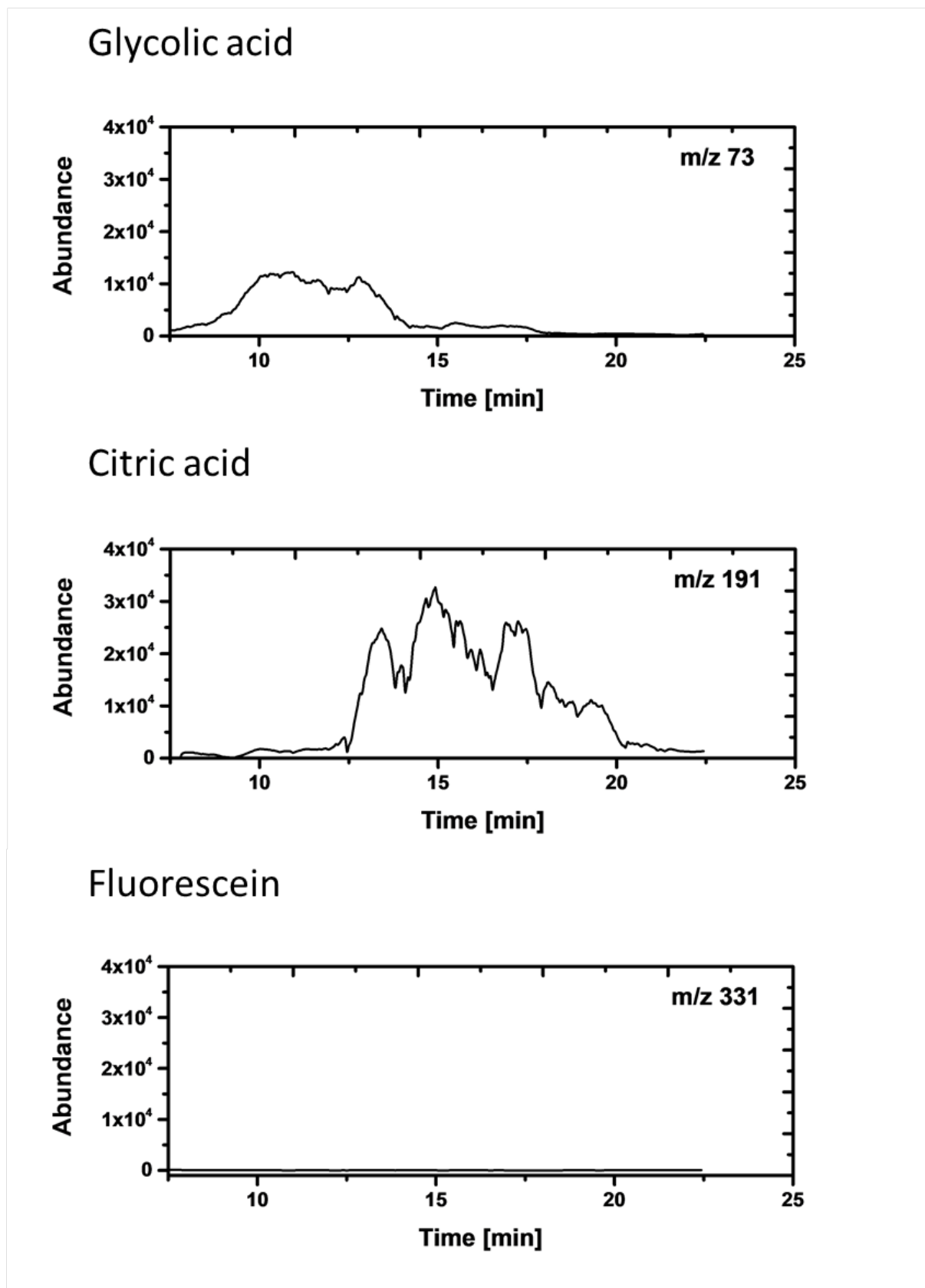


Figure 4.11: Selected ion isotachopherograms for glycolic acid ($m/z=73$), citric acid ($m/z=191$) and fluorescein ($m/z=331$).

Chapter 5

FFITP enhanced ISFET Based Biosensor

5.1 Introduction

Biomarkers are objectively measurable biological characteristics that can be used to diagnose, monitor or predict the risk of disease [1]. For example, BRCA1 mutations are genetic markers for breast cancer risk [14], high blood glucose indicative for diabetes, creatinine clearance related to kidney function, and prostate specific antigen (PSA) is a protein biomarker for prostate cancer [50]. With "omics" approaches such as transcriptomics, proteomics, glycomics and metabolomics, the number of known biomarkers increases exponentially. A critical issue in the use of these biomarkers to inform treatment is the development of analytical techniques being able to cope with the large variety in physicochemical properties and dynamic range in plasma and urine. As many biomarkers of interest are present at low concentration against a more concentrated and complex chemical background, their concentration needs to be raised selectively so that it can be detected without interferences. Isotachopheresis (ITP) is a mode of electrophoresis, where the sample is placed in a discontinuous electrolyte system, comprised of a leading and trailing electrolyte (LE and TE, respectively). The key advantages of isotachopheresis are that the sample can be concentrated and separated in the same time. The combination of ITP and FFE has the advantage that the sample can be continuously separated and also concentrated as already discussed in the other chapters. However detection in FFITP is a challenging task, The most common method to detect the sample is done by optical detection. Optical detection has several limitations. First of all the sample has to be labeled which is not always possible. The bigger problem in FFITP or in ITP general is the fact that the sample will stack to next to each other, which makes difficult to distinguish the sample. To solve this problem spacer are put in between the sample [51]inano2000capillaryoerlemans1981isotachopheresis. Finding the right spacer however is

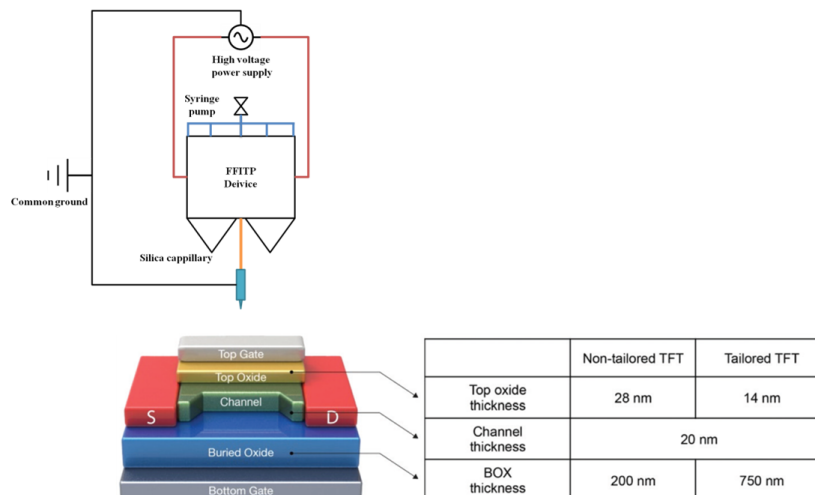


Figure 5.1: Schematic operation of the FFITP-DGFET.

relative complicated. In order to overcome this limitation of the optical sensor a more elegant detection method is required. One of the possibilities is the Ion-sensitive field-effect transistors (ISFETs). Since an ISFET is a electrochemical sensor which can be used for various analyte which also includes biological samples [52]rothberg2011integrated. Self-amplified transistor immunosensor under dual gate (DGFET) was recently suggested [35] to improve the sensitivity and the stability of the ion-sensitive field-effect transistor. The connection of the FFITP to the DGFET is beneficial for both of the technology. From the FFITP side the DGFET sensor is a label free sensor which could solve the limitation of the optical sensor. Also the combination of FFITP-DGFET is beneficial of the point of view from the DGFET. Since the major problem of the DGFET is the high sensitivity which is resulting also to detect unwanted signal, therefore purification of the sample is needed. Especially in real biological application it is common that the sample of interest has much lower concentration than the other proteins. It is also common in early disease detection that the sample has a very low concentration. Therefore the pre-concentration ability of the FFITP will enable to increase the concentration of the sample which result to increase the detection limit. We demonstrate the online coupling of an FFITP device with DGFET operation, enabling continuous analyte concentration and purification before injection into the DGFET, as illustrated in 5.1.

5.2 Experimental

5.2.1 Chemicals

All buffers were prepared as follows with resulting pH value of 7.5. The leading buffer was made by 5 mM TRIS hydrochloride, the terminating buffer by 10 mM TRIS Glycine

buffer solution. The sample was prepared by mixing 10 pg/mL (GFP) full length protein (ab119740), Fluorescein mixed with TE. All chemicals were purchased from Sigma Aldrich (Germany) with the exception of GFP, which was purchased from Life Technology (Germany).

5.2.2 Surface modification for attaching GFP antibody to the sensor

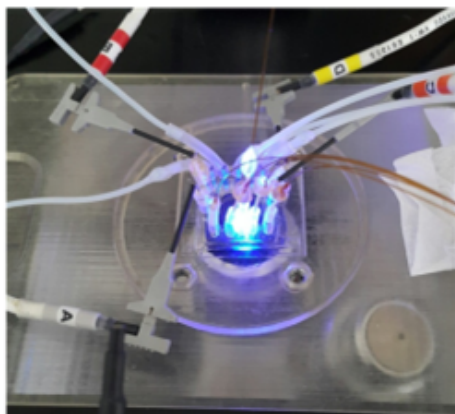
Antibodies (Anti-GFP antibody ChIP Grade (ab290)) were used to detect Green fluorescent protein (GFP). Surface modification was needed that for attaching the antibodies. First, the extended gate (EG) was put in Oxygen plasma for 5 min with 30 watt, in order to make -OH at the surface. Then 5 percent APTES (500 μ L + 9.5 mL ethanol), was injected to the EG for 1 hour to build $-NH_2$. 1 M of succinic anhydride which was mixed with Dimethylformamide (DMF) was used for 16 hours in a incubator of temperature 37 degree too build -COOH. In order to enhance the bonding between -COOH and $-NH_2$, 4 M EDC (1-Ethyl-3-(3-dimethylaminopropyl) carbodiimide) was mixed with 0.1 M NHS (N-Hydroxysuccinimide) for 15 minutes. Finally GFP antibodies were injected with a concentration of 200 ng/mL for 1 hour in room temperature. In order to wash out the non attached antibodies the EG was washed out with phosphate buffer solution. To avoid that non wanted protein attached to the surface 10 percent bovine serum albumin (BSA) was injected for 1 hour. All chemicals were purchased from Sigma Aldrich (Germany) with the exception of GFP antibodies, which were purchased from Life Technology (Germany).

5.2.3 Experiment setup

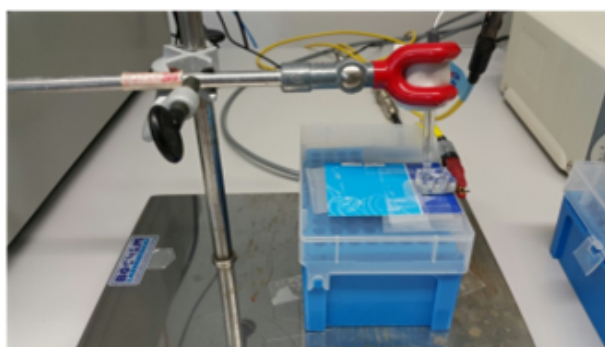
The FFITP device was mounted on Canon) inverted microscope as in the former chapters. Blue LED was used and the picture were taken by a fluorescence filter set. neMesys low pressure pump was used to inject the sample and buffer to the FFITP device and also to the DGFET with a flow rate 20 μ L. DGFET was connected to the Probe station via using the Semiconductor analyzer (B1500A). 5.2 shows the experimental setup where the top left side shows the microfluidic chip, the bottom left is the extended gate, and the right side is the probe station. The FFITP device was directly coupled to the EG sensing part of the DGFET via a 100 μ m wide and 30 cm long fused silica capillary. The threshold voltage was measure through the probe station and the semiconductor analyser.

5.3 Experimental Procedures

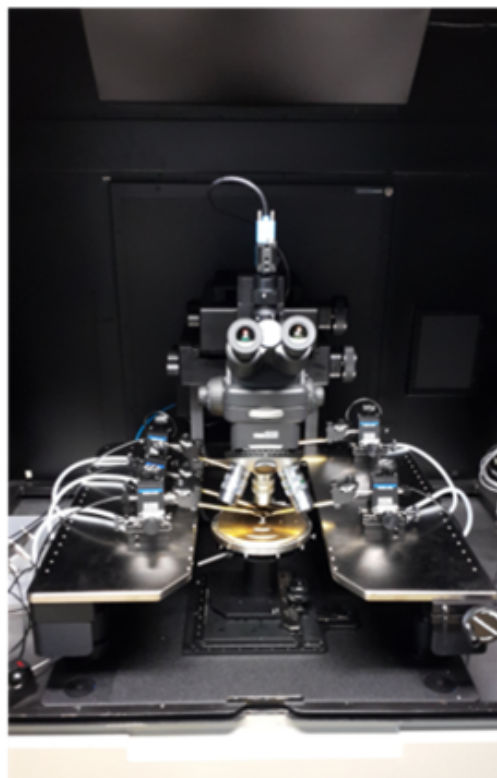
The FFITP process was done as the former chapter. The concentrated GFP through the FFITP device was collected to the sensing part of the DGFET with a volume of 100



Microfluidic chip



EG sensing part



Semiconductor analyzer

Figure 5.2: 3 Left top: FFITP with connector. Left bottoms: EG-DG FET where the antibody and the antigens was injected. Right bottom: Probe station where the DGFET was mounted

μL . In order to ensure that the GFP was properly injected to the DGFET sensing part fluorescein was additionally used for optical guidance. The change of the threshold voltage due to the concentrated GFP was measured after 30 min so that the GFP can react with the antibody. Additionally a negative curve was measured where the no antibody were bind at the surface of the DGFET for negative control.

5.4 Result and Discussion

Before coupling FFITP to the GFP we had to test first the ITP process and also the DGFET with the GFP antigen and antibody. Therefore each of the experiment was first done individually.

5.4.1 FFITP

The FFITP process of 10 ng/ml GFP with TRIS buffer with a flow rate of 20 $\mu\text{L}/\text{min}$ was observed so that we can confirm our designed ITP condition. 5.3 shows the FFITP process. It can be observed when the electric field is applied the GFP is concentrating (5.3 A) and when no voltage is applied the GFP is dissipating (5.3 B). 5.3 C shows the zoomed region of the FFITP process where it can be once more observe that the GFP is concentrating during it flows trough the outlet

5.4.2 DGFET

In order to check whether the antibody ant the GFP is function properly the DGFET was tested alone. Here the concentration of GFP was increased from 1 fg/ml to 10 $\mu\text{g}/\text{ml}$ with a concentration increase of factor ten. PBS buffer was used for this experiment, and the GFP was let for 20 min so that they can react with the antibody and the change of the gate voltage was measured. 5.4 shows the result of the gate voltage and also the the change of the threshold voltage. Positive control means that the gate voltage was measured with existence of GFP antibody and vice versa negative is without the antibody. It could be observed that the threshold voltage in increasing when the GFP concentration increase.

5.4.3 FFITP-DGFET connection

By connecting FFITP and DGFET three major problems were able to occur. First, since FFITP use an electric field for the ITP process, this electric field could be transferred to the DGFET and could make some problems. Second, fluorescein was used as optical guidance so that we can ensure that the sample is injected to the DGFET. Here however fluorescein could be disturb the DGFET signal since fluorescein itself has also a charge there the influence of fluorescein was also considered. At last since DGFET was originally tested under PBS buffer, however FFITP needs a TRIS buffer for the ITP process, therefore the buffer change from PBS buffer to TRIS buffer was studied.

Influence of the electric field from FFITP to the DGFET

DGFET is measuring the change of the threshold voltage. Also it known that the FET is possible to break due to an electric field two possible problems were able to think. First, although the FFITP is connected to the DGFET through a fused silica tube there exist possibilities that the high electric field of FFITP will damage the DGFET. The second possible scenario was that the FFITP electric field will shift the threshold voltage. Therefore an experiment was done to observe this problem. The fluorescein was used as sample with an initial concentration of 100 μM . The voltage across the FFITP device was increased from 100 V to 500 V. As shown in ?? no voltage shift and also no damage

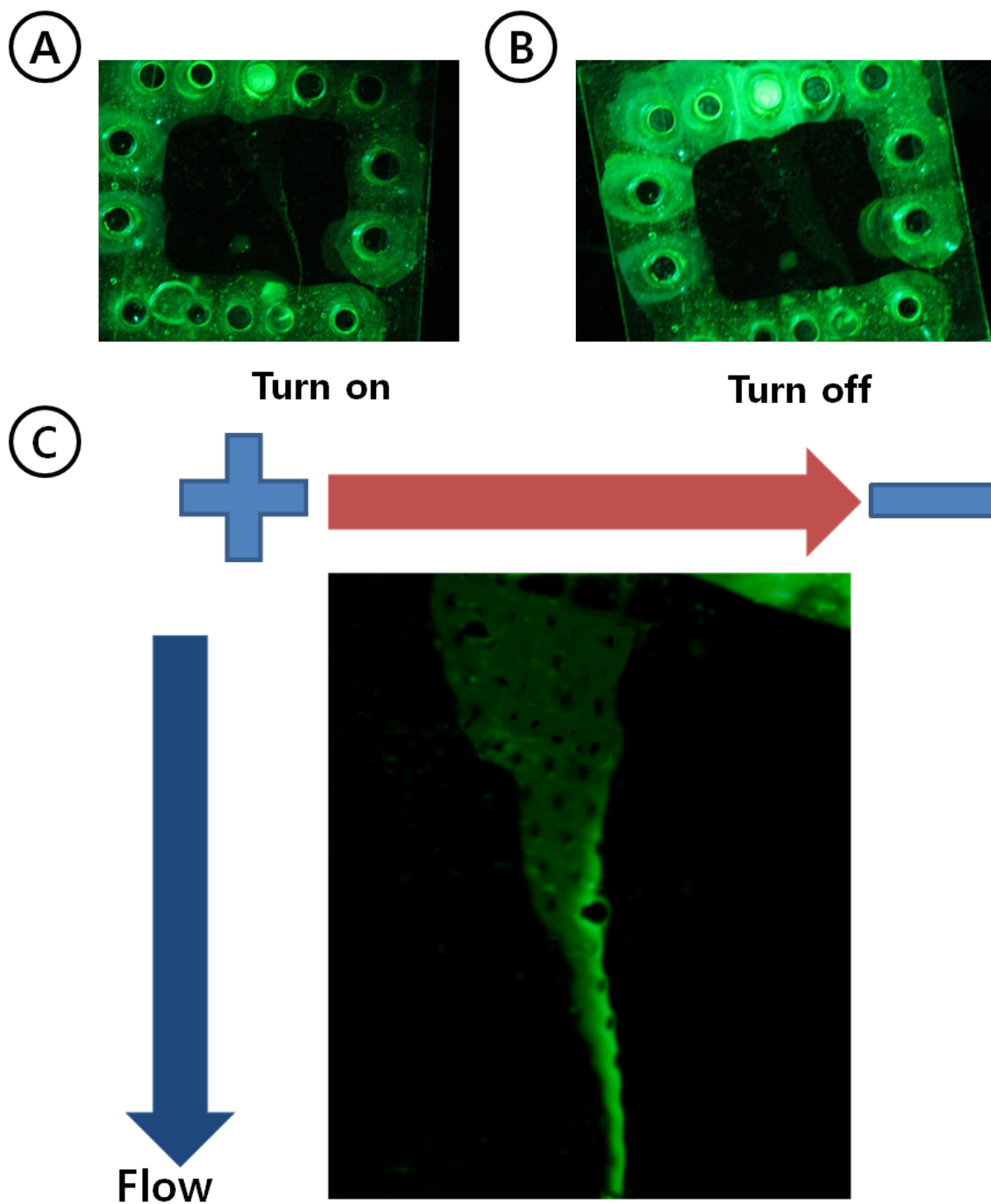


Figure 5.3: The ITP process of GFP. (A) Electric field on (B) Electric field off (C) The zoomed version when the electric field is applied

of the chip was observed. We believe that the resistance of the fused silica tube is high enough so that amount of delivered current is neglectable.

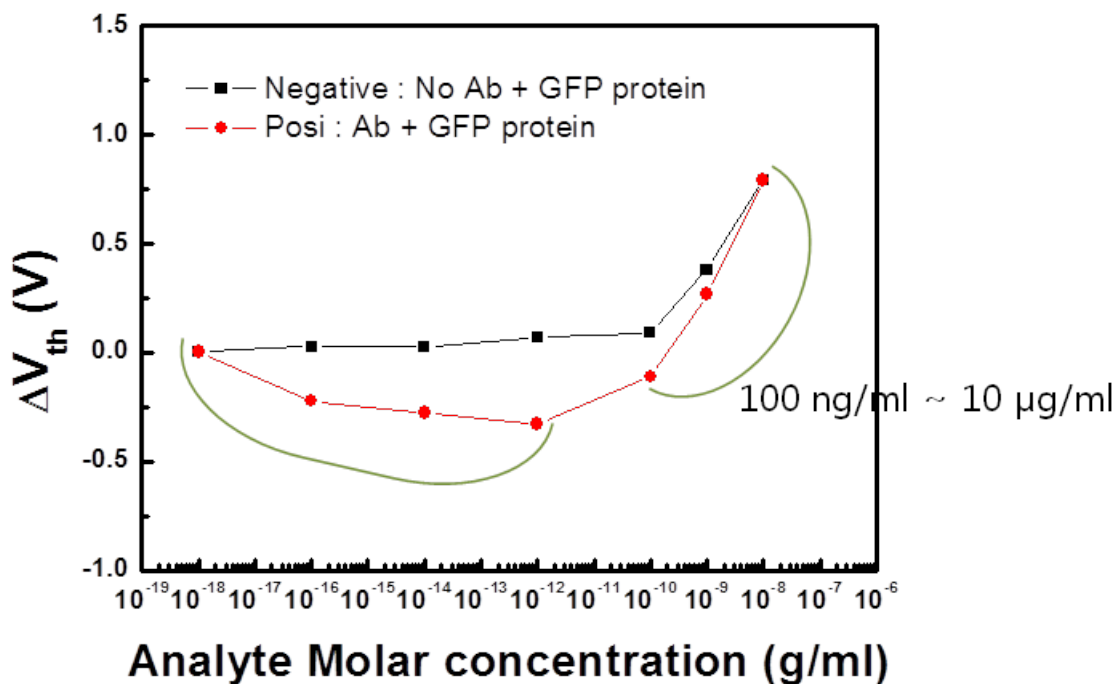


Figure 5.4: The concentration change from DGFET with GFP in PBS buffer

Influence of fluorescein to the DGFET

GFP was used initially as sample since it is possible to observe through a fluorescent microscope. However, we have discovered that the detection limit of GFP was 200 nM, which was already too low since the initial concentration was less than 1 nM. Since the FFITP is able to concentrate about 100-fold, even after FFITP it was difficult to observe the GFP. Therefore, fluorescein was needed for optical guidance so that we can ensure that the GFP is entering the DGFET. Here the concern was whether fluorescein has any influence on the threshold change, since fluorescein also has a charge. Therefore, fluorescein was injected through the FFITP to the DGFET, and the threshold voltage change of the DGFET was observed. As shown in 5.6, also in this case we were not able to see any influence of fluorescein. This gives us the conclusion that fluorescein can be used for optical guidance.

Influence of TRIS buffer to the DGFET

To test the compatibility of the TRIS buffer, a simple experiment was done where the concentration of GFP was increased from 1 fg/ml to 1 ng/ml. Also, as fluorescein was used for optical guidance, it was also tested for the concentration influence of fluorescein. Figure 5.7 (right) shows the threshold voltage shift according to the concentration of the GFP, where it can be obtained that the threshold voltage decreases as the concentration of GFP increases. Also, no influence was detected from fluorescein. The graph was made by

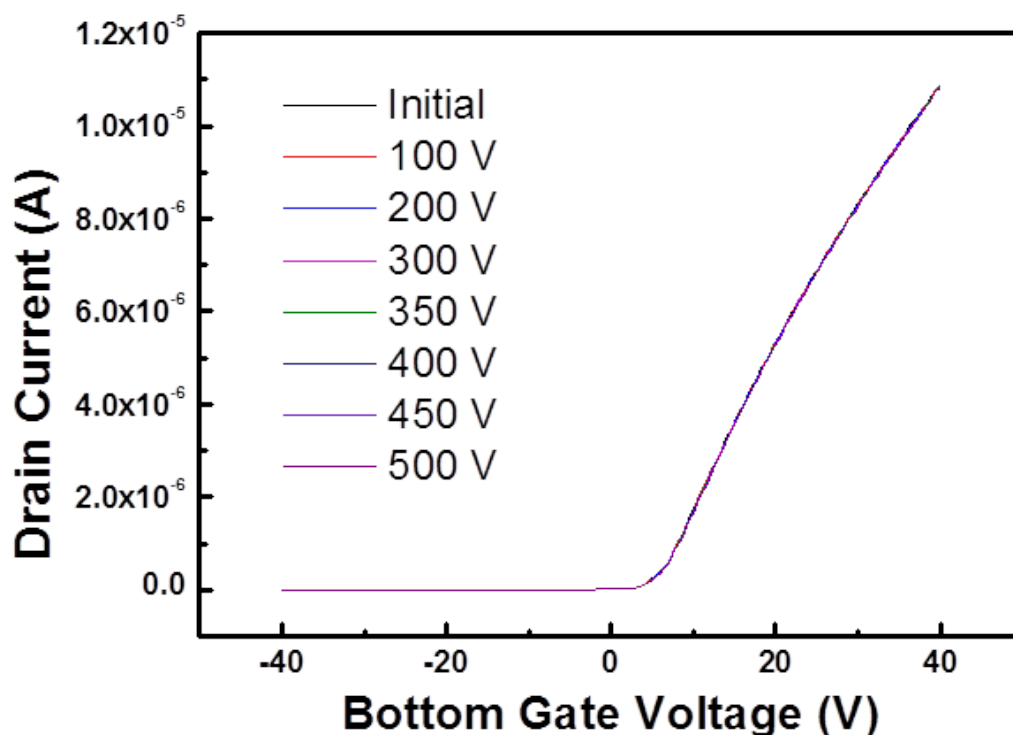


Figure 5.5: The V-I curve by increasing the voltage at the FFITP device.

subtracting of the signal which was achieved with antibodies (Positive signal) and without the antibodies (Negative control)

5.4.4 Coupling of FFITP and DGFET

Since all of the data so far was promising for the final step we connected the FFITP device to the DGFET. With a 10 pg/mL initial concentration of GFP and 2 nM of fluorescein. TRIS buffer was used for this experiment. It was able to observe a threshold voltage change from -0.04451 V to -0.0134 V. Also no influence was observed from fluorescein. Based on these encouraging initial results, we are confident that the online coupling of FFITP-DGFET is possible.

5.5 Conclusion

The connection of FFITP and DGFET is beneficial for both device. DGFET is solving the limitation of the optical detection from the FFITP side. While the FFITP will be able to purify the sample and also simultaneously concentrated the desired sample so that the detection limit of the DGFET will increase. The compatibility of the buffer and

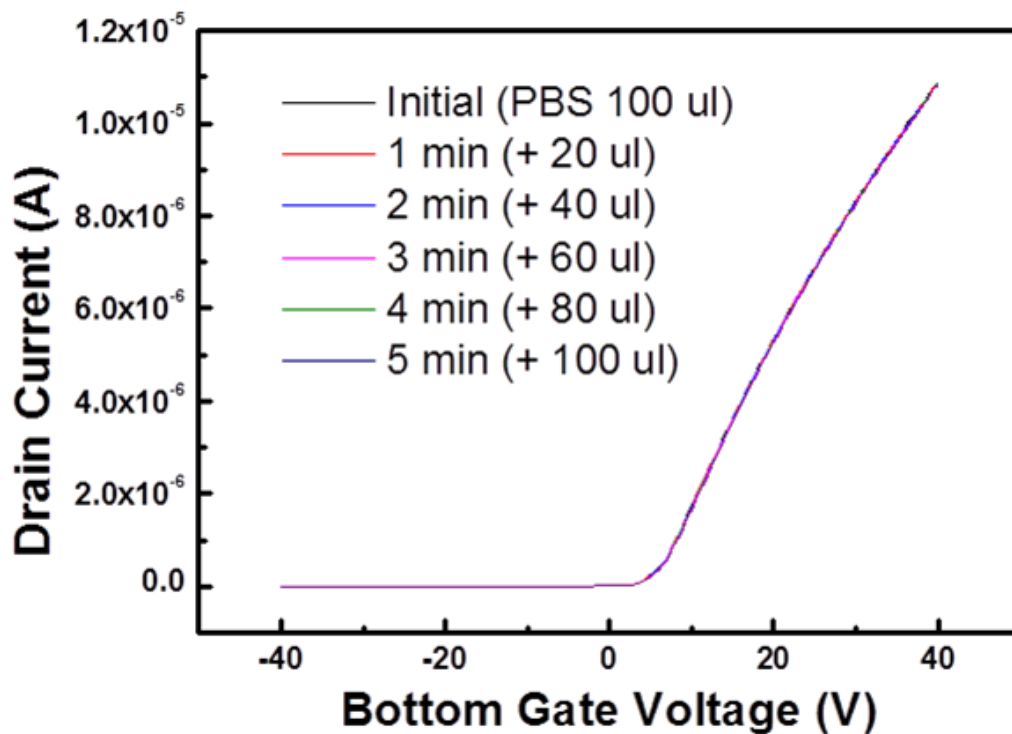


Figure 5.6: The V-I curve with injection of fluorescein to the DGFET via FFITP.

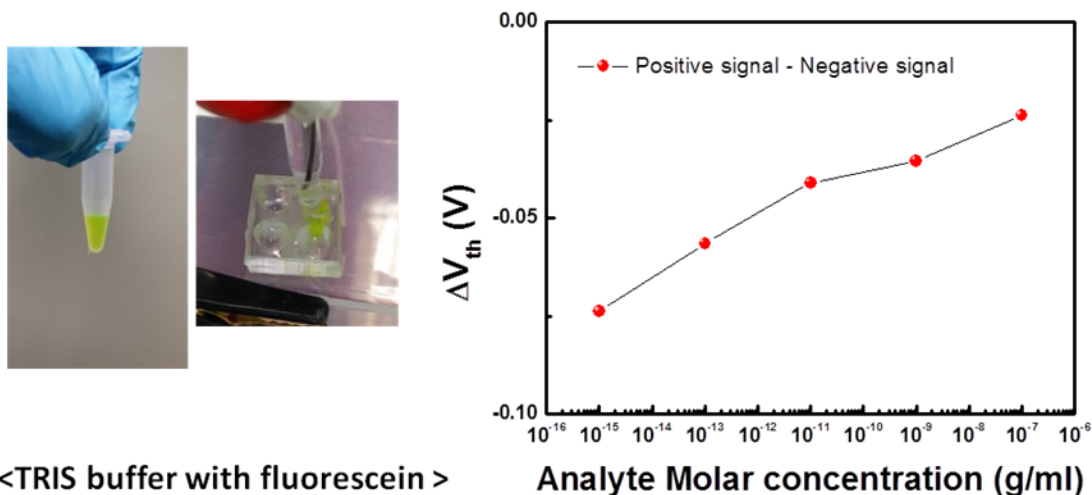


Figure 5.7: Left: TRIS buffer which was injected to the EG via pipette. Right: the threshold voltage change when the GFP concentration was increased from 1 fg/ml to 1 ng/ml

the influence of the electric field to FFITP to the DGFET were tested where the threshold

voltage has changed from -0.04451 V to -0.0134 V before FFITP (GFP: 10 pg/mL, fluorescein 2nM) and after FFITP. Also no influence was observed from fluorescein. Based on these encouraging initial results, we are confident that the online coupling of FFITP-DGFET will solve problems either where the concentration of the target analytes is very low compared to contaminants. However due to the low threshold shift which had an average shift less than 50 mV, where in normal case a signal change of 1V is achieved. We were not confident enough to trust our standard curve and therefore we were not able to conclude the concentration effort of the FFITP. Therefore further studies are required to optimize the condition in DGFET and FFITP.

Chapter 6

Conclusion

A free-flow Isothachophoresis chip was directly connected to an Electrospray-Ionisation-Mass-Spectrometry (ESI-MS) and a Dual-Gate-Field-Effect-Transistor (DGFET). Isothachophoresis is a separation based on two buffers (leading and terminating) with ions of different mobility presence of electric field. This method makes enable focusing of the sample while allowing separation. Free-flow electrophoresis (FFE) separation methods have been developed and investigated for continuous sample preparation and mild separation conditions make it also interesting for online monitoring and detection applications. Here we have combined both methods into continuous free-flow isothachophoresis using micro fabricated glass. The microfluidic device was designed and its pattern was transferred by conventional photolithography and etched by HF/HCl mixture. The device consists of five inlets (I), a separation (main) chamber with the size of $23 * 15mm$, two side chambers for connecting the electrodes and five outlets (O). The three middle inlets are split with a binary tree structure for equal distribution of samples and buffers. Two outer two inlets used to guide flow direction into the main chamber. The side chambers are separated from the main chamber by 25 micro meter wide channels to prevent gas bubbles entering the main chamber. The outlets are designed in similar fashion as the inlets. The relationship with the ITP process and the flow rate as well as the relation chip with the electric field strength and the ITP process was studied. Where it could be observed that the concentration of the ITP process is increasing when the flow rate was lower and the electric was higher, however bubble generation was able to observe when the applied electric field was higher than 1000 V. With this result we were able to conclude the optimal condition for the FFITP chip was when the flow rate was $2 \mu L/min$ and the voltage was 500 V. In order to scan the concentrated the target sample, hydrodynamic control was used in such way that the focus stream was moving to a desired output. Here three method was compared which was applying positive pressure at outlet, applying positive pressure at inlet, and applying negative pressure at the inlet. After comparing the settling time and the shift precision of the three methods we could conclude that applying positive pressure was giv-

ing the best result with a settling time of 45 second and control precision of 30 μm . The online connection with the FFITP-ESI-MS was realized with fused silica tubing. Citric acid, Glycolic acid was used as a target sample and Fluorescein was used as contaminant. Also Alexa flour 488 was used as optical guidance to ensure the position of Citric acid and Glycolic acid. A concentration factor of 3.2 was able to observe and also a fluidic scanning was done which was detected by the ESI-MS. Also a fluidic scanning was demonstrated where it could be Citric acid and Glycolic acid was concentrated which had no interference in the time domain and Fluorescein not able to observed in the entire ESI-MS data output. With this result we could conclude that the online coupling of FFITP to ESI-MS decouples the separation and detection timeframe because the electrophoretic separation takes place perpendicular to the flow direction, which can be beneficial for monitoring (bio)chemical changes and/or extensive MSn studies. Also a feasibility test was done of the FFITP-DGFET. Green fluorescent protein (GFP) was used as target sample where fluorescein was used as an optical guidance. Although we were not able to conclude the exact concentration factor due to several problems, we were able to conclude that the online connection of FFITP to DGFET increases the signal output which was a positive sign that the coupling would lower the detection limit of the sensor. With the encouraging result of the online coupling FFITP-MS and FFITP-DGFET we were able to conclude that the FFITP chip can be used as an interface for sample concentration and purification. This leads to encourage us to do further study with application where the sample should be extracted from a solution where the contaminant has a high concentration and the target sample has a low concentration which should be collect or observed for a relative long time domain.

Chapter 7

Appendix

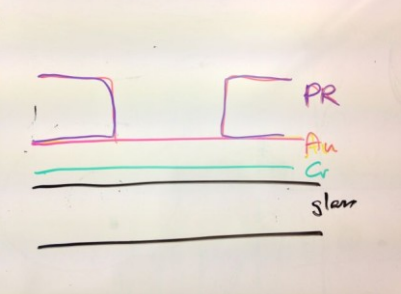
7.1 fabrication protocol

This is the detail process document for the chip fabrication

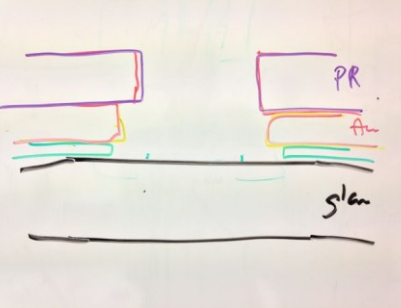
7.1.1 Glass chip

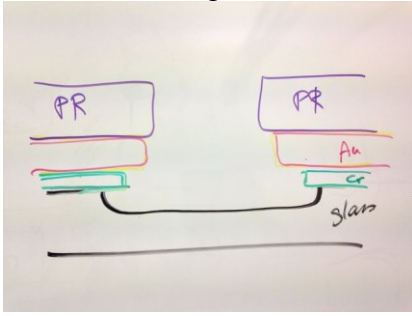
Step	Process	Comment
1	Bottom wafer	
2	<p>Substrate Borofloat BF33-500 μm (#subs114)</p> <p>NL-CLR-Cupboard cleanroom Supplier: Schott Glas: www.schott.com/borofloat</p> <ul style="list-style-type: none"> • Type: Borofloat 33 • C.T.E.: $3.25 \times 10^{-6} \text{ K}^{-1}$ • Tglass: 525°C • T anneal: 560°C • Tsoftening: 820 °C <ul style="list-style-type: none"> • Diameter: 100.0 mm ± 0.3 mm • Thickness: 0.5 mm ± 0.025 mm • Roughness: < 1.0 nm • TTV: < 5 μm • Surface: DSP • Edge: C-edge • Flat: 32.5 mm (Semi) • Sec. Flat: 18 mm (acc to SEMI) • Price 40 euro <ul style="list-style-type: none"> • Etch rate HF 25%: 1μm/min • Etch rate BHF (1:7): 20-25 nm/min • Etchrate HF 1%: 8.6 nm/min 	Number of wafers = 2
3	<p>Clean HNO3 1&2 (#clean105)</p> <p>NL-CLR-WB16</p> <ul style="list-style-type: none"> • Beaker 1: HNO₃ (99%) 5min • Beaker 2: HNO₃ (99%) 5min 	
4	<p>Quick Dump Rinse (QDR) (#clean119)</p> <p>NL-CLR-Wet benches</p> <p>Recipe 1 QDR: 2 cycles of steps 1 till 3, 1- fill bath 5 sec 2- spray dump 15 sec 3- spray-fill 90 sec 4- end fill 200 sec</p> <p>Recipe 2 cascade rinsing: continuous flow Rinse till the DI resistivity is > 10 ΩM</p>	
5	<p>Substrate rinsing/drying Semitool (#clean121)</p> <p>NL-CLR-Wet Benches Semitool spin rinser dryer</p> <p>Apply always a single rinsing step (QDR) before using the Semitool</p> <p>Use dedicated wafer carrier of rinser dryer</p> <p>Parameters/step</p> <ul style="list-style-type: none"> • rinse in DI: 30 sec: 600 rpm • Rinse in DI: 10.0 MΩ; 600 rpm • N2 purge: 10sec; 600 rpm • drying 1: 280 sec; 1600 rpm • drying 2: 0000 - 0000 <p>Unload wafer</p>	
6	<p>Sputtering of Cr (#film117)</p> <p>NL-CLR-Sputterke Eq.Nr. 37</p>	10 nm

	<p>Cr Target (gun #: see mis logbook)</p> <ul style="list-style-type: none"> • Use Ar flow to adjust process pressure. • Base pressure: < 1.0 e-6mbar • Sputter pressure: 6.6 e-3mbar • power: 200W • Depositionrate = 15 nm/min 	
7	<p>Sputtering of Au (#film136)</p> <p>NL-CLR-Eq.Nr. 37 / Sputterke Au Target (gun #: see mis logbook)</p> <ul style="list-style-type: none"> • use Ar flow to adjust pressure • Base pressure: < 1.0 e-6mbar • Sputter pressure: 6.6 e-3mbar • power: 200W • Depositionrate = 45-50 nm/min. • MAX THICKNESS: 250 NM 	150 nm
8	<p>Dehydration bake (#lith102)</p> <p>NL-CLR-WB21/22 dehydration bake at hotplate</p> <ul style="list-style-type: none"> • temp. 120°C • time: 5min 	Continue immediately with priming the step!
9	<p>Priming (liquid) (#lith101)</p> <p>NL-CLR-WB21/22 Primer: HexaMethylDiSilazane (HMDS) use spincoater:</p> <ul style="list-style-type: none"> • program: 4000 (4000rpm, 30sec) 	
10	<p>Coating Olin Oir 907-17 (#lith105)</p> <p>NL-CLR-WB21 Coating: Primus spinner</p> <ul style="list-style-type: none"> • olin oir 907-17 • spin Program: 4000 (4000rpm, 30sec) <p>Prebake: hotplate</p> <ul style="list-style-type: none"> • time 90 sec • temp 95 °C 	1.7 um
11	<p>Alignment & Exposure Olin OiR 907-17 (#lith121)</p> <p>NL-CLR- EV620 Electronic Vision Group EV620 Mask Aligner</p> <ul style="list-style-type: none"> • Hg-lamp: 12 mW/cm² • Exposure Time: 4sec 	mask channels
12	<p>Development Olin OiR resist (#lith111)</p> <p>NL-CLR-WB21 After exposurebBake : hotplate</p> <ul style="list-style-type: none"> • time 60sec • temp 120°C <p>development: developer: OPD4262</p> <ul style="list-style-type: none"> • time: 30sec in beaker 1 • time: 15-30sec in beaker 2 	

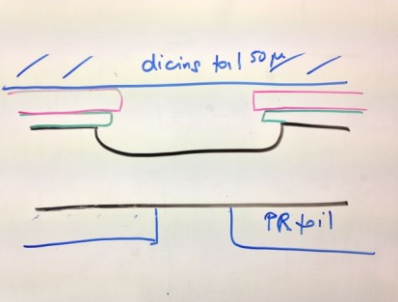
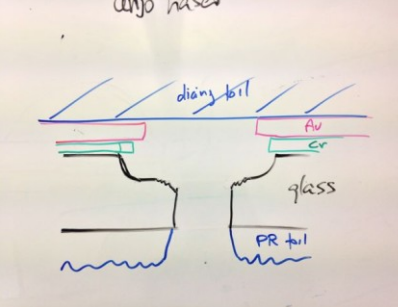
13	<p>Quick Dump Rinse (QDR) (#clean119)</p> <p>NL-CLR-Wet benches Recipe 1 QDR: 2 cycles of steps 1 till 3, 1- fill bath 5 sec 2- spray dump 15 sec 3- spray-fill 90 sec 4- end fill 200 sec Recipe 2 cascade rinsing: continuous flow Rinse till the DI resistivity is > 10 ΩM</p>	
14	<p>Substrate drying (#clean120)</p> <p>NL-CLR-WB Single wafer dryer • speed: 2500 rpm, 60 sec with 30 sec N₂ flow</p>	
15	<p>Postbake Olin OiR resist (#lith109)</p> <p>NL-CLR-WB21 postbake: Hotplate • temp 120°C • time 10min</p>	t=30min
16	<p>Inspection by optical microscope (#metro101)</p> <p>NL-CLR- Nikon Microscope • dedicated microscope for lithography inspection</p>	
17	<p>Cleaning by UV/Ozone (#clean109)</p> <p>NL-CLR-UV PRS 100 reactor -To improve wetting for wet chemical etching of chromium and oxide layers coated with olin oir resist. -To remove resist residues Time: variable</p>	
18	<p>Etching of gold (#etch136)</p> <p>NL-CLR-WB10 Use dedecated beaker with gold etch • recipe: KI:I₂:DI = (4:1:40) • add 40g KI and 10g I₂ to 400ml DI water • temp.: 20°C Etchrates = xx nm/min (check rate with dummy wafer!) Excessive underetching of Cr occurs because of a galvanic reaction with gold. To minimize this make sure you do not overetch the chromium.</p>	
19	<p>Quick Dump Rinse (QDR)</p> <p>NL-CLR-Wet benches Recipe 1 QDR: 2 cycles of steps 1 till 3,</p>	

	(#clean119)	1- fill bath 5 sec 2- spray dump 15 sec 3- spray-fill 90 sec 4- end fill 200 sec Recipe 2 cascade rinsing: continuous flow Rinse till the DI resistivity is > 10 ΩM	
20	Etching of chromium (#etch134)	NL-CLR-WB10 Use dedicated beaker with chromium etch (standard) • temp.:20°C Etchrates = 60nm/min, Check always the etchrate with dummy wafer!	
21	Quick Dump Rinse (QDR) (#clean119)	NL-CLR-Wet benches Recipe 1 QDR: 2 cycles of steps 1 till 3, 1- fill bath 5 sec 2- spray dump 15 sec 3- spray-fill 90 sec 4- end fill 200 sec Recipe 2 cascade rinsing: continuous flow Rinse till the DI resistivity is > 10 ΩM	
22	Etching of gold (#etch136)	NL-CLR-WB10 Use dedecated beaker with gold etch • recipe: KI:I ₂ :DI = (4:1:40) • add 40g KI and 10g I ₂ to 400ml DI water • temp.: 20°C Etchrates = xx nm/min (check rate with dummy wafer!) Excessive underetching of Cr occurs because of a galvanic reaction with gold. To minimize this make sure you do not overetch the chromium.	
23	Quick Dump Rinse (QDR) (#clean119)	NL-CLR-Wet benches Recipe 1 QDR: 2 cycles of steps 1 till 3, 1- fill bath 5 sec 2- spray dump 15 sec 3- spray-fill 90 sec 4- end fill 200 sec Recipe 2 cascade rinsing: continuous flow Rinse till the DI resistivity is > 10 ΩM	
24	Etching of chromium (#etch134)	NL-CLR-WB10 Use dedicated beaker with chromium etch (standard) • temp.:20°C Etchrates = 60nm/min, Check always the etchrate with dummy wafer!	in order to make sure all Cr is gone,

25	<p>Quick Dump Rinse (QDR) (#clean119)</p> <p>NL-CLR-Wet benches Recipe 1 QDR: 2 cycles of steps 1 till 3, 1- fill bath 5 sec 2- spray dump 15 sec 3- spray-fill 90 sec 4- end fill 200 sec Recipe 2 cascade rinsing: continuous flow Rinse till the DI resistivity is > 10 ΩM</p>	
26	<p>Substrate rinsing/drying Semitool (#clean121)</p> <p>NL-CLR-Wet Benches Semitool spin rinser dryer Apply always a single rinsing step (QDR) before using the Semitool Use dedicated wafer carrier of rinser dryer Parameters/step</p> <ul style="list-style-type: none"> • rinse in DI: 30 sec: 600 rpm • Rinse in DI: 10.0 MΩ; 600 rpm • N2 purge: 10sec; 600 rpm • drying 1: 280 sec; 1600 rpm • drying 2: 0000 - 0000 <p>Unload wafers</p>	
27	<p>Surface profile measurement (#metro105)</p> <p>NL-CLR-Veeco Dektak 8</p>	<p>measure thickness stack, to allow measurement of channel depth afterward</p> 
28	<p>Cleaning by UV/Ozone (#clean109)</p> <p>NL-CLR-UV PRS 100 reactor -To improve wetting for wet chemical etching of chromium and oxide layers coated with olin or resist. -To remove resist residues Time: variable</p>	
29	<p>Etching in HF/HCl 25%/2.5% (#etch131UPDATE)</p> <p>NL-CLR-WB09 or 10 Use private beaker for etching: HF (25%) Add one part HF (50%) to one part DI to dilute etch solution. Add one part HCl to 10 parts HF</p> <ul style="list-style-type: none"> • temp.: 20°C <p>Etch rates (function of load):</p>	<p>First etch step to about 4.8 um, than slow etch towards 5.0 um using BHF</p>

	<ul style="list-style-type: none"> • borofloat BF33: 1 $\mu\text{m}/\text{min}$ in 25% HF <p>BHF (1:7 dilution) for last step. Etchrate 23 nm/min.</p>	
30	<p>Quick Dump Rinse (QDR) (#clean119)</p> <p>NL-CLR-Wet benches Recipe 1 QDR: 2 cycles of steps 1 till 3, 1- fill bath 5 sec 2- spray dump 15 sec 3- spray-fill 90 sec 4- end fill 200 sec Recipe 2 cascade rinsing: continuous flow Rinse till the DI resistivity is $> 10 \Omega\text{M}$</p>	
31	<p>Substrate rinsing/drying Semitool (#clean121)</p> <p>NL-CLR-Wet Benches Semitool spin rinser dryer Apply always a single rinsing step (QDR) before using the Semitool Use dedicated wafer carrier of rinser dryer Parameters/step</p> <ul style="list-style-type: none"> • rinse in DI: 30 sec: 600 rpm • Rinse in DI: 10.0 MΩ; 600 rpm • N2 purge: 10sec; 600 rpm • drying 1: 280 sec; 1600 rpm • drying 2: 0000 - 0000 <p>Unload wafers</p>	
32	<p>Surface profile measurement (#metro105)</p> <p>NL-CLR-Veeco Dektak 8</p>	<p>measure etch depth</p> 
33	<p>Repeat from 28, and continue etching until depth=5μm. Be aware subtract the PR/Cr/Au film from the profilometer data (PR thickness + 160 nm). Use BHF Er=23 nm/min for last etch steps to slow down.</p>	<p>Precision required 5.0\pm0.2 μm.</p>
34	<p>Quick Dump Rinse (QDR) (#clean119)</p> <p>NL-CLR-Wet benches Recipe 1 QDR: 2 cycles of steps 1 till 3, 1- fill bath 5 sec 2- spray dump 15 sec 3- spray-fill 90 sec 4- end fill 200 sec Recipe 2 cascade rinsing: continuous flow</p>	

		Rinse till the DI resistivity is > 10 ΩM	
35	Substrate rinsing/drying Semitool (#clean121)	NL-CLR-Wet Benches Semitool spin rinser dryer Apply always a single rinsing step (QDR) before using the Semitool Use dedicated wafer carrier of rinser dryer Parameters/step <ul style="list-style-type: none"> • rinse in DI: 30 sec: 600 rpm • Rinse in DI: 10.0 MΩ; 600 rpm • N2 purge: 10sec; 600 rpm • drying 1: 280 sec; 1600 rpm • drying 2: 0000 - 0000 Unload wafers	
36	Clean HNO3 1&2 (#clean105)	NL-CLR-WB16 <ul style="list-style-type: none"> • Beaker 1: HNO₃ (99%) 5min • Beaker 2: HNO₃ (99%) 5min 	Stripping resist
37			
38			
39	Lamination of BF 410 foil (#lith145)	NL-CLR-GBC 3500 PRO Laminator Ordyl BF 410 dry resist foil Laminate BF 410 foil on one side <ul style="list-style-type: none"> • Protect hotplate with Aluminium foil • Put wafer on hotplate, 100 °C, 180 sec • Remove thick PET layer from BF 410 foil • Apply BF 410 foil with roller • Protect carry-paper with plain A4 paper • Close carrier and laminate • Temp: 130 °C ('carry 'preset) • Speed: 2 ('carry 'preset) • Remove and cool down wafer • Cut the wafer out of foil 	
40	Alignment and exposure BF410 (#lith135)	NL-CLR-EVG 20 Electronic Vision Group 20 Mask Aligner <ul style="list-style-type: none"> • Hg-lamp: 12 W.cm² • Exposure time: 20 sec (BF 410) Remark: DSP alignment with foil on both sides <ul style="list-style-type: none"> • Remove the foil with a "knife" to achieve a clear view of the aligning marks • After development protect the aligning mask with tape again! 	Using holes mask
41	UV dicing foil (Adwill D-210)	NL-CLR- Dicing foil Information: Thickness: 125um	On other side as BF410

	<p>(#back104)</p> <p>Material: 100um PET + 25um Acrylic (adhesive) Adhesion before UV: 2000 mN/25mm Adhesion after UV : 15 mN/25mm UV irradiation : Luminance > 120mW/cm² and Quality > 70mJ/cm² (wave length: 365nm)</p>	
42	<p>Development BF410 foil (#lith136)</p> <p>Carre-TST-HCM Spray Developer Na₂CO₃: MERCK 1.06392.0500 Na₂CO₃:H₂O = 15g : 7.5liters (+ 1 cup Antifoam)</p> <ul style="list-style-type: none"> • Temp: 32°C • Time: 3min • Rinsing • Spin drying <p>Due to non-uniform development turn sample by 180° after half the time - small features might need longer development time</p>	
43	<p>Powderblasting of glass (#etch120)</p> <p>NL-Carre-BIOS Powderblaster For feature size >100µm</p> <ul style="list-style-type: none"> • Particles: 30µm Al₂O₃ • Pressure: 4.6bar • Massflow: 3-12 g/min • Etchrate appr. 91µm per g/cm² 	<p>Powderblast into, maybe through the dicing foil</p>
44		
45	<p>Removal of foil and particles after powderblasting (#clean139)</p> <p>Outside cleanroom - use own facility Start with removal of foil</p> <ul style="list-style-type: none"> • remove dicing foil manually • remove powderblast foil manually • rinse wafer with water (by spraying) to remove powderblast particles • strip foil in Na₂CO₃¹ solution, time >30 min • rinse wafer with water time > few minutes • ultrasonic cleaning in water, time >10 min • ultrasonic cleaning in fresh water, time >10 min • drying of substrate by spinning or N₂ gun <p>Note 1: For silicon substrates the stripping procedure in Na₂CO₃ solution is critical.</p>	

		<p>The Na₂CO₃ solution may create a rough surface. #If wafer bonding is needed the silicon surface should be protected by an oxide film.</p>	
46	<p>Removal of particles (#clean110)</p>	<p>NL-CLR-Wet Bench11 Removal of particles generated by powderblasting and /or metal lift-off. Use ultrasonic bath 1 Use dedicated metal beakers and carriers</p> <ul style="list-style-type: none"> • beaker 1: Aceton technical, > 10 min , ultrasonic • beaker 2: Isopropanol technical > 10min, ultrasonic • beaker 3: DI water > 10min, ultrasonic 	
47	<p>Quick Dump Rinse (QDR) (#clean119)</p>	<p>NL-CLR-Wet benches Recipe 1 QDR: 2 cycles of steps 1 till 3, 1- fill bath 5 sec 2- spray dump 15 sec 3- spray-fill 90 sec 4- end fill 200 sec Recipe 2 cascade rinsing: continuous flow Rinse till the DI resistivity is > 10 ΩM</p>	
48	<p>Substrate drying (#clean120)</p>	<p>NL-CLR-WB Single wafer dryer</p> <ul style="list-style-type: none"> • speed: 2500 rpm, 60 sec with 30 sec N₂ flow 	
49	<p>Surface profile measurement (#metro105)</p>	<p>NL-CLR-Veeco Dektak 8</p>	<p>Here the exact channel depth is determined</p>
50			
51	<p>Etching of gold (#etch136)</p>	<p>NL-CLR-WB10 Use dedecated beaker with gold etch</p> <ul style="list-style-type: none"> • recipe: KI:I₂:DI = (4:1:40) • add 40g KI and 10g I₂ to 400ml DI water • temp.: 20°C <p>Etchrates = xx nm/min (check rate with dummy wafer!) Excessive underetching of Cr occurs because of a galvanic reaction with gold. To minimize this make sure you do not overetch the chromium.</p>	
52	<p>Etching of chromium (#etch134)</p>	<p>NL-CLR-WB10 Use dedicated beaker with chromium etch (standard)</p>	

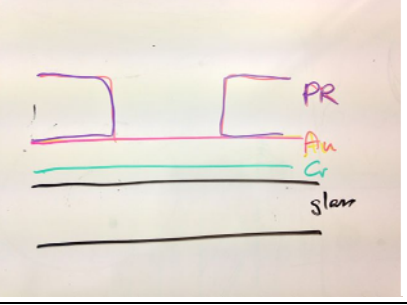
		<ul style="list-style-type: none"> temp.:20°C Etchrates = 60nm/min, Check always the etchrate with dummy wafer!	
53	Etching of gold (#etch136)	NL-CLR-WB10 Use dedecated beaker with gold etch <ul style="list-style-type: none"> recipe: KI:I₂:DI = (4:1:40) add 40g KI and 10g I₂ to 400ml DI water temp.: 20°C Etchrates = xx nm/min (check rate with dummy wafer!) Excessive underetching of Cr occurs because of a galvanic reaction with gold. To minimize this make sure you do not overetch the chromium.	
54	Etching of chromium (#etch134)	NL-CLR-WB10 Use dedicated beaker with chromium etch (standard) <ul style="list-style-type: none"> temp.:20°C Etchrates = 60nm/min, Check always the etchrate with dummy wafer!	
55	Clean HNO3 1&2 (#clean105)	NL-CLR-WB16 <ul style="list-style-type: none"> Beaker 1: HNO₃ (99%) 5min Beaker 2: HNO₃ (99%) 5min 	Both new top wafer and bottom wafer
56	Etching in KOH standard (#etch138)	NL CLR WB17 use dedicated beaker 1 or 2 <ul style="list-style-type: none"> 25wt% KOH (standard recipe) temp.: 75°C use stirrer Etchrates: Si <100> = 1µm/min Si <111> = 12.5nm/min SiO ₂ (thermal) = 180nm/hr SiRN < 0.6nm/hr (LPCVD ??)	To obtain good prebond
57	Clean HNO3 1&2 (#clean105)	NL CLR WB16 <ul style="list-style-type: none"> Beaker 1: HNO₃ (99%) 5min Beaker 2: HNO₃ (99%) 5min 	
57	Clean Piranha		To obtain good prebond
58	EV620 Aligning & Prebonding (#bond104)	NL-CLR-EV620 mask aligner Program: xxxxx <ul style="list-style-type: none"> SDB Direct Bond tool 4" Bond chuck SDB Substrate1 4" Substrate2 4" Separation 30 µm No exposure SDB Piston Bond time 60 sec Instructions: <ul style="list-style-type: none"> Align alignmarks of of top wafer to crosshairs 	

		<ul style="list-style-type: none"> • Check prebonding by using IR-setup 	
59	-position waferstack in press -Temp:650 Fahrenheit - Apply force: 'Max.pressure Dorothee' *clean chuck with acetone *position wafers (centre) *turn on heating *apply pressure T>550 F *Max.pressure: if valve is closed tightly, max		
60	At Mic-Mec Lab. temp:600-650 C, t=60min. Place stack on Si-wafer carrier		
61			
62			Dicing bonded wafers
63	<p>Dicing of a Silicon wafer (#back101)</p> <p>NI-CLR- Disco DAD dicing saw Applications: Silicon wafers, bonded silicon-silicon wafers (max 1.1mm) See #back103 for laminate of Nitto STW T10 dicing foil (80 μm) See #back104 for laminate of UV dicing foil (250μm)</p> <p>Parameters dicing: Wafer work size: 110 mm for a standard 100 mm silicon wafer Max. Feed speed: 10 mm/sec X, Y values: correspond respectively to Ch1 and Ch2 and those values are determined by mask layout Saw type NBC-Z 2050 Select in blade menu: NBC-Z-2050</p> <p>Blade info: Exposure 1.3 mm (maximum dicing depth for a new blade) Width: 50 μm Spindle revolutions: 30. 000 rpm Depth settings: Maximum cut depth: 1.1 mm Foil thickness: See foil info Min. blade heighth: 50 μm</p>	<p>dicing from single side, completely though the wafer</p>	

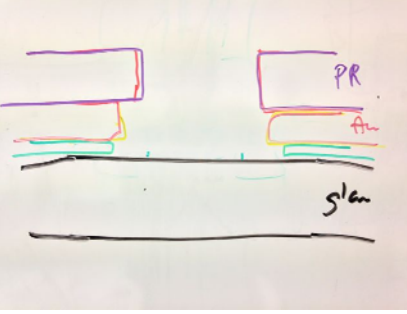
7.1.2 SU8 chip

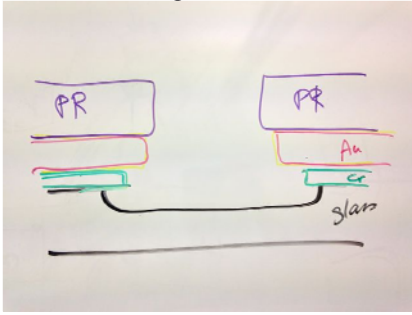
Step	Process	Comment
1	5 um channel wafer	
2	<p>Substrate Borofloat BF33-500 μm (#subs114)</p> <p>NL-CLR-Cupboard cleanroom Supplier: Schott Glas: www.schott.com/borofloat</p> <ul style="list-style-type: none"> • Type: Borofloat 33 • C.T.E.: $3.25 \times 10^{-6} \text{ K}^{-1}$ • Tglass: 525°C • T anneal: 560°C • Tsoftening: 820 °C <ul style="list-style-type: none"> • Diameter: 100.0 mm ± 0.3 mm • Thickness: 0.5 mm ± 0.025 mm • Roughness: < 1.0 nm • TTV: < 5 μm • Surface: DSP • Edge: C-edge • Flat: 32.5 mm (Semi) • Sec. Flat: 18 mm (acc to SEMI) • Price 40 euro <ul style="list-style-type: none"> • Etch rate HF 25%: 1 μm/min • Etch rate BHF (1:7): 20-25 nm/min • Etchrate HF 1%: 8.6 nm/min 	Number of wafers = 2
3	<p>Clean HNO3 1&2 (#clean105)</p> <p>NL-CLR-WB16</p> <ul style="list-style-type: none"> • Beaker 1: HNO₃ (99%) 5min • Beaker 2: HNO₃ (99%) 5min 	
4	<p>Quick Dump Rinse (QDR) (#clean119)</p> <p>NL-CLR-Wet benches</p> <p>Recipe 1 QDR: 2 cycles of steps 1 till 3, 1- fill bath 5 sec 2- spray dump 15 sec 3- spray-fill 90 sec 4- end fill 200 sec</p> <p>Recipe 2 cascade rinsing: continuous flow Rinse till the DI resistivity is > 10 ΩM</p>	
5	<p>Substrate rinsing/drying Semitool (#clean121)</p> <p>NL-CLR-Wet Benches Semitool spin rinser dryer</p> <p>Apply always a single rinsing step (QDR) before using the Semitool</p> <p>Use dedicated wafer carrier of rinser dryer</p> <p>Parameters/step</p> <ul style="list-style-type: none"> • rinse in DI: 30 sec; 600 rpm • Qrinse in DI: 10.0 MΩ; 600 rpm • N2 purge: 10sec; 600 rpm • drying 1: 280 sec; 1600 rpm • drying 2: 0000 - 0000 <p>Unload wafer</p>	
6	<p>Sputtering of Cr (#film117)</p> <p>NL-CLR-Sputterke Eq.Nr. 37</p>	10 nm

	<p>Cr Target (gun #: see mis logbook)</p> <ul style="list-style-type: none"> • Use Ar flow to adjust process pressure. • Base pressure: < 1.0 e-6mbar • Sputter pressure: 6.6 e-3mbar • power: 200W • Depositionrate = 15 nm/min 	
7	<p>Sputtering of Au (#film136)</p> <p>NL-CLR-Eq.Nr. 37 / Sputterke Au Target (gun #: see mis logbook)</p> <ul style="list-style-type: none"> • use Ar flow to adjust pressure • Base pressure: < 1.0 e-6mbar • Sputter pressure: 6.6 e-3mbar • power: 200W • Depositionrate = 45-50 nm/min. • MAX THICKNESS: 250 NM 	150 nm
8	<p>Dehydration bake (#lith102)</p> <p>NL-CLR-WB21/22 dehydration bake at hotplate</p> <ul style="list-style-type: none"> • temp. 120°C • time: 5min 	Continue immediately with priming the step!
9	<p>Priming (liquid) (#lith101)</p> <p>NL-CLR-WB21/22 Primer: HexaMethylDiSilazane (HMDS) use spincoater:</p> <ul style="list-style-type: none"> • program: 4000 (4000rpm, 30sec) 	
10	<p>Coating Olin Oir 907-17 (#lith105)</p> <p>NL-CLR-WB21 Coating: Primus spinner</p> <ul style="list-style-type: none"> • olin oir 907-17 • spin Program: 4000 (4000rpm, 30sec) <p>Prebake: hotplate</p> <ul style="list-style-type: none"> • time 90 sec • temp 95 °C 	1.7 um
11	<p>Alignment & Exposure Olin OiR 907-17 (#lith121)</p> <p>NL-CLR- EV620 Electronic Vision Group EV620 Mask Aligner</p> <ul style="list-style-type: none"> • Hg-lamp: 12 mW/cm² • Exposure Time: 4sec 	mask channels (layet number 10)
12	<p>Development Olin OiR resist (#lith111)</p> <p>NL-CLR-WB21 After exposurebBake : hotplate</p> <ul style="list-style-type: none"> • time 60sec • temp 120°C <p>development: developer: OPD4262</p> <ul style="list-style-type: none"> • time: 30sec in beaker 1 • time: 15-30sec in beaker 2 	

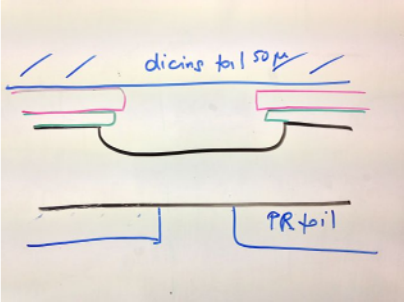
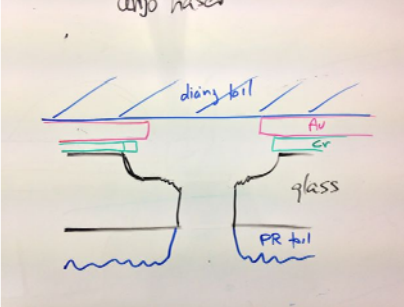
13	<p>Quick Dump Rinse (QDR) (#clean119)</p> <p>NL-CLR-Wet benches Recipe 1 QDR: 2 cycles of steps 1 till 3, 1- fill bath 5 sec 2- spray dump 15 sec 3- spray-fill 90 sec 4- end fill 200 sec Recipe 2 cascade rinsing: continuous flow Rinse till the DI resistivity is > 10 ΩM</p>	
14	<p>Substrate drying (#clean120)</p> <p>NL-CLR-WB Single wafer dryer • speed: 2500 rpm, 60 sec with 30 sec N₂ flow</p>	
15	<p>Postbake Olin OiR resist (#lith109)</p> <p>NL-CLR-WB21 postbake: Hotplate • temp 120°C • time 10min</p>	t=30min
16	<p>Inspection by optical microscope (#metro101)</p> <p>NL-CLR- Nikon Microscope • dedicated microscope for lithography inspection</p>	
17	<p>Cleaning by UV/Ozone (#clean109)</p> <p>NL-CLR-UV PRS 100 reactor -To improve wetting for wet chemical etching of chromium and oxide layers coated with olin oir resist. -To remove resist residues Time: variable</p>	
18	<p>Etching of gold (#etch136)</p> <p>NL-CLR-WB10 Use dedecated beaker with gold etch • recipe: KI:I₂:DI = (4:1:40) • add 40g KI and 10g I₂ to 400ml DI water • temp.: 20°C Etchrates = xx nm/min (check rate with dummy wafer!) Excessive underetching of Cr occurs because of a galvanic reaction with gold. To minimize this make sure you do not overetch the chromium.</p>	
19	<p>Quick Dump Rinse (QDR)</p> <p>NL-CLR-Wet benches Recipe 1 QDR: 2 cycles of steps 1 till 3,</p>	

	(#clean119)	<p>1- fill bath 5 sec 2- spray dump 15 sec 3- spray-fill 90 sec 4- end fill 200 sec Recipe 2 cascade rinsing: continuous flow Rinse till the DI resistivity is > 10 ΩM</p>	
20	Etching of chromium (#etch134)	<p>NL-CLR-WB10 Use dedicated beaker with chromium etch (standard) • temp.:20°C Etchrates = 60nm/min, Check always the etchrate with dummy wafer!</p>	
21	Quick Dump Rinse (QDR) (#clean119)	<p>NL-CLR-Wet benches Recipe 1 QDR: 2 cycles of steps 1 till 3, 1- fill bath 5 sec 2- spray dump 15 sec 3- spray-fill 90 sec 4- end fill 200 sec Recipe 2 cascade rinsing: continuous flow Rinse till the DI resistivity is > 10 ΩM</p>	
22	Etching of gold (#etch136)	<p>NL-CLR-WB10 Use dedecated beaker with gold etch • recipe: KI:I₂:DI = (4:1:40) • add 40g KI and 10g I₂ to 400ml DI water • temp.: 20°C Etchrates = xx nm/min (check rate with dummy wafer!) Excessive underetching of Cr occurs because of a galvanic reaction with gold. To minimize this make sure you do not overetch the chromium.</p>	
23	Quick Dump Rinse (QDR) (#clean119)	<p>NL-CLR-Wet benches Recipe 1 QDR: 2 cycles of steps 1 till 3, 1- fill bath 5 sec 2- spray dump 15 sec 3- spray-fill 90 sec 4- end fill 200 sec Recipe 2 cascade rinsing: continuous flow Rinse till the DI resistivity is > 10 ΩM</p>	
24	Etching of chromium (#etch134)	<p>NL-CLR-WB10 Use dedicated beaker with chromium etch (standard) • temp.:20°C Etchrates = 60nm/min, Check always the etchrate with dummy wafer!</p>	in order to make sure all Cr is gone,

25	<p>Quick Dump Rinse (QDR) (#clean119)</p> <p>NL-CLR-Wet benches Recipe 1 QDR: 2 cycles of steps 1 till 3, 1- fill bath 5 sec 2- spray dump 15 sec 3- spray-fill 90 sec 4- end fill 200 sec Recipe 2 cascade rinsing: continuous flow Rinse till the DI resistivity is > 10 ΩM</p>	
26	<p>Substrate rinsing/drying Semitool (#clean121)</p> <p>NL-CLR-Wet Benches Semitool spin rinser dryer Apply always a single rinsing step (QDR) before using the Semitool Use dedicated wafer carrier of rinser dryer Parameters/step</p> <ul style="list-style-type: none"> • rinse in DI: 30 sec: 600 rpm • Qrinse in DI: 10.0 MΩ; 600 rpm • N2 purge: 10sec; 600 rpm • drying 1: 280 sec; 1600 rpm • drying 2: 0000 - 0000 <p>Unload wafers</p>	
27	<p>Surface profile measurement (#metro105)</p> <p>NL-CLR-Veeco Dektak 8</p>	<p>measure thickness stack, to allow measurement of channel depth afterward</p> 
28	<p>Cleaning by UV/Ozone (#clean109)</p> <p>NL-CLR-UV PRS 100 reactor -To improve wetting for wet chemical etching of chromium and oxide layers coated with olin or resist. -To remove resist residues Time: variable</p>	
29	<p>Etching in HF/HCl 25%/2.5% (#etch131UPDATE)</p> <p>NL-CLR-WB09 or 10 Use private beaker for etching: HF (25%) Add one part HF (50%) to one part DI to dilute etch solution. Add one part HCl to 10 parts HF</p> <ul style="list-style-type: none"> • temp.: 20°C <p>Etchrates (function of load):</p>	<p>First etch step to about 4.8 um, than slow etch towards 5.0 um using BHF</p>

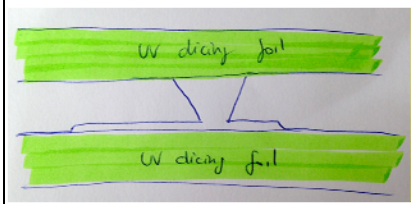
	<ul style="list-style-type: none"> • borofloat BF33: 1 $\mu\text{m}/\text{min}$ in 25% HF <p>BHF (1:7 dilution) for last step. Etchrate 23 nm/min.</p>	
30	<p>Quick Dump Rinse (QDR) (#clean119)</p> <p>NL-CLR-Wet benches Recipe 1 QDR: 2 cycles of steps 1 till 3, 1- fill bath 5 sec 2- spray dump 15 sec 3- spray-fill 90 sec 4- end fill 200 sec Recipe 2 cascade rinsing: continuous flow Rinse till the DI resistivity is $> 10 \Omega\text{M}$</p>	
31	<p>Substrate rinsing/drying Semitool (#clean121)</p> <p>NL-CLR-Wet Benches Semitool spin rinser dryer Apply always a single rinsing step (QDR) before using the Semitool Use dedicated wafer carrier of rinser dryer Parameters/step</p> <ul style="list-style-type: none"> • rinse in DI: 30 sec; 600 rpm • Qrinse in DI: 10.0 MΩ; 600 rpm • N2 purge: 10sec; 600 rpm • drying 1: 280 sec; 1600 rpm • drying 2: 0000 - 0000 <p>Unload wafers</p>	
32	<p>Surface profile measurement (#metro105)</p> <p>NL-CLR-Veeco Dektak 8</p>	<p>measure etch depth</p> 
33	<p>Repeat from 28, and continue etching until depth=5μm. Be aware subtract the PR/Cr/Au film from the profilometer data (PR thickness + 160 nm). Use BHF Er=23 nm/min for last etch steps to slow down.</p>	<p>Precision required 5.0\pm0.2 μm.</p>
34	<p>Quick Dump Rinse (QDR) (#clean119)</p> <p>NL-CLR-Wet benches Recipe 1 QDR: 2 cycles of steps 1 till 3, 1- fill bath 5 sec 2- spray dump 15 sec 3- spray-fill 90 sec 4- end fill 200 sec Recipe 2 cascade rinsing: continuous flow</p>	

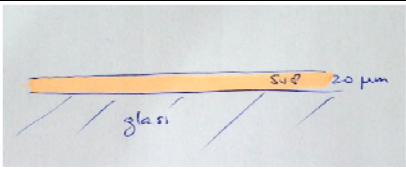
		Rinse till the DI resistivity is > 10 ΩM	
35	Substrate rinsing/drying Semitool (#clean121)	NL-CLR-Wet Benches Semitool spin rinser dryer Apply always a single rinsing step (QDR) before using the Semitool Use dedicated wafer carrier of rinser dryer Parameters/step <ul style="list-style-type: none"> • rinse in DI: 30 sec; 600 rpm • Rinse in DI: 10.0 MΩ; 600 rpm • N2 purge: 10sec; 600 rpm • drying 1: 280 sec; 1600 rpm • drying 2: 0000 - 0000 Unload wafers	
36	Clean HNO3 1&2 (#clean105)	NL-CLR-WB16 <ul style="list-style-type: none"> • Beaker 1: HNO₃ (99%) 5min • Beaker 2: HNO₃ (99%) 5min 	Stripping resist
37			
38			
39	Lamination of BF 410 foil (#lith145)	NL-CLR-GBC 3500 PRO Laminator Ordyl BF 410 dry resist foil Laminate BF 410 foil on one side <ul style="list-style-type: none"> • Protect hotplate with Aluminium foil • Put wafer on hotplate, 100 °C, 180 sec • Remove thick PET layer from BF 410 foil • Apply BF 410 foil with roller • Protect carry-paper with plain A4 paper • Close carrier and laminate • Temp: 130 °C ('carry 'preset) • Speed: 2 ('carry 'preset) • Remove and cool down wafer • Cut the wafer out of foil 	
40	Alignment and exposure BF410 (#lith135)	NL-CLR-EVG 20 Electronic Vision Group 20 Mask Aligner <ul style="list-style-type: none"> • Hg-lamp: 12 W.cm² • Exposure time: 20 sec (BF 410) Remark: DSP alignment with foil on both sides <ul style="list-style-type: none"> • Remove the foil with a "knife" to achieve a clear view of the aligning marks • After development protect the aligning mask with tape again! 	Using holes mask (Layer number 30)
41	UV dicing foil (Adwill D-210)	NI-CLR- Dicing foil Information: Thickness: 125um	On other side as BF410

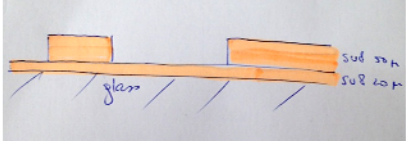
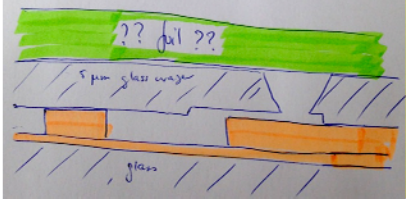
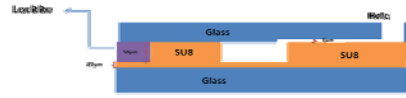
	<p>(#back104)</p> <p>Material: 100um PET + 25um Acrylic (adhesive) Adhesion before UV: 2000 mN/25mm Adhesion after UV : 15 mN/25mm UV irradiation : Luminance > 120mW/cm² and Quality > 70mJ/cm² (wave length: 365nm)</p>	
42	<p>Development BF410 foil (#lith136)</p> <p>Carre-TST-HCM Spray Developer Na₂CO₃: MERCK 1.06392.0500 Na₂CO₃:H₂O = 15g : 7.5liters (+ 1 cup Antifoam)</p> <ul style="list-style-type: none"> • Temp: 32°C • Time: 3min • Rinsing • Spin drying <p>Due to non-uniform development turn sample by 180° after half the time - small features might need longer development time</p>	 <p>The diagram shows a cross-section of a wafer. At the top, there is a layer labeled 'dicing foil 50µm'. Below it, there are two rectangular regions representing features. Underneath these features, there is a layer labeled 'PR foil'. The wafer is shown with a central hole.</p>
43	<p>Powderblasting of glass (#etch120)</p> <p>NL-Carre-BIOS Powderblaster For feature size >100µm</p> <ul style="list-style-type: none"> • Particles: 30µm Al₂O₃ • Pressure: 4.6bar • Massflow: 3-12 g/min • Etchrate appr. 91µm per g/cm² 	<p>Powderblast into, maybe through the dicing foil</p>
44		 <p>The diagram shows a cross-section of a wafer. At the top, there is a layer labeled 'dicing foil'. Below it, there are two rectangular regions representing features. Underneath these features, there is a layer labeled 'glass'. At the bottom, there is a layer labeled 'PR foil'. The wafer is shown with a central hole.</p>
45	<p>Removal of foil and particles after powderblasting (#clean139)</p> <p>Outside cleanroom - use own facility</p> <p>Start with removal of foil</p> <ul style="list-style-type: none"> • remove dicing foil manually • remove powderblast foil manually • rinse wafer with water (by spraying) to remove powderblast particles • strip foil in Na₂CO₃¹ solution, time >30 min • rinse wafer with water time > few minutes • ultrasonic cleaning in water, time >10 min • ultrasonic cleaning in fresh water, time >10 min • drying of substrate by spinning or N₂ gun <p>Note 1: For silicon substrates the stripping procedure in Na₂CO₃ solution is critical.</p>	

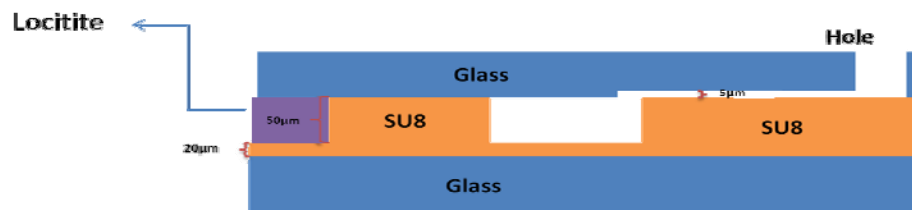
		<p>The Na₂CO₃ solution may create a rough surface. #If wafer bonding is needed the silicon surface should be protected by an oxide film.</p>	
46	<p>Removal of particles (#clean110)</p>	<p>NL-CLR-Wet Bench11 Removal of particles generated by powderblasting and /or metal lift-off. Use ultrasonic bath 1 Use dedicated metal beakers and carriers</p> <ul style="list-style-type: none"> • beaker 1: Aceton technical, > 10 min , ultrasonic • beaker 2: Isopropanol technical > 10min, ultrasonic • beaker 3: DI water > 10min, ultrasonic 	
47	<p>Quick Dump Rinse (QDR) (#clean119)</p>	<p>NL-CLR-Wet benches Recipe 1 QDR: 2 cycles of steps 1 till 3, 1- fill bath 5 sec 2- spray dump 15 sec 3- spray-fill 90 sec 4- end fill 200 sec Recipe 2 cascade rinsing: continuous flow Rinse till the DI resistivity is > 10 ΩM</p>	
48	<p>Substrate drying (#clean120)</p>	<p>NL-CLR-WB Single wafer dryer</p> <ul style="list-style-type: none"> • speed: 2500 rpm, 60 sec with 30 sec N₂ flow 	
49	<p>Surface profile measurement (#metro105)</p>	<p>NL-CLR-Veeco Dektak 8</p>	<p>Here the exact channel depth is determined</p>
50			
51	<p>Etching of gold (#etch136)</p>	<p>NL-CLR-WB10 Use dedecated beaker with gold etch</p> <ul style="list-style-type: none"> • recipe: KI:I₂:DI = (4:1:40) • add 40g KI and 10g I₂ to 400ml DI water • temp.: 20°C <p>Etchrates = xx nm/min (check rate with dummy wafer!) Excessive underetching of Cr occurs because of a galvanic reaction with gold. To minimize this make sure you do not overetch the chromium.</p>	
52	<p>Etching of chromium (#etch134)</p>	<p>NL-CLR-WB10 Use dedicated beaker with chromium etch (standard)</p>	

		<ul style="list-style-type: none"> temp.: 20°C Etchrates = 60nm/min, Check always the etchrate with dummy wafer!	
53	Etching of gold (#etch136)	NL-CLR-WB10 Use dedecated beaker with gold etch <ul style="list-style-type: none"> recipe: KI:I₂:DI = (4:1:40) add 40g KI and 10g I₂ to 400ml DI water temp.: 20°C Etchrates = xx nm/min (check rate with dummy wafer!) Excessive underetching of Cr occurs because of a galvanic reaction with gold. To minimize this make sure you do not overetch the chromium.	
54	Etching of chromium (#etch134)	NL-CLR-WB10 Use dedicated beaker with chromium etch (standard) <ul style="list-style-type: none"> temp.: 20°C Etchrates = 60nm/min, Check always the etchrate with dummy wafer!	
55	Clean HNO₃ 1&2 (#clean105)	NL-CLR-WB16 <ul style="list-style-type: none"> Beaker 1: HNO₃ (99%) 5min Beaker 2: HNO₃ (99%) 5min 	
56	UV dicing foil (Adwill D-210)	NI-CLR- Dicing foil Information: Thickness: 125um Material: 100um PET + 25um Acrylic (adhesive) Adhesion before UV: 2000 mN/25mm Adhesion after UV : 15 mN/25mm UV irradiation : Luminance > 120mW/cm ² and Quality > 70mJ/cm ² (wave length: 365nm)	On channel side
57	UV dicing foil (Adwill D-210)	NI-CLR- Dicing foil Information: Thickness: 125um Material: 100um PET + 25um Acrylic (adhesive) Adhesion before UV: 2000 mN/25mm Adhesion after UV : 15 mN/25mm UV irradiation : Luminance > 120mW/cm ² and Quality > 70mJ/cm ² (wave length: 365nm)	On back side ??? Perhaps another type of foil, since you might want to remove only the channel side foil for bonding. The UV foil needs a flood expose. Be aware that the foil should be able to withstand 150 degrees.



	Send to KIST	
59	50 um SU8 channel wafer	
60	Piranha clean 2 h @ 120 °C	New glass wafer?
62	Rinse & dry HOW???	
64	Oxygen treatment TEPLA 300 E 230 W, 600 s	Proceed immediately with next step
66	Lamination Photosensitive SU8 20um?? Laminator DH360 Fiol brand, thickness 20 um?? Roll speed 1 at 78 °C	Let the foil relax for 20 minutes before proceeding. Keep foil in yellow light until exposure!
68	Adhesion bake Hotplate in room ???? 300s @ 90 °C	Let the foil relax for 20 minutes before proceeding
70	PET film peel	Manual
72	Soft bake Hotplate in room ???? 300s @ 90 °C	Let the foil relax for 20 minutes before proceeding
74	Alignment & Exposure SU8 Suss MA6 • Hg-lamp: 12 mW/cm ² • Exposure Time: 240 sec	Flood exposure, no mask?
76	Post bake Hotplate in room ???? 300s @ 90 °C	
80	Lamination Photosensitive SU8 50 um?? Laminator DH360 Fiol brand, thickness 50 um?? Roll speed 1 at 78 °C	Let the foil relax for 20 minutes before proceeding. Keep foil in yellow light until exposure!
82	Adhesion bake Hotplate in room ???? 300s @ 90 °C	Let the foil relax for 20 minutes before proceeding
84	PET film peel	Manual

86	Soft bake	Hotplate in room ???? 300s @ 90 °C	Let the foil relax for 20 minutes before proceeding
87	Prepare 5 um wafer	Flood expose UV Where? Power? How long?	Preparation of 5 um wafer for bonding, so that there is no delay after development. Remove only UV foil from front side?
88	Alignment & Exposure SU8	Suss MA6 • Hg-lamp: 12 mW/cm² • Exposure Time: 225 sec	Which mask?
90	Develop	MR Dev 600 (PGMEA) • Temp:???? °C • Time: 240 s • Rinse in IPA • Dry with N ₂	Proceed directly to microcopy
92	Microscopy check	What, where	 Proceed immediately to bonding
94	Bonding	Suss SB 6 • Initial separation? • Pressure? • Temperature: 150 °C • Time?	5 um wafer facing down?? onto 50 um SU8 wafer Alignment by eye, precision 300 um 
100	Dicing	What, where, settings? • Blade? • Speed?	How do you protect inlet holes during dicing? Dicing foil?
110	Enhance bond strength	Which UV source, where? Loctite 3491 • 1000W • 120 sec	Apply loctite on outside of structure. Will it glue the dicing foil? 
110	Remove dicing foil	UV flood expose has already been done	Right before using the chip.



Final Structure layout

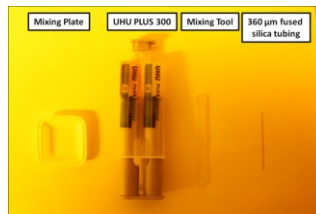
7.2 Connector mounting protocol

This is the protocol to bond the connectors for the tubing

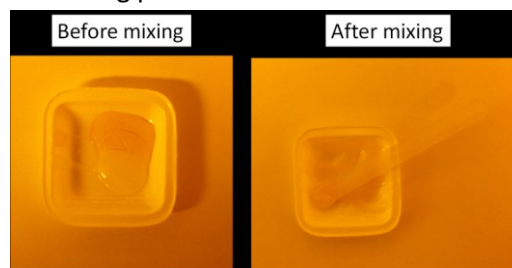
<Connector mounting protocol >

- 1) Clean the glass chip with Nitrogen gas (Nitrogen gun).
- 2) Turn on the hot plate with temperature of 120 °C
- 3) Mix the UHU PLUS Endfest 300

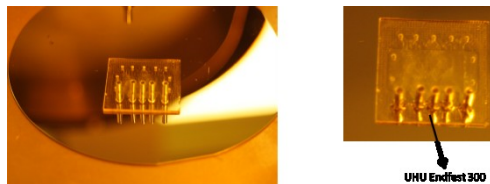
Preparation:



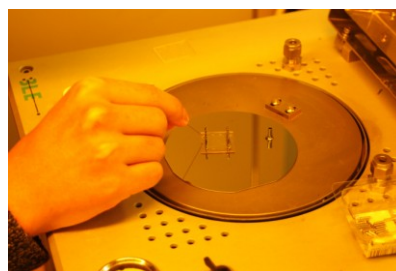
Mix the UHU plus 300 in the Mixing plate



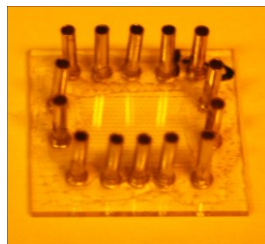
- 4) Put bootlace ferrules at the inlets. Carefully put the UHU in the outer side of the ferrules. Cure it for 10 min with a Temperature 120 °C



- 5) Repeat the process #5 also for the other Inlets



- 6) Seal the ferrules for no leakage. Cure it for 10 min with a Temperature 120 °C



- 7) Rest the Chip for at least 2 hours (Overnight it when it is possible)

7.3 Cleaning protocol

This is the protocol to clean the chip

7.3.1 Glass chip

<Cleaning protocol for 5 μm Glass chip>

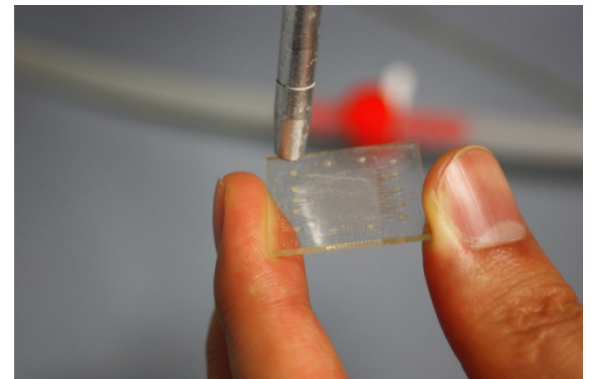
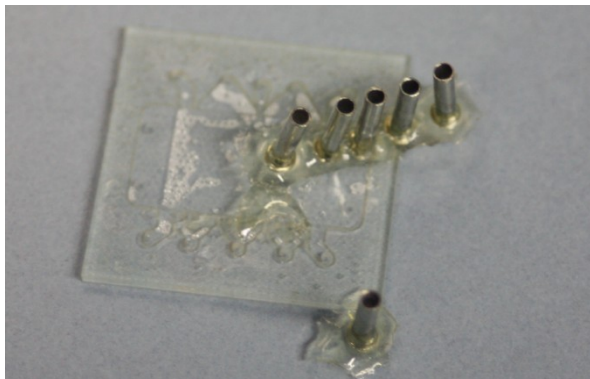
1. Mix isopropanol with water (2:10 ratio) in a beaker



2. Let FFITP device in sonicator for 2 hours in 80°C



3. The connector will be removed after process (2) than dry the chip with Nitrogen Gun
(Keep slight distance with the chip, don't use too high pressure)



4. Let the FFITP device in the solution and sonicate it (15 min, 80°C)



5. Repeat step (3) & (4) three times and then rinse it with kimtex paper



6. To remove the rest water inside the FFITP put the chip inside vacuum (Use Oxygen Plasma machine)

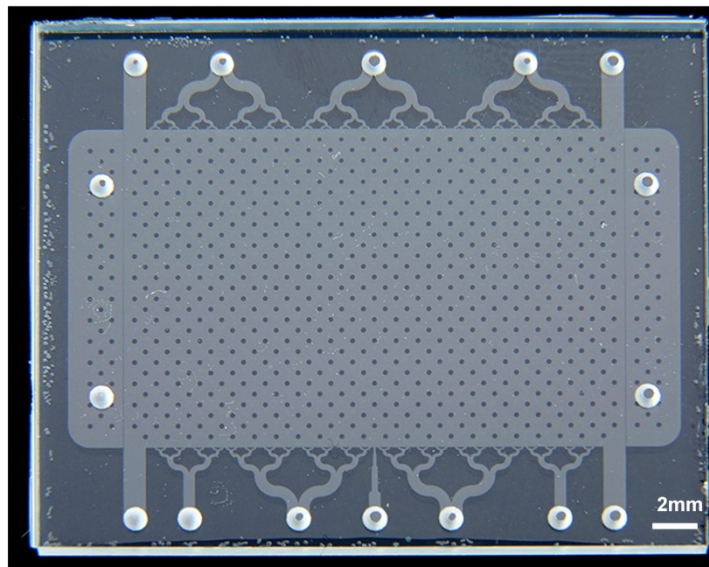


- Push the red button (turning on the machine)
- Press the Ventilation (open the machine)
- Put the FFITP inside
- Close and press (Pump)
- Wait for 5 min
- Press the Ventilation (open the machine)
- Remove the chip
- Close and press (Pump)

7. To remove all the rest inside and outside the FFITP device put the chip inside a oven



- a. Turn on the oven
- b. Press time 1a and select 00:10
- c. Press time 2a and select 06:00
- d. Press T1 and select 400 °C
- e. The chip will be clean



7.3.2 SU8 chip

<Cleaning protocol for 5 μm Glass chip>

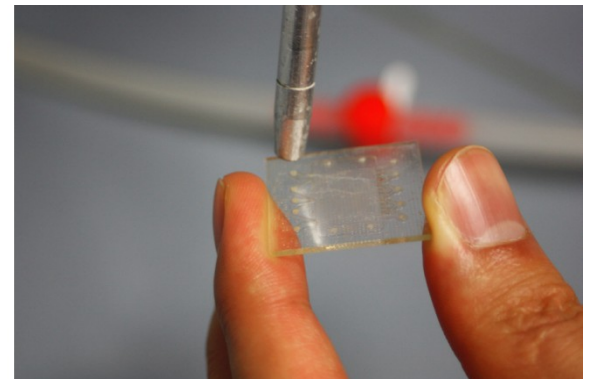
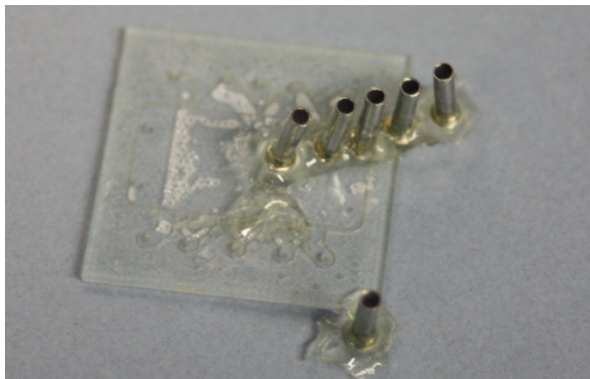
1. Mix isopropanol with water (2:10 ratio) in a beaker



2. Let FFITP device in sonicator for 2 hours in 80°C



3. The connector will be removed after process (2) than dry the chip with Nitrogen Gun
(Keep slight distance with the chip, don't use too high pressure)



4. Let the FFITP device in the solution and sonicate it (15 min, 80°C)



5. Repeat step (3) & (4) three times and then rinse it with kimtex paper

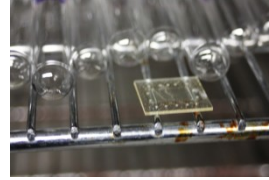


6. To remove the rest water inside the FFITP put the chip inside vacuum (Use Oxygen Plasma machine)



- Push the red button (turning on the machine)
- Press the Ventilation (open the machine)
- Put the FFITP inside
- Close and press (Pump)
- Wait for 5 min
- Press the Ventilation (open the machine)
- Remove the chip
- Close and press (Pump)

7. To remove all the rest inside and outside the FFITP device put the chip inside a oven with 70 degree.



Bibliography

- [1] Paul Atkinson, Amanda Coffey, Sara Delamont, John Lofland, and Lyn Lofland. *Handbook of ethnography*. Sage, 2001.
- [2] Jozef L Beckers. Steady-state models in electrophoresis: From isotachopheresis to capillary zone electrophoresis. *Electrophoresis*, 16(1):1987–1998, 1995.
- [3] Christian Benz, Michael Boomhoff, Johannes Appun, Christoph Schneider, and Detlev Belder. Chip-based free-flow electrophoresis with integrated nanospray mass-spectrometry. *Angewandte Chemie International Edition*, 54(9):2766–2770, 2015.
- [4] Geert AJ Besselink, Paul Vulto, Rob GH Lammertink, Stefan Schlautmann, Albert van den Berg, Wouter Olthuis, Gerard HM Engbers, and Richard Schasfoort. Electroosmotic guiding of sample flows in a laminar flow chamber. *Electrophoresis*, 25(21-22):3705–3711, 2004.
- [5] Eric R. Castro and Andreas Manz. Present state of microchip electrophoresis: State of the art and routine applications. *Journal of Chromatography A*, 1382:66 – 85, 2015. ISSN 0021-9673. doi: <http://dx.doi.org/10.1016/j.chroma.2014.11.034>. URL <http://www.sciencedirect.com/science/article/pii/S0021967314017920>. Editors' Choice {IX}.
- [6] Anne Chartogne, Ubbo R Tjaden, and Jan Van der Greef. A free-flow electrophoresis chip device for interfacing capillary isoelectric focusing on-line with electrospray mass spectrometry. *Rapid Communications in Mass Spectrometry*, 14(14):1269–1274, 2000.
- [7] Li-Jing Cheng and Hsueh-Chia Chang. Switchable ph actuators and 3d integrated salt bridges as new strategies for reconfigurable microfluidic free-flow electrophoretic separation. *Lab on a Chip*, 14(5):979–987, 2014.
- [8] Vladislav Dolník, Shaorong Liu, Stevan Jovanovich, et al. Capillary electrophoresis on microchip. *Electrophoresis*, 21(1):41–54, 2000.
- [9] Frans Matheus Everaerts, Jo L Beckers, and Theo PEM Verheggen. *Isotachopheresis: theory, instrumentation and applications*, volume 6. Elsevier, 2011.
- [10] John B Fenn, Matthias Mann, Chin Kai Meng, Shek Fu Wong, and Craig M Whitehouse. Electrospray ionization for mass spectrometry of large biomolecules. *Science*, 246(4926):64–71, 1989.
- [11] John B Fenn, Matthias Mann, Chin Kai Meng, Shek Fu Wong, and Craige M Whitehouse. Electrospray ionization-principles and practice. *Mass Spectrometry Reviews*, 9(1):37–70, 1990.

- [12] Alisdair R Fernie, Richard N Trethewey, Arno J Krotzky, and Lothar Willmitzer. Metabolite profiling: from diagnostics to systems biology. *Nature Reviews Molecular Cell Biology*, 5(9):763–769, 2004.
- [13] Bryan R Fonslow and Michael T Bowser. Free-flow electrophoresis on an anodic bonded glass microchip. *Analytical chemistry*, 77(17):5706–5710, 2005.
- [14] P Andrew Futreal, Qingyun Liu, Donna Shattuck-Eidens, Charles Cochran, Keith Harshman, Sean Tavtigian, L Michelle Bennett, Astrid Haugen-Strano, Jeff Swensen, Yoshio Miki, et al. Brca1 mutations in primary breast and ovarian carcinomas. *Science*, 266(5182):120–122, 1994.
- [15] Petr Gebauer and Petr Boček. Theory of zone separation in isotachophoresis: A diffusional approach. *Electrophoresis*, 16(1):1999–2007, 1995.
- [16] Petr Gebauer, Zdena Malá, and Petr Boček. Recent progress in analytical capillary isotachophoresis. *Electrophoresis*, 32(1):83–89, 2011.
- [17] Petr Gebauer, Zdena Malá, and Petr Boček. Electrolyte system strategies for anionic isotachophoresis with electrospray-ionization mass-spectrometric detection. 2. isotachophoresis in moving-boundary systems. *Electrophoresis*, 34(24):3245–3251, 2013.
- [18] Kurt Hannig. New aspects in preparative and analytical continuous free-flow cell electrophoresis. *Electrophoresis*, 3(5):235–243, 1982.
- [19] H von Helmholtz. Ueber einige gesetze der vertheilung elektrischer ströme in körperlichen leitern mit anwendung auf die thierisch-elektrischen versuche. *Annalen der Physik*, 165(6):211–233, 1853.
- [20] Sabrina Hoffstetter-Kuhn, Reinhard Kuhn, and Horst Wagner. Free flow electrophoresis for the purification of proteins: I. zone electrophoresis and isotachophoresis. *Electrophoresis*, 11(4):304–309, 1990.
- [21] Vlastimil Hruška and Bohuslav Gaš. Kohlrausch regulating function and other conservation laws in electrophoresis. *Electrophoresis*, 28(1-2):3–14, 2007.
- [22] Stephen C Jacobson, Lance B Koutny, Roland Hergenroeder, Alvin W Moore Jr, and J Michael Ramsey. Microchip capillary electrophoresis with an integrated postcolumn reactor. *Analytical Chemistry*, 66(20):3472–3476, 1994.
- [23] Dirk Janasek, Joachim Franzke, and Andreas Manz. Scaling and the design of miniaturized chemical-analysis systems. *Nature*, 442(7101):374–380, 2006.

- [24] Dirk Janasek, Michael Schilling, Joachim Franzke, and Andreas Manz. Isotachophoresis in free-flow using a miniaturized device. *Analytical chemistry*, 78(11):3815–3819, 2006.
- [25] Dirk Janasek, Michael Schilling, Andreas Manz, and Joachim Franzke. Electrostatic induction of the electric field into free-flow electrophoresis devices. *Lab on a Chip*, 6(6):710–713, 2006.
- [26] Stefan Köhler, Christian Benz, Holger Becker, Erik Beckert, Volker Beushausen, and Detlev Belder. Micro free-flow electrophoresis with injection molded chips. *Rsc Advances*, 2(2):520–525, 2012.
- [27] Stefan Köhler, Stefan Nagl, Stefanie Fritzsche, and Detlev Belder. Label-free real-time imaging in microchip free-flow electrophoresis applying high speed deep uv fluorescence scanning. *Lab on a chip*, 12(3):458–463, 2012.
- [28] Dietrich Kohlheyer, Geert AJ Besselink, Rob GH Lammertink, Stefan Schlautmann, Sandeep Unnikrishnan, and Richard BM Schasfoort. Electro-osmotically controllable multi-flow microreactor. *Microfluidics and Nanofluidics*, 1(3):242–248, 2005.
- [29] Dietrich Kohlheyer, Geert AJ Besselink, Stefan Schlautmann, and Richard BM Schasfoort. Free-flow zone electrophoresis and isoelectric focusing using a microfabricated glass device with ion permeable membranes. *Lab on a Chip*, 6(3):374–380, 2006.
- [30] Dietrich Kohlheyer, Jan CT Eijkel, Stefan Schlautmann, Albert Van Den Berg, and Richard BM Schasfoort. Microfluidic high-resolution free-flow isoelectric focusing. *Analytical chemistry*, 79(21):8190–8198, 2007.
- [31] Dietrich Kohlheyer, Jan CT Eijkel, Stefan Schlautmann, Albert van den Berg, and Richard BM Schasfoort. Bubble-free operation of a microfluidic free-flow electrophoresis chip with integrated pt electrodes. *Analytical chemistry*, 80(11):4111–4118, 2008.
- [32] Dietrich Kohlheyer, Jan CT Eijkel, Albert van den Berg, and Richard Schasfoort. Miniaturizing free-flow electrophoresis—a critical review. *Electrophoresis*, 29(5):977–993, 2008.
- [33] Ludmila Křivánková and Petr Boček. Continuous free-flow electrophoresis. *Electrophoresis*, 19(7):1064–1074, 1998.
- [34] Gwo-Bin Lee, Shu-Hui Chen, Guan-Ruey Huang, Wang-Chou Sung, and Yen-Heng Lin. Microfabricated plastic chips by hot embossing methods and their applications for dna separation and detection. *Sensors and Actuators B: Chemical*, 75(1):142–148, 2001.

- [35] I-K Lee, M Jeun, H-J Jang, W-J Cho, and KH Lee. A self-amplified transistor immunosensor under dual gate operation: highly sensitive detection of hepatitis b surface antigen. *Nanoscale*, 7(40):16789–16797, 2015.
- [36] Zdena Malá, Petr Gebauer, and Petr Boček. Recent progress in analytical capillary isotachopheresis. *Electrophoresis*, 36(1):2–14, 2015.
- [37] Andreas Manz and Jan CT Eijkel. Miniaturization and chip technology. what can we expect? *Pure and Applied Chemistry*, 73(10):1555–1561, 2001.
- [38] Theresa McDonnell and Janusz Pawliszyn. Capillary isotachopheresis with concentration gradient detection. *Analytical chemistry*, 63(17):1884–1889, 1991.
- [39] Adam Marcus Namisnyk. *A survey of electrochemical supercapacitor technology*. PhD thesis, University of Technology, Sydney, 2003.
- [40] Pamela N Nge, Chad I Rogers, and Adam T Woolley. Advances in microfluidic materials, functions, integration, and applications. *Chemical reviews*, 113(4):2550–2583, 2013.
- [41] Gregor Ocvirk, Mark Munroe, Thompson Tang, Richard Oleschuk, Ken Westra, and D Jed Harrison. Electrokinetic control of fluid flow in native poly (dimethylsiloxane) capillary electrophoresis devices. *Electrophoresis*, 21(1):107–115, 2000.
- [42] David Perrett. 200 years of electrophoresis. *Chromatog. Today December*, pages 4–7, 2010.
- [43] RNA Prebiotic. Polymer microstructures formed by moulding in capillaries. *Nature*, 376:581–584, 1995.
- [44] Jeff E Prest, Sara J Baldock, Peter R Fielden, Nicholas J Goddard, and Bernard J Treves Brown. Analysis of amino acids by miniaturised isotachopheresis. *Journal of Chromatography A*, 1051(1):221–226, 2004.
- [45] Jeff E Prest, Sara J Baldock, Peter R Fielden, Nicholas J Goddard, Royston Goodacre, Richard O’Connor, and Bernard J Treves Brown. Miniaturised free flow isotachopheresis of bacteria using an injection moulded separation device. *Journal of Chromatography B*, 903:53–59, 2012.
- [46] Joselito P Quirino and Shigeru Terabe. Sample stacking of cationic and anionic analytes in capillary electrophoresis. *Journal of Chromatography A*, 902(1):119–135, 2000.

- [47] Daniel E Raymond, Andreas Manz, and H Michael Widmer. Continuous sample pretreatment using a free-flow electrophoresis device integrated onto a silicon chip. *Analytical Chemistry*, 66(18):2858–2865, 1994.
- [48] Richard D Smith, Joseph A Loo, Rachel R Ogorzalek Loo, Mark Busman, and Harold R Udseth. Principles and practice of electrospray ionization-mass spectrometry for large polypeptides and proteins. *Mass Spectrometry Reviews*, 10(5):359–452, 1991.
- [49] Otto Stern. Zur theorie der elektrolytischen doppelschicht. *Zeitschrift für Elektrochemie und angewandte physikalische Chemie*, 30(21-22):508–516, 1924.
- [50] Leon Sun, Judd W Moul, James M Hotaling, Edward Rampersaud, Phillipp Dahm, Cary Robertson, Nicholas Fitzsimons, David Albala, and Thomas J Polascik. Prostate-specific antigen (psa) and psa velocity for prostate cancer detection in men aged \geq 50 years. *BJU international*, 99(4):753–757, 2007.
- [51] P Just Svendsen and Carsten Rose. Separation of proteins using ampholine carrier ampholytes as buffer and spacer ions in an isotachopheresis system. *Science Tools, The LKB Instrument Journal*, 17(1):13–17, 1970.
- [52] Alexey Tarasov, Mathias Wipf, Ralph L Stoop, Kristine Bedner, Wangyang Fu, Vitaliy A Guzenko, Oren Knopfmacher, Michel Calame, and Christian Schonenberger. Understanding the electrolyte background for biochemical sensing with ion-sensitive field-effect transistors. *ACS nano*, 6(10):9291–9298, 2012.
- [53] Staffan Wall. The history of electrokinetic phenomena. *Current Opinion in Colloid & Interface Science*, 15(3):119–124, 2010.
- [54] Younan Xia, Milan Mrksich, Enoch Kim, and George M Whitesides. Microcontact printing of octadecylsiloxane on the surface of silicon dioxide and its application in microfabrication. *Journal of the American Chemical Society*, 117(37):9576–9577, 1995.
- [55] Chao-Xuan Zhang and Andreas Manz. High-speed free-flow electrophoresis on chip. *Analytical chemistry*, 75(21):5759–5766, 2003.